

CALCIUM CARBONATE-BASED PARTICLES AND CAPSULES FOR THERAPEUTIC ENZYMES

Aantal woorden: 28207

Laura Van Poelvoorde

Stamnummer: 01206084

Promotor: Prof. dr. ir. Andre Skirtach

Copromotor: dr. Bogdan Parakhonskiy

Masterproef voorgelegd voor het behalen van de graad master in de richting Master of Science in de industriële wetenschappen: biochemie

Academiejaar: 2016 - 2017



CALCIUM CARBONATE-BASED PARTICLES AND CAPSULES FOR THERAPEUTIC ENZYMES

Aantal woorden: 28207

Laura Van Poelvoorde

Stamnummer: 01206084

Promotor: Prof. dr. ir. Andre Skirtach

Copromotor: dr. Bogdan Parakhonskiy

Masterproef voorgelegd voor het behalen van de graad master in de richting Master of Science in de industriële wetenschappen: biochemie

Academiejaar: 2016 - 2017



“The author and the promoter give the permission to use this thesis for consultation and to copy parts of it for personal use. Every other use is subject to the copyright laws, more specifically the source must be extensively specified when using the results from this thesis”.

Promotor:

Prof. Dr. Ir. Andre Skirtach

Author:

Laura Van Poelvoorde

Acknowledgements

This thesis was made to fulfil the requirements for the degree of Master of Science in Industrial Sciences: Biochemistry at Ghent University. The research in this work and the description were accomplished thanks to the support of many, and I would like to take this opportunity to express my gratitude.

First, I want to thank my promotor Prof. Dr. Ir. Andre Skirtach and my tutor Dr. Bogdan Parakhonskiy for the possibility to temporarily join the Department of Molecular Biotechnology. Also, I want to thank them for their guidance, for teaching me various techniques and the confidence, that I would provide good results. I am also grateful for their help, suggestions and corrections in the manuscript of this thesis.

Furthermore, I want to thank Dr. Lynn De Backer and Dr. Felix Sauvage for the help with the liposomes and the access to the ultracentrifuge. I want to thank Dr. Ekaterina Lengert for performing the SEM images. Also, I want to thank Dr. Margot Vansteenland for the access and explanation for the microplate reader.

In addition, I would like to thank the whole lab group and other thesis students for the enjoyable working atmosphere.

Finally, I would like to thank my friends and family for their constant support, advice, encouragement through my studies and for reading this thesis.

Abstract

CaCO₃ particles are very useful microparticles, because of the low synthesis costs, simple synthesis method, the porosity that leads to easy loading, the biocompatibility, the low toxicity and the mild decomposition conditions. However, these CaCO₃ particles cannot easily be used by itself, due to the instability in water based solutions, which is maximum 1 day, and the weak protection of loaded materials. A less time consuming and expensive method than the use of polyelectrolytes, is the use of alginate based hydrogels. The stability of the alginate based hydrogels is minimum 6 days. These particles are compared with liposomes made from DOPC, because liposomes are already frequently used in controlled drug delivery.

In this study, various carriers are loaded with ALP and they are compared based on their loading capacity, their stability and their enzyme activity. Seven types of carriers were obtained, namely CaCO₃ particles, alginate based hydrogels, calcium alginate based hydrogels and silver alginate based hydrogels with and without a CaCO₃ core and finally liposomes.

The loading capacity of the vaterite particles is 19.9% for the small particles and 16.1% for the large particles. However, ALP is a relatively inexpensive enzyme, so if a more expensive enzyme is used, it will be more interesting to take in account the loading efficiency. The loading capacity of the liposomes is much higher, namely 100%.

Even though the small vaterite particles have a higher loading capacity than the large vaterite particles, the percentage of active ALP of the large particles is higher, namely 55.2%, than the small vaterite particles, namely 32.3%. In the XPS data it is indicated that there is more ALP on the surface of the large particles. The higher loading capacity and the lower amount of ALP of the small particles could indicate that there is ALP present in the particles. When the vaterite particles are gelatinized through alginate, the percentage of active ALP decreases to 23.3% for the small particles and 27.2% for the large particles. When links are made with silver, there is no detection of activity. However, when these links are made with CaCl₂, there is still activity detected for the small particles and large particles, namely 10% and 4.6% respectively, and it decreases even more when the CaCO₃ core is removed to 4.2% for the small particles and 2.4% for the large particles. The percentage of active ALP in the liposomes is 57.5%

Keywords

Alkaline phosphatase, alginate based hydrogel, CaCO₃ particle, enzyme activity, DOPC, loading capacity, stability

Abstract (Dutch)

CaCO₃ partikels zijn zeer nuttige micropartikels door hun lage synthesekosten, simpele synthesemethode, de porositeit dat leidt tot de gemakkelijke lading van ALP, de biocompatibiliteit en de milde decompositiecondities. Echter kunnen deze CaCO₃ partikels niet gemakkelijk op zichzelf worden gebruikt door hun instabiliteit in watergebaseerde oplossingen, waarin ze maximaal 1 dag stabiel zijn en hun zwakke bescherming van het geladen materiaal. Een minder tijdsintensieve en dure methode dan het gebruik van poly-elektrolyten is het gebruik van alginaat gebaseerde hydrogels. De stabiliteit van deze alginaat gebaseerde hydrogels is minimaal 6 dagen. Deze partikels worden vervolgens vergeleken met liposomen gemaakt van DOPC, omdat liposomen al vaak worden gebruikt in gecontroleerde drug delivery.

In deze studie worden verschillende carriers geladen met ALP en worden ze vergeleken op basis van hun ladingscapaciteit, hun stabiliteit en hun enzymactiviteit. Er worden 7 verschillende types carriers verkregen, namelijk CaCO₃ partikels, alginaatgebaseerde hydrogels, calciumalginaatgebaseerde hydrogels en zilveralginaat hydrogels met en zonder CaCO₃ kern en tenslotte liposomen.

De ladingscapaciteit van vaterietpartikels is 19.9% voor de kleine partikels en 16.1% voor de grote partikels. Echter, ALP is een relatief goedkoop enzym, dus als er een duurder enzym wordt gebruikt, is het interessant om rekening te houden met de ladingsefficiëntie. De ladingscapaciteit van de liposomen is veel hoger, namelijk 100%.

De kleine vaterietpartikels hebben dus een hogere ladingscapaciteit, dan de grote vaterietpartikels, maar het percentage van actief ALP is hoger in de grote partikels, namelijk 55.2%, dan de kleine partikels, namelijk 32.3%. In de XPS-data wordt er aangegeven dat er meer ALP op de oppervlakte is van de grote partikels. De hogere ladingscapaciteit en lagere hoeveelheid aan ALP van de kleine vaterietpartikels kan aantonen dat er ALP aanwezig is in de partikels. Als deze vaterietpartikels worden gelatiniseerd met alginaat, zal het percentage aan actief ALP dalen tot 23.3% voor de kleine partikels en 27.2% voor de grote partikels. Als er vervolgens linken worden gemaakt met zilver, wordt er geen activiteit meer gedetecteerd. Echter, als deze linken worden gemaakt met CaCl₂, dan wordt er nog steeds activiteit gedetecteerd voor de kleine en grote partikels, namelijk respectievelijk 10% en 4.6%. Deze zal verder dalen als de CaCO₃ kern wordt verwijderd tot 4.2% voor de kleine partikels en 2.4% voor de grote partikels. Het percentage aan actief ALP in de liposomen is 57.5%

Kernwoorden

Alkalische fosfatase, alginaatgebaseerde hydrogel, CaCO₃ partikel, DOPC, enzymactiviteit, ladingscapaciteit, stabiliteit

Table of Contents

1	List with abbreviations	2
2	List with tables and figures	4
2.1	Tables	4
2.2	Figures	4
2.3	Graph	5
3	Introduction	8
4	Literature	10
4.1	Microparticles and other carriers	10
4.1.1	Calcium carbonate particles	11
4.1.2	Liposomes	13
4.1.3	Red Blood Cells and Red blood cell-like capsules	14
4.1.4	Poly(lactic-acid-co-glycolide) particles	16
4.2	Loading	17
4.3	Encapsulation	17
4.3.1	Layer-by-layer structures	18
4.3.2	Alginate capsules	20
4.4	Release	22
4.5	Enzymes	24
4.5.1	Alkaline phosphatase	24
4.5.2	Human guanylate kinase	26
4.6	Drug delivery	26
4.7	Cellular uptake and intracellular release	28
4.7.1	Mechanical stability of polymeric capsules	28
4.7.2	Influence of the size and shape on the cellular uptake	28
4.7.3	Intracellular release of content from capsule	29
5	Goals	30
5.1	CaCO ₃ particles and encapsulated CaCO ₃ particles	30
5.1.1	Loading capacity	30
5.1.2	Stability	30
5.1.3	Activity of the enzyme loaded to the particles	30
5.2	Comparison of the liposomes with CaCO ₃ particles	30

6	Material and Methods.....	32
6.1	Calcium carbonate particles	32
6.1.1	Formation of calcium carbonate particles.....	32
6.1.2	ALP loading	33
6.1.3	Optical Microscopy.....	34
6.1.4	Scanning Electron Microscopy.....	34
6.1.5	FTIR spectroscopy.....	34
6.1.6	Stability of the particles	34
6.1.7	Enzymatic activity measurements.....	35
6.1.8	XPS measurements.....	35
6.1.9	Toxicity test.....	36
6.2	Alginate particles.....	36
6.2.1	Particles synthesis	36
6.2.2	Stability of the particles	37
6.2.3	Enzymatic activity measurements.....	37
6.3	Liposomes.....	37
6.3.1	Particles synthesis	37
6.3.2	Enzymatic activity measurements.....	38
7	Results and discussion.....	40
7.1	Calcium carbonate particles	40
7.1.1	Optimization of time and concentration for ALP loading	41
7.1.2	Stability of the particles	43
7.1.3	Amount of active ALP in the particles.....	47
7.1.4	XPS measurements.....	49
7.1.5	Toxicity	50
7.2	Alginate particles.....	51
7.2.1	Stability of the particles	52
7.2.2	Amount of active ALP in the particles.....	53
7.3	Liposomes.....	56
8	Conclusion	58
9	Future perspectives.....	60
9.1	Expected manuscripts	60
10	References.....	62

I.	Appendix: SEM images of alginate based hydrogels	1
----	--	---

1 List with abbreviations

ADP	Adenosine-5'-diphosphate
AKI	Acute kidney injury
ALP	Alkaline phosphatase
ATP	Adenosine-5'-triphosphate
CaCl₂	Calcium chloride
CaCO₃	Calcium carbonate
CD	Crohn's disease
DMF	Dimethylformamide
DMSO	Dimethylsulfoxide
DNA	Deoxyribonucleic acid
DS	Dextran sulphate
EDTA	Ethylenediaminetetraacetic acid
EDX	Energy-Dispersive X-ray spectroscopy
EG	Ethylene glycol
ERT	Enzyme Replacement Therapy
FDA	U.S. Food and Drug Administration
FTIR	Fourier Transform Infrared
G	α -L-guluronic acid
GDP	Guanosine-5'-monophosphate
GMP	Guanosine-5'-monophosphate
GMPK	Guanylate kinase
GPI	Glucosylphosphatidylinositol
GSH	Glutathione
Hb	Haemoglobin
hGMPK	Human Guanylate kinase
IBD	Inflammatory Bowel Disease
IgG	Immunoglobulin G
LbL	Layer-by-layer

LPS	Lipopolysaccharide
M	β -D-mannuronic acid
MF	Melamine formaldehyde
NaAlg	Sodium alginate
NaCO₃	Sodium carbonate
PAH	Poly(allylamine hydrochloride)
PBS	Phosphate Buffered Saline
PEG	Poly(ethylene glycol)
PEM	Polyelectrolyte multilayer
PLA	Poly(lactic acid)
PLGA	Poly(lactic-acid-co-glycolide)
pNPP	p-Nitrophenyl phosphate
PS	Polystyrene
PSS	Polystyrene sulfonate
RBC	Red blood cell
TNSALP	Tissue-non-specific alkaline phosphatase
UC	Ulcerative colitis
XPS	X-ray Photoelectron Spectroscopy

2 List with tables and figures

2.1 Tables

Table 1: Results of EDX of large particles dissolved in PBS 46

Table 2: SEM images of the various small and large alginate based hydrogels 1

2.2 Figures

Figure 1. Different forms of calcium carbonate, namely aragonite, calcite and vaterite. 12

Figure 2: Schematic description of LbL-capsule synthesis by direct (a and b) or indirect methods (c). Alternate layers of oppositely charged polyelectrolytes (grey and black layers) are assembled on a core by sequential deposition or spraying. Enzyme-containing cores (a) and sacrificial cores (c) are decomposed afterward, followed by enzyme loading for (c). Crystallized enzymes are dissolved (b). The final result in all preparation methods is a polyelectrolyte-shell encapsulating enzymes in its confinement (Rother C. & Nidetzky B., 2014). 20

Figure 3: Covalent or non-covalent systems in drug delivery. (A) After identifying whether surface immobilized or encapsulated delivery is preferred (B), a variety of triggers can be utilized for controlled release (C) (Doane T. L. & Burda C., 2011)..... 27

Figure 4. Chemical precipitation procedure for small particles. The reaction between calcium ions and carbonate ions with addition of ethylene glycol (EG) (in aqueous solution)..... 32

Figure 5. Chemical precipitation procedure for large particles. The reaction between calcium ions and carbonate ions (in aqueous solution)..... 32

Figure 6: SEM images of small (A) with a size of $1.150 (\pm 0,074) \mu\text{m}$ and large (B) with a size of $2.307 (\pm 0.385) \mu\text{m}$ vaterite particles..... 40

Figure 7: FTIR spectra of small vaterite particles (1), large vaterite particles (2) and calcite particles (3) without ALP. A band typical for calcite is marked at 712 cm^{-1} and 873 cm^{-1} and band characteristic for vaterite is marked at 745 cm^{-1} , 878 cm^{-1} and 1085 cm^{-1} 41

Figure 8: Scanning Electron Microscopy images of the recrystallization process from vaterite particles (A), to vaterite and calcite particles (B), to calcite (C) particles 44

Figure 9: Scanning Electron Microscopy images of the transformation of vaterite particles (A) to hydroxyapatite (B) particles 44

Figure 10: FTIR spectra of calcium carbonate particles without ALP before (1 and 5) and after (2, 3, 4, 6, 7, 8) one week of incubation in the different solvents. (1) Initial large vaterite particles; (2) Large particles incubated in H_2O ; (3) Large particles incubated in NaCl ; (4) Large particles incubated in PBS ; (5) Initial small vaterite particles; (6) Small particles incubated in H_2O ; (7) Small particles incubated in NaCl ; (8) Small particles incubated in PBS . A band typical for hydroxyapatite is marked at 961 cm^{-1} , a band typical for calcite is marked at 873 cm^{-1} and 712 cm^{-1} and a band typical for vaterite is marked at 1085 cm^{-1} , 878 cm^{-1} and 745 cm^{-1} 45

Figure 11: Enzymatic reaction mechanism of p-nitrophenylphosphate to p-nitrophenol with ALP. 47

Figure 12: FTIR spectra of small (A) and large (B) alginate based hydrogels in comparison with CaCO₃ particles (1); (2) alginate particles; (3) silver alginate particles with a CaCO₃ core; (4) silver alginate particles after addition of ascorbic acid; (5) calcium alginate particles with a CaCO₃ core. Bands characteristic for small silver alginate particles are 712 cm⁻¹, 800 cm⁻¹, 878 cm⁻¹ and 1085 cm⁻¹. Bands characteristic for large silver alginate particles are 612 cm⁻¹, 712 cm⁻¹, 745 cm⁻¹, 800 cm⁻¹, 878 cm⁻¹ and 1085 cm⁻¹. Specific bands for calcium alginate particles with a CaCO₃ core are 745 cm⁻¹, 878 cm⁻¹ and 1085 cm⁻¹. 51

2.3 Graph

Graph 1: Loading capacity (A) and loading efficiency (B) for small (●) and large (▲) vaterite particles dependent on the time of ALP absorption, by measuring the ALP concentration after dissolving the particles in EDTA (Dissolution method) and measuring the ALP concentration in the supernatans (Supernatans method)..... 42

Graph 2: Loading capacity (A) and loading efficiency (B) for small (●) and large (▲) particles dependent on the of the initial ALP concentrations, by measuring the ALP concentration after dissolving the particles in EDTA (Dissolution method) and measuring the ALP concentration in the supernatans (Supernatans method)..... 43

Graph 3: The dynamics of the composition of the samples for different ALP concentrations, namely 0, 0.5 and 10 mg/mL, with different sizes, namely small (A) and large (B) particles, incubated in different solutions, namely PBS, NaCl and H₂O. The recrystallization process started after 2 hours of ALP loading..... 46

Graph 4: Absorbance spectra with a low standard deviation (± 0,005) of 1 mg of small (●) and large (▲) vaterite particles loaded with an initial concentration of 10 mg/mL ALP after the addition of substrate pNPP in function of different time intervals of adding stop solution. 48

Graph 5: Intensity of the absorbance of the enzyme activity measurement measured at 405 nm of recrystallized small (A) and large (B) particles loaded with an initial concentration of 0,5 mg/mL ALP and 10 mg/mL. The particles are incubated in three solvents, namely H₂O, PBS and NaCl. 48

Graph 6: Amount of nitrogen in the small (●) and large (▲) particles, dependent on the different initial ALP concentrations, namely 0.5, 1, 4 and 10 mg/mL. 49

Graph 7: Results of the toxicity normalized to the control cells of small and large particles, loaded with different initial ALP concentrations, namely 0.5, 10 and 20 mg/mL. 50

Graph 8: The dynamics of the composition of the samples of small and large CaCO₃ particles in comparison with different alginate based hydrogels, such as alginate particles (CaCO₃/Alg), silver alginate particles with CaCO₃ core (CaCO₃/AgAlg) and calcium alginate particles with CaCO₃ core (CaCO₃/CaAlg)..... 52

Graph 9: The percentage of active ALP in the intermediate steps of the formation of silver alginate particles, namely starting with ALP loaded CaCO₃ particles (1), next the addition of alginate (10 mg/mL) (2), subsequently AgNO₃ (0.5 M) (3) is added and finally ascorbic acid (0.1 M) (4) is added.53

Graph 10: The percentage of active ALP in small (●) and large (▲) particles dependent on the different alginate concentrations, namely 0, 3, 5, 7, and 10 mg/mL.....54

Graph 11: Absorption spectra of ALP loaded small (A) and large (B) particles with different coating: CaCO₃ particles (1), CaCO₃ particles with alginate (5 mg/mL) layer (2) and CaCO₃ particles with alginate layer crosslinked with different AgNO₃ concentrations, namely 0.1 M (3a), 0.25 M (3b), 0.5 M (3c) and 0.75 M (3d).54

Graph 12: The percentage of active ALP in small and large ALP loaded CaCO₃ (1) particles, alginate particles (2), alginate particles linked with different concentration of CaCl₂, namely 0.1 M (3a) and 0.5 M (3b) and finally after the addition of ascorbic acid (0.1M) to the alginate particles linked with 0.1 M CaCl₂ (4a) and 0.5 M CaCl₂ (4b).55

Graph 13: Loading capacity of the liposomes, small vaterite particles and large vaterite particles, measured with the dissolution method and the supernatans method, loaded with an initial ALP concentration of 10 mg/mL.56

Graph 14: The percentage of active ALP of the liposomes, small vaterite particles and large vaterite particles, measured with the dissolution method and the supernatans method, loaded with an initial ALP concentration of 10 mg/mL.....57

3 Introduction

The goal of this thesis is to develop carriers for therapeutic enzymes, that will be delivered to the human body. Free enzymes don't survive long in the human body, because of low bioavailability and short half-lives. The bio-availability of the enzymes is limited due to among others a rapid metabolism and opsonisation of the immune system. By using carriers based upon microparticles, the enzymes are protected. These carriers cannot only be used to deliver drugs, but they can also be used in the chemical, physical and food industry.

Over the years, a lot of different micro- and nanocarriers have been developed from various materials such as liposomes, cells, polymeric electrolytes. Most capsules, used in this thesis, are assembled out of calcium carbonate (CaCO_3) particles. The advantage of these particles is the porosity, which allows more effective encapsulation. Also, CaCO_3 particles have low synthesis costs, a simple synthesis method, biocompatibility, low toxicity and mild decomposition conditions.

In this thesis, the stability, the adsorption and the activity of the adsorbed enzyme in large and small CaCO_3 particles, alginate based hydrogels and liposomes are compared. Liposomes are used for the comparison with the CaCO_3 particles and alginate based hydrogels, because liposomes are the most common and well-investigated nanocarriers for targeted drug delivery.

4 Literature

4.1 Microparticles and other carriers

Microparticles have significant advantages as drug delivery systems: the possibility to accurately control the release rate of the incorporated drug over periods of hours to months, an effective protection of the encapsulated active agent against degradation, an easy administration and a desired, pre-programmed drug release profiles, that can be provided which will match the therapeutic needs of the patient (Singh M. N. et al, 2010).

The diameter of microparticles is within the range of a few micrometres. In comparison nanoparticles are much smaller with a diameter within the range between a few nanometres to 900 nanometres. This size range is important for in vivo applications, because nanoparticles can also be used for drug delivery through blood circulation. Microparticles are very attractive, because of the simplicity of their characterization and imaging with the use of a conventional microscope. Also aggregation can be easily prevented, there is a superior loading capacity and they have a large surface area for modification (Delcea M. et al, 2011).

These microparticles can be composed of several materials. The most commonly used materials are hollow polyelectrolyte microcapsules made of sodium poly(styrene sulfonate) (PSS), poly(allylamine hydrochloride) (PAH) multilayers and a core composed of melamine formaldehyde (MF) or polystyrene (PS) (Dejugnat C. & Sukhorukov G.B., 2004; Sukhorukov G.B. et al, 1999), polylactic acid (PLA) particles (Shenoy D. B. et al, 2003), CaCO₃ cores (Antipov A. A. et al, 2003), cells (Neu B. et al, 2008), silica particles (Itoh Y. et al, 2004) and gold nanoparticles (Schneider G. & Decher G., 2004).

These cores will need to be extracted from its capsules. However, to dissolve MF core to oligomers hydrochloric acid or a few water-soluble solvents, such as dimethylformamide (DMF) or dimethylsulfoxide (DMSO), can be used. During this process, slow diffusion of these oligomers causes a high osmotic pressure. Consequently, this osmotic pressure can cause ruptures in the capsule, but it can also happen that some residue of the oligomers can stay behind in the capsule. The same problem occurs with PLA cores, that will be dissolved in organic solvents. These solvents can also be used to dissolve PS cores. These will cause instability and a change in structure of the capsules (Dejugnat C. & Sukhorukov G.B., 2004; Delcea M. et al, 2011; Dong W. et al, 2005; Sukhorukov G.B. et al, 1999). Also, cells can be used, but the disadvantage of using cells as core, is their variety in shape and size.

The previous discussed cores are organic, so they are hard to dissolve in water, in contrary to inorganic cores. These cores will also cause less rupture of the capsule, because it dissolves into ions. However silica cores will give aggregation problems, which is not suitable for loading, and the dissolution can only be achieved with the highly corrosive hydrofluoric acid (Itoh Y. et al, 2004). Gold particles have to be extracted with a hazardous potassium cyanide solution (Schneider G. & Decher G., 2004). Because of all these disadvantages, CaCO₃ will be chosen as core material due to its porosity and the easy dissolution in ethylenediaminetetraacetic acid (EDTA). Also, porous particles, such as CaCO₃, allow more effective encapsulation of

molecules than smooth particles, such as silica and polystyrene. The disadvantage of CaCO_3 is its irregular size and the control of the aggregation, that has to be controlled as much as possible (Antipov A. A. et al, 2003; Parakhonskiy B. V. et al, 2014a).

4.1.1 Calcium carbonate particles

Mimicking the biological behaviour is a promising strategy to enhance the cellular targeting efficacy in drug delivery systems. There is often an association with shape-specific, anisotropic and noncovalent interactions between biological molecules. For the medical application of anisotropic particles, inhalation is viewed as an important area, because of its favourable hydrodynamic properties. For the uptake of drug carriers into cells, the shape of the particles is an important factor. There has been a relatively high penetration rate in cells observed with cubical, semispherical and elliptical shapes in comparison with spherical capsules, produced from the same material (Donatan S. et al, 2016).

As already discussed, calcium carbonate (CaCO_3) particles are useful for the making of microparticles in drug delivery systems, because they have low synthesis costs, the method to make the particles is not difficult, the particles are very porous so they are easy to load, it is biocompatible, it is not toxic and has mild decomposition conditions (Donatan S. et al, 2016; Parakhonskiy B. et al, 2015). Other applications of CaCO_3 are as templates for the assembly of microparticles built by the layer-by-layer technique (LbL). It is possible to load these particles with proteins and especially enzyme-catalysed reactions are important, due to the possibility of a high loading capacity retaining the microcapsules and preserving their catalytic activity (Donatan S. et al, 2016). The last years, the use of proteins as therapeutic compounds is increasing for the treatment of diseases and tissue repair systems (Yilmaz Z. E. et al, 2016). The disadvantages of the CaCO_3 cores are their high polydispersity and non-spherical shapes, therefore aggregation and stability can be an issue (Delcea M. et al, 2011; Parakhonskiy B. V. et al, 2014a). These parameters can be altered by changing the concentration, adding a solution with high viscosity or make use of the ultrasound or magnetic stirring. By lowering the concentration, the particles will be smaller, because of the smaller chance of aggregation. Also by magnetic stirring or by using ultrasound the size should be reduced (Trushina D. B. et al, 2015).

There are three forms of anhydrous polymorphs of CaCO_3 , namely aragonite, vaterite and the very stable calcite. The three polymorphs have different characteristic properties. The most stable conformation in nature is calcite, which has a rhombohedral unit cell, found to form large single-crystal particles with often a cubic-like crystalline form. Vaterite and aragonite are thermodynamically unstable and can be stabilized kinetically or biochemically. Vaterite has a hexagonal unit cell and is usually found as polycrystalline spherical particles. It is metastable and it can easily recrystallize to stable and cubic-like calcite, when it is kept in a solution for several hours. This recrystallization to calcite is due to growing surface-to-volume ratio and enhanced solubility with decreasing particle size (Kirboga S. & Oner M., 2013; Parakhonskiy B. et al, 2012; Svenskaya Y. et al, 2016; Volodkin D. V. et al, 2010). Therefore the phase transition is energetically favourable, because vaterite particles have a higher Gibbs free energy than

calcite particles (Parakhonskiy B. V. et al, 2014a; Sawada K., 1997). The third type of the polymorphs is aragonite with an orthorhombic form, which is often found to form needle-like crystals. Aragonite is a useful biomedical material, because it is denser than calcite and can be used as an anticancer drug carrier, scaffold for bone repair and tissue engineering (Islam K. N. et al, 2011).

When the calcium carbonate precipitates from the solution, the initial composition of the different polymorphs is determined by the thermodynamics and kinetics. Calcite will precipitate at lower temperatures, in contrary to aragonite, which dominates at higher temperatures (Ogino T. et al, 1987). At higher levels of supersaturation vaterite will be precipitated.

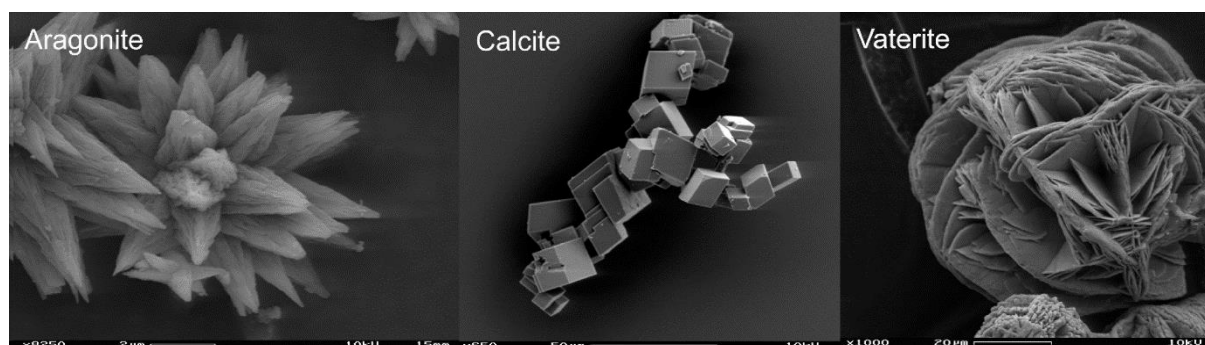


Figure 1. Different forms of calcium carbonate, namely aragonite, calcite and vaterite.

Vaterite is the most promising polymorph, because of the high porosity and surface area, which can result in high loading capacity and the potential release of therapeutic compound. It is also biocompatible, it has a high cell uptake efficiency and it can decompose rapidly under mild conditions. In other application areas, such as biomineralization or nanomaterial processing, CaCO_3 particles are used in a diverse range of shapes. To obtain vaterite it is required to use a supersaturated salt solution, with an optimal temperature between 20°C and 50°C . The control of the size of the particles is very important for further use in the biomedical sector, because the particles should be small enough for blood circulation. The formation of vaterite is simple, where sodium carbonate (NaCO_3) and calcium chloride (CaCl_2) are mixed and precipitated. The shape of the particles can be controlled by the ratio of the salts NaCO_3 and CaCl_2 , but also by adding ethylene glycol (Donatan S. et al, 2016; Parakhonskiy B. V. et al, 2014a; Trushina D. B. et al, 2015). Various inorganic and organic additives, especially those with carboxylic, phosphonate, sulfonate, hydroxyl, carboxylate and amino groups, are responsible for the vaterite morphology. By changing the concentration of the additive, molecular weight and the number of functional groups will control the growth rate, the crystal habit and stability, particle size and surface morphology. Currently vaterite is being actively used in bone implants, abrasives, cleaners and absorbers, but also for encapsulation and drug delivery (Trushina D. B. et al, 2014).

4.1.1.1 The different shapes of CaCO_3 particles

Various morphologies of CaCO_3 particles have been reported, namely isotropic, which are spherical and cubical, and anisotropic, which are elliptical and star-like, particles. The surface morphology, crystallinity, porosity and loading capacity of the resulting CaCO_3 particles are

controlled in function of the reaction time, the concentration of the initial salt solutions, the solubility of salts and the mixing speed. Also, the addition of ethylene glycol can be a parameter.

Spherical shaped CaCO_3 particles are obtained, when the two salts are mixed in equal amounts. Elliptical CaCO_3 are created when nonequimolar concentrations of two salts are used. Star-like particles are believed to be formed, because of the aggregation of vaterite nuclei, which is the result of the competition of the forming of nuclei and crystal growth. These particles have a larger surface area, than the spherical or elliptical particles (Parakhonskiy B. V. et al, 2014a). If high initial concentrations of salts are used, then there will be the formation of spherical, elliptical and rhomboidal CaCO_3 particles. For synthesis in nonequilibrium conditions with a low ethylene glycol (EG) concentration, the shape of the CaCO_3 particles transforms to a star-like morphology and if the concentration of calcium ion is ± 10 times lower than that of carbonate ions, there will be the formation of elongated distorted ellipsoidal. Spherical particles were obtained when the concentration of carbonate ions is ± 10 times lower than that of calcium ions.

EG has a high viscosity, so the solution becomes more viscous, leading to a lesser movement of ions, thus reducing the size and the solubility of CaCO_3 particles. EG prevents the recrystallization of CaCO_3 particles from spherical vaterite to cubic-like calcite. The addition of EG to the solution reduces the transformation energy and the rate of the recrystallization process (Donatan S. et al, 2016; Parakhonskiy B. V. et al, 2014a). At low EG (25%) and relatively high salt concentrations (1 M) spherical particles are obtained, but these showed a strong tendency to aggregate. This could be caused by the high amounts of salts, present at the start of the reaction in a small local volume. By increasing the EG concentration or decreasing the salt concentration, agglomeration can be avoided, while obtaining separate particles. The size of particles obtained at a higher percent of EG are smaller than those synthesized at a lower content of EG (Donatan S. et al, 2016). If there is an increase in EG to 50%-80% in the reaction medium, the density will increase and the stability of precipitated CaCO_3 particles will be reduced. A high concentration of carbonate ions leads to the formation of anisotropic rhomboidal or ellipsoidal geometries. In contrary a low concentration results in isotropic spherical particles (Donatan S. et al, 2016).

Another approach to control the phases and morphology of CaCO_3 is by adding additives, such as water-soluble additives and copolymers (Parakhonskiy B. V. et al, 2014a).

4.1.2 Liposomes

Liposomes are bilayer vesicles, these mostly consists of self-assembled natural and synthetic lipid molecules (Discher D. E. & Eisenber A., 2002) and they are effective systems for enzyme microencapsulation, because they can contain water-soluble enzymes within their aqueous confinement (Walde P. & Ichikawa S., 2001). They are frequently used in controlled drug delivery (Discher D. E. & Eisenber A., 2002; Park B. et al, 2010; Ruyschaert T. et al, 2004) and for encapsulating enzymes in biosensing applications. They are the most common and well-investigated nanocarriers for targeted drug delivery. Depending on the used method, they can

form unilamellar vesicles, that contains one bilayer, multilamellar vesicles, that contains more bilayer or multivesicular vesicles, that consists of multiple bilayer shells within one vesicle (Walde P. & Ichikawa S., 2001).

There are four types of synthesis methods, namely liposome preparation from dried lipid film by the addition of enzyme solution and shaking. The dried lipid film is prepared by solvent evaporation of an organic amphiphilic solution. A second type of method is a reverse-phase evaporation starting from emulsions from which the organic phase removed by evaporation. A third method is liposome preparation using micelle-forming detergents, that are removed from the lipid containing solution by dialysis and the fourth method is based on the microinjection of dissolved lipids into an enzyme solution (Rother C. & Nidetzky B., 2014).

All these methods have potentially adverse effects on enzyme stabilisation due to sonification, cycles of freezing and thawing, extrusion or contact with organic solvents. Additionally, the observable activity of a liposome-based enzymatic microcapsule depends on how effective the mass transfer across the membrane of the liposomal vesicle is. The permeability and permselectivity of liposomes can be influenced to some extent by using physical or chemical methods (Walde P. & Ichikawa S., 2001), such as the use of magnetic fields (Ramundo-Orlando A. et al, 2000), detergents (Yoshimoto M. et al, 2002), insertion of membranes porines, that will serve as size-selective filters. Another characteristic of liposome is their low exhibition of process stability, due to a low durability and resistance to stress, such as osmotic pressure and mechanical forces. By the use of temperature (Hotz J. & Meier W., 1998) or UV-induced (Graff A. et al, 2001) cross-linking polymerization in the hydrophobic membrane interior (Graff A. et al, 2001) can improve this stability. Finally the entrapment efficiency depends mainly on the lipid concentration, that is used during the encapsulation step (Walde P. & Ichikawa S., 2001).

In this thesis, the first method will be used. Various methods will start from a dried lipid film. This is advantageous, because direct contact between the enzyme and the organic solvents will be avoided, so protein denaturation is prevented (Mozafari M. R. et al, 2008; Walde P. & Ichikawa S., 2001). The amphiphilic molecules, that later constitute the liposomes, are dissolved in an organic solvent, such as chloroform. Next, the solvent will be removed at an elevated temperature or reduced pressure. Hereafter an aqueous enzyme solution is added and under intensive shaking, to desorb the dried lipid film multilayers from the solid surface of the vessel used, the formation of multilamellar vesicles occurs. These vesicles have typically heterogeneous sizes and the number of lipid layers can vary considerably. These multilamellar vesicles can undergo further modification using different procedures, such as repeating freezing and thawing. This will increase the relative abundance of multivesicular vesicle structures. Another procedure is sonification, which will result in the formation of unilamellar vesicles (Walde P. & Ichikawa S., 2001).

4.1.3 Red Blood Cells and Red blood cell-like capsules

Liposomes have a limited stability and a low permeability for polar molecules, but they are already used as drug delivery systems in pharmaceuticals and cosmetics (Lasic D. D., 1994).

Microcapsules formed by LbL from polyelectrolytes are an improvement, because they are permeable to small polar molecules and resistant to chemical and physical influences (Bäumler H. et al, 2000; Caruso F. et al, 1997). Liposomes and microcapsules composed from polyelectrolytes are limited by their spherical shape, which precludes producing capsules with anisotropic properties. Biological cells are more interesting because of their large variety in shapes and sizes.

The encapsulation of these cells or sub-cellular elements by itself have interesting applications in biotechnology and immunology, because it would provide cells or element protection against external influences and allow their compartmentalization. The main requirement for successful polyelectrolyte layer growth with LbL on a template is a sufficiently high electric charge on the substrate surface. Most particles from biological origin have already a pronounced surface charge density, but the problem with biological templates is their limited membrane stability. Strong interactions with the adsorbing polyelectrolyte molecules can lead to membrane rupture and breakdown of the template structure. To stabilize for example red blood cells (RBC), glutardialdehyde can be used, which will form cross-linked haemoglobin and will prevent osmotically-driven haemolysis (Neu B. et al, 2008). Another disadvantage of this carrier is the complex structure of the biological surface, where the negative surface charge is largely provided by sialic acid residues attached to glycoproteins. Hence, the surface charge is non-homogeneously distributed in a layer of several nanometres thickness (Donath E. et al, 1996; Donath E. & Voigt A., 1986; Sharp K. A. & Brooks D. E., 1985). So, it is possible that the first layers of adsorbing polyelectrolytes do not fully compensate for this spatially-distributed surface charge of the cell surface. This leads to a reversal of the surface potential only from the third layer onwards (Neu B. et al, 2008), in comparison to for example alternating adsorption onto charged latex particles, which always results in a reversal of the surface charge, independently of the layer number (Donath E. et al, 1997). The resulting microcapsules are exact copies of the biological template, exhibit elastic properties and have a permeability which can be controlled by experimental parameters (Neu B. et al, 2008).

RBCs have several properties, that make them interesting drug carriers. They are biodegradable and they can circulate for a long period of time. They can easily be handled by means of several techniques for the encapsulation of different molecules, without affecting their morphological, immunological and biochemical properties. Also, they have a large volume available for the encapsulation of drugs. RBCs can protect the encapsulated substance from premature inactivation and degradation and protect the organism against the toxic effects of the drugs. Finally, they can act as active bioreactors due to the presence of several enzymatic activities, that can convert selected prodrugs into diffusible active drugs (Magnani M. et al, 2002).

Any drug, such as peptides, nucleic acids, and other drugs, can potentially be encapsulated into RBCs. However, not all molecules are suitable because rapid leakage through the red cell membrane, molecules may be toxic for the cell itself. Also some enzymes, such as ALP, are produced by the RBCs, thus not interesting for some experiments (Biagiotti S. et al, 2011).

The encapsulation of the RBCs can be achieved by direct encapsulation of membrane-diffusible drug molecules or by the internalization of impermeant prodrugs susceptible to be metabolically converted into diffusible active drugs.

RBCs have a unique biconcave discoidal morphology and has sophisticated biological functionalities (James J. P. et al, 2012), such as the flexibility to squeeze through capillary vessels, the ability to circulate long-term in human body and the ability to deliver oxygen, all of which are made possible by their special physical properties and chemical composition. Especially the ability to deform and squeeze is important for the circulation in mammals, hereafter the vesicles recover to their initial shape after passing through capillaries (Chasis J. A. & Mohandas N., 1986).

To mimic this flowing character of the RBCs in blood capillaries of a smaller size, it is important to fabricate microcapsules with a biconcave discoidal morphology. This will prove a favourable surface-area-to-volume ratio, which allows the RBC's to undergo deformation, while maintaining a constant surface area (Chasis J. A. & Mohandas N., 1986). The templates will determine the morphology and size (Shchepelina O. et al, 2010) and Ca(OH)_2 is hereby very interesting. Although pure Ca(OH)_2 is prismatic in shape (Hardikar V. V. & Matijevic E., 2001), the presence of dextran sulphate (DS) in the reaction solution will result in particles with a biconcave discoidal morphology (She S. et al, 2013). The deformation of these particles in microcapillaries is mainly due to the hollow structure and good elasticity of the capsule wall, which facilitates the recovery after the liberation of the microcapillary (She S. et al, 2013). This deformation is different from other RBC-mimicking particles, such as discoidal poly(lactic-acid-co-glycolide) (PLGA) (Doshi N. et al, 2009), 2-hydroxy ethyl acrylate hydrogel particles (Merkel T. J. et al, 2011) and poly(ethylene glycol) (PEG) particles (Haghooie R. et al, 2010). PLGA and 2-hydroxy ethyl acrylate hydrogel particles will be stretched (Doshi N. et al, 2009; Merkel T. J. et al, 2011) and the PEG particles prefer to bend instead of stretching and keep their length constant in the constriction (Haghooie R. et al, 2010). These deformations can still be different from the deformation of RBC's, because RBC's are filled with haemoglobin (Hb) (She S. et al, 2012). So, after optimization of the chemical composition and wall structure, the RBC-like capsules can be filled with osmotically active drugs. Another important feature of RBCs is that they carry and release oxygen, so it is important that RBC-like capsules have the capacity of binding and releasing oxygen. This can be achieved by the assembly of additional layers of Hb onto the RBC-like capsules (Duan L. et al, 2007).

4.1.4 Poly(lactic-acid-co-glycolide) particles

Poly(lactic-acid-co-glycolide) (PLGA) is of considerable interest to use as a base material for biomedical applications because of its biocompatibility, it is approved for clinical use in humans by the U.S. Food and Drug Administration (FDA), the biodegradation rate is tailored depending on the molecular weight and the copolymer ratio, it has potential to modify surface properties to provide better interaction with biological materials and it is suitable for export to countries where implantation of animal-derived products is unpopular (Gentile P. et al, 2014).

4.2 Loading

The loading of particles comprises adsorbing molecules onto adsorbents or inside the capsule. For drug delivery, the loading of molecules inside the capsule is of utmost importance. There are various methods to achieve this. Firstly, there is “true” encapsulation, where the encapsulated protein is entrapped in the interior of the capsules. This can be achieved by reversible shrinking and expansion by pH and light. When there is an increase in pH of the solution, the size of the pores will increase and the molecules will penetrate the capsules. When there is a decrease in pH the process will be reversed and the pores will close and entrap the molecules. For encapsulation with the use of light, the use of special molecules, such as azobenzene molecules, is required. When there is an exposure to light, the molecules will undergo a transition of cis- to trans-configuration, which will close the pores and thus entrap the molecules. Another way to achieve this is by irreversible shrinking by temperature and salt concentration, which has an important effect on the morphology of polyelectrolytes. When a critical threshold is surmounted, the interplay between hydrophobic and electrostatic interactions induces irreversible shrinking. This method will produce mechanically strong capsules (Skirtach A. G. et al, 2011). A second method is co-precipitation, where the loading molecules are loaded on a core material before coating. The molecule will be administered to the core material or at the same time as the synthesis of the core (Petrov A. I. et al, 2005).

The size and shape play an important role in the loading capacity of particles. The shape influences its morphology, which affects the loading capacity and the catalytic activity. An increase of the EG concentration enhances the porosity and as a result the protein loading capacity (Donatan S. et al, 2016). Proteins are large molecules and the immobilisation in the pores depends on the particle type and the ratio of external and internal surfaces, but it will mostly be adsorbed on the external surface. Rhomboidal calcite particles, such as calcite, have the smallest surface area and thus the smallest loading capacity. This is due to their largely nonporous nature. In contrary star-like particles exhibit a better protein loading capacity, because of their external surface (Donatan S. et al, 2016). The size of particles affects the loading, smaller particles possess higher loading capacity than larger ones for the same weight of material (Parakhonskiy B. V. et al, 2014a).

The enzymatic activity is proportional to the loading capacity, but not all molecules contribute to the activity. The activity of the enzymes encapsulated in rhomboidal particles is the lowest, consistent with the lowest loading capacity of these particles. Nevertheless, the loading capacity of star-like particles is slightly higher, but the enzyme activity is significantly higher, because of the larger roughness and surface area compared to spherical and elliptical particles of comparable sizes. Many molecules are located on the surface, without penetrating the particle. However, enzyme molecules can enter inside the porous structure of elliptical particles. This will slow down the release of the reaction product molecules (Donatan S. et al, 2016).

4.3 Encapsulation

A substance may be encapsulated for a number of reasons, for example for the protection of reactive material from their environment, for safe and convenient handling of the materials

which are otherwise toxic or noxious, for taste masking and modification of physical properties of the drugs (Singh M. N. et al, 2010). The cores will be covered with polymers to attain capsules, which can contain several molecules. These polymers include polyelectrolytes (Sukhorukov G.B. et al, 1999), proteins (Caruso F. & Möhwald H., 1999), deoxyribonucleic acid (DNA) (Vinogradova O. I. et al, 2005), lipids (Moya S. et al, 2001), viruses (Delcea M. et al, 2011; Yoo P. J. et al, 2006), biocompatible polyions (Itoh Y. et al, 2004), charged golden nanoparticles, dendrimers.

While selecting a polymer the product requirements, such as stabilization, reduced volatility, release characteristics, environmental conditions, etc. should be taken into consideration. The polymer should be capable of forming a film that is cohesive with the core material and should be chemically compatible and non-reactive with the core material and provide the desired coating properties, such as strength, flexibility, impermeability, optical properties and stability (Singh M. N. et al, 2010).

There is a broad spectrum of approaches to encapsulate substances in the capsule interior and to release them at the specific target by external stimuli (Delcea M. et al, 2011).

4.3.1 Layer-by-layer structures

Polymeric multilayer capsules assembled with the layer-by-layer (LbL) technique are promising candidates for more complex tasks of storage, encapsulation and release. The mechanical stability, elasticity, morphology, biocompatibility, permeability and surface characteristics can be easily adjusted. Polyelectrolyte multilayer (PEM) capsules are multifunctional and various stimuli can affect and control their properties (Delcea M. et al, 2011). Polymeric multilayer capsules are an important class of vehicles, often designed for mimicking naturally occurring delivery systems, in contrast to nano- and microparticles, liposomes and red blood cells (Donatan S. et al, 2016). The main properties of the polymers depend on their molecular weight, the persistence length and grafting ratio/charge density of functional groups. These parameters in turn determine the melting temperature, their thermal properties, hydrodynamic radius and configuration.

This technique offers flexibility of design and multifunctionality and they can be used in a broad range of drug delivery applications. It is based on the sequential adsorption of oppositely charged polyelectrolytes on a preformed charged template core, that is chemically dissolved after the coating process (Donatan S. et al, 2016; Rother C. & Nidetzky B., 2014). Another possibility for layer assembly is to spray the dissolved polyelectrolytes onto the core (Rother C. & Nidetzky B., 2014). This method appeals to the fact, that the polyelectrolyte multilayer shell is permeable to small molecules and ions, used to dissolve the core and the shell impermeable to larger molecules, that are encapsulated (Skirtach A. G. et al, 2011). Often the combination of weakly negatively charged polystyrene sulfonate (PSS) and strongly positively charged polyallylamine hydrochloride (PAH) are used (Rother C. & Nidetzky B., 2014).

As discussed in 4.1 there is a variety of inorganic and organic templates, that can be used for the fabrication of capsules, such as MF, PS, NP, PLA, CaCO₃ cores, silica particles and cells

(Delcea M. et al, 2011). The choice of the core is very important in producing efficient hollow capsules, because the properties, such as size, shape and ease of removal, will dominate the properties of the capsules (Itoh Y. et al, 2004).

The LbL structure preparation can be divided into direct and indirect encapsulation methods, as shown in Figure 2. Direct methods involve the incorporation of the enzyme into a solid porous structure such as mesoporous silica (Yu A. et al, 2005) or CaCO₃ (Petrov A. I. et al, 2005; Volodkin D. V. et al, 2004), by either adsorption or co-precipitation. Next the cores will be surrounded by polyelectrolyte layers. Finally CaCO₃ within the microparticles can be easily decomposed by the addition of EDTA at a neutral pH, so the size of the microcapsules depends on the size of the core (Volodkin D. V. et al, 2004). Another method for direct enzyme encapsulation within the LbL structures is the use of a colloidal core, which consists of the enzyme directly in a crystalline (Trau D. & Renneberg R., 2003) or in an aggregated (Balabushevitch N. G. et al, 2001) form. This method is very difficult due to the high solubility of the enzymes. In indirect methods of LbL structure formation, the enzyme is absent during the preparation and a sacrificial core, such as MF (Balabushevitch N. G. et al, 2003; Ghan R. et al, 2004; Tiourina O. P. & Sukhorukov G.B., 2002), CaCO₃ (Volodkin D. V. et al, 2003), polystyrene and silica (Schuetz P. & Caruso F., 2003), will be used, that will be dissolved later and hollow capsules are obtained. Some cores, such as polystyrene and MF cannot be removed completely (Skirtach A. G. et al, 2011; Volodkin D. V. et al, 2004). This partial dissolution leads to microspheres, which also can take up enzymes upon incubation (Sakr O. S. & Borchard G., 2013). Hereafter the pores should be opened, so the enzymes can diffuse into the capsules. This can be achieved by reversible expansion by pH increase (Ghan R. et al, 2004; Tiourina O. P. & Sukhorukov G.B., 2002), but there are also other methods that can be used. These are discussed further in 4.4.

These capsules can be affected by certain stimuli to control the size of the capsules and the loading or release of the molecules. This is a result of the molecular weight, flexibility and density of charged groups of the polymers (Glinel K. et al, 2002).

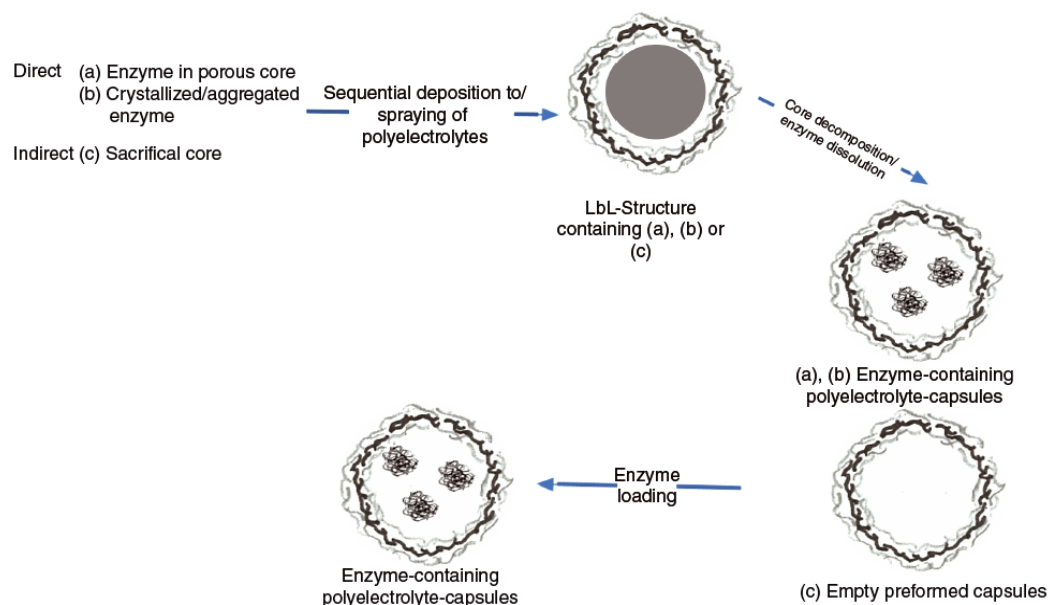


Figure 2: Schematic description of LbL-capsule synthesis by direct (a and b) or indirect methods (c). Alternate layers of oppositely charged polyelectrolytes (grey and black layers) are assembled on a core by sequential deposition or spraying. Enzyme-containing cores (a) and sacrificial cores (c) are decomposed afterward, followed by enzyme loading for (c). Crystallized enzymes are dissolved (b). The final result in all preparation methods is a polyelectrolyte-shell encapsulating enzymes in its confinement (Rother C. & Nidetzky B., 2014).

To achieve the assembly of polyelectrolyte multilayers with the use of sequential adsorption, the non-adsorbed excess polyelectrolyte has to be removed by a membrane filtration (Voigt A. et al, 1999) or a cycle of centrifugation and resuspension (Manning G. S., 1977). The membrane filtration provides the highest quality of microcapsules, because of the minimal particle aggregation during the total preparation process of adsorption and washing cycles and because this method has a high adaptation capacity to meet all the requirements of a great variety of chemical and colloid chemical systems (Voigt A. et al, 1999).

An important factor is the number of layers, because capsules with an even layer number and a balanced ratio between positively and negatively charged monomers show a heat-induced shrinking and an increase in wall thickness. Hereby is a solid sphere for high incubation temperatures or long incubation times achieved. The shrinkage is caused by the decreased water/polyelectrolyte interface and it will be less pronounced when there is an increase in layer number, due to a higher layer thickness and thus more material should be rearranged. Capsules with an odd number of layers and an excess of positive charges will swell with the increase in temperature until it ruptures, because their wall will be too thin to keep integrity. This is caused by the trend of the multilayers to increase the mutual distance between charges, so the tendency to reduce the polymer/water interface is exceeded by the unbalanced ratio between the polyelectrolytes (Köhler K. et al, 2005).

4.3.2 Alginate capsules

Alginates are linear copolymers of 1-4 linked β -D-mannuronic acid (M) and α -L-guluronic acid (G). Along the chain with homopolymeric regions of M and G are arranged in a block-wise pattern, interspaced with regions of alternating structures (Haug A. et al, 1966). The physicochemical properties, such as the affinity to cations, gelling properties and chain stiffness, of the polymer is dependent on the ratio and the order of G and M units. Alginates form gels with divalent cations, such as Ca^{2+} , that preferentially bind to the G-blocks in the alginate (Kohn R. & Larsen B., 1972; Stokke B. T. et al, 1993), thus the length of the G-blocks is the main structural feature contributing to gel formation (Skjåk-Braek G. et al, 1986; Smidsrod O. & Haug A., 1968). Commercially, this is available as a sodium salt (NaAlg). Alginate is frequently employed due to its biocompatibility and good morphological and mechanical properties (Raj N. K. K. & Sharma C. P., 2003). There is a tremendous interest in alginate based hydrogel materials, because of their biocompatibility, relatively low cost and low toxicity (Lee K. Y. & Mooney D. J., 2012). Moreover they are suitable for many biological components including cells (Blandino A. et al, 2000; Husain Q. et al, 1985; Kierstan M. & Bucke C., 1977; Srivastava R. et al, 2005), due to the relatively inert aqueous environment within the matrix, the mild room temperature encapsulation process, high gel porosity allow high diffusion rates of

macromolecules (Kikuchi A. et al, 1997; Strand B. L. et al, 2008) and the ability to control this porosity with simple one-step coating procedures. It is used in the biotechnology industry as a thickening agent, a gelling agent and a colloidal stabilizer (Amsden B. & Turner N., 1999; Gåserød O. et al, 1998; Liu L. et al, 1997; Thu B. et al, 1996). The gentle and cell friendly mechanism of gelation has led to extensive use in medicine, including cell therapy and tissue engineering applications (Melvik J. E. & Dornish M., 2004).

Often CaCO_3 particles are included in the alginate beads, which are soluble in acidic aqueous media and less soluble in neutral or alkali media, so when there is contact between the bead and an acidic medium, the CaCO_3 will be leached out, leaving a void within the beads (Han M. R. et al, 2007). Other advantages of CaCO_3 microparticles are the low cost, biocompatibility (Parakhonskiy B. V. et al, 2013), mild decomposition conditions (Svenskaya Y. et al, 2013) and porous structure (Trushina D. B. et al, 2015; Volodkin D. V. et al, 2003). Due to the porosity a variety of molecules can be incorporated, such as insulin (Volodkin D. V. et al, 2010), oxidised glucose (Stein E. W. et al, 2006), therapeutic enzymes (Yashchenok A. et al, 2010), photodynamic dyes. These CaCO_3 can't easily be used by itself, due to its instability in water based solutions and weak protection of loaded materials (Svenskaya Y. et al, 2013). Therefore protection is needed by encapsulation (Sergeeva A. et al, 2015), which is currently achieved by using electrostatic deposition of a number of polyelectrolytes, which is an expensive and time consuming technique (Lengert E. et al, 2016).

An example of alginate based hydrogels, are silver alginate microspheres. This is a simple fabrication method, where the pores of porous calcium carbonate microparticles are filled with sodium alginate. The gelling of the sodium alginate is achieved by the presence of silver ions. Finally by adding ascorbic acid, it initiates the expansion of silver particles and the dissolution of calcium carbonate, which results in hollow plasmonic microspheres (Lengert E. et al, 2016). This is interesting because these are highly effective Surface enhanced Raman scattering (SERS) structures. SERS is a versatile and powerful technique for rapid identification and sensing of different analytes, such as drugs, pollutants, biomolecules, microorganisms and cancerous cells. However, SERS depends strongly on material, morphology and the incident light for the excitation of surface plasmons. Therefore, the unique properties of silver are very interesting, such as the localized plasmon resonance and the capability to concentrate an electromagnetic field at the interparticular junctions. Silver is more interesting than gold, because of its stronger resonance and smaller imaginary part of the refractive index in the resonance frequency (Schlücker S., 2011).

Another way to form an alginate-based hydrogel is through gelation in an aqueous solution, with the aid of divalent cations, such as Ca^{2+} and Mg^{2+} (Ouwere C. et al, 1998). Ionic bonds will occur by electrostatic interactions between the alginate and the Ca^{2+} , which leads to the formation of mechanically stable networks (Melzoch K. et al, 1994). CaCO_3 will be included in the alginate beads and when there is contact with an acidic medium, the CaCO_3 will be leached out. This will leave void volumes within the beads (Han M. R. et al, 2007).

4.4 Release

There are three main types of stimuli, that will influence the release, namely those based on manipulating physical principles, affecting chemical composition or influencing biological reaction (Wuytens P. et al, 2014). These can be related to the properties of polymers, the interaction with external fields or actions and the functions of molecules (Delcea M. et al, 2011).

When using chemical methods, the locality of the action is very important, because all chemical stimuli possess a non-local character, so the effects that are transferred through a solution and act on the whole network of polymers, will affect the whole capsule. An example of a chemical methods is by controlling the pH of the solution, this will result in the repulsion of the prevailing charged groups and tends to increase the spacing between polymers. This can be used for encapsulation by closing the pores of the capsules or for release, so the encapsulated materials can leave the interior of the capsules (Liang K. et al, 2014). In vivo the different pH values of different organs can act as a trigger for the release. The advantage of this method is that reversible permeability is possible, however there will be weak mechanical properties and the pH in biological applications cannot be changed. Another chemical method is by changing the salt concentration, because the effect of salt on polyelectrolyte multilayer capsules, takes place on the whole surface of the microcapsules. Salt ions will increase the osmotic pressure, so the interaction of the polymers forming the polyelectrolyte multilayer shells will loosen, which will lead to disintegration of microcapsules and the release of loaded materials (Dong W. et al, 2005). The decrease of the interaction between polymers can be used upon addition of a high salt concentration for the fusion of capsules (Zhang R. et al, 2010). The ionic strength affects many capsules, but in biological applications the salt concentration needs to remain constant. Solvents are frequently used for manipulating, forcing and encapsulating molecules (Lvov Y. M. et al, 2010). Finally, there are electrochemical methods for release, where for example polypyrrole is a good agent for reducing the permeability of microcapsules. This has a high potential for sensing applications and it has the possibility of using electrical field pulses to induce release. However there is only a limited volume of applicability, because it has to be in the vicinity of an electrode (Andreeva D. V. et al, 2006).

There are also a variety of biological methods for release, where the microcapsules will be affected by proteins, peptides or other biologically relevant molecules or by enzymatic degradation (Ghan R. et al, 2004). For the encapsulation of enzymes there are a variety of possibilities, such as enzyme incorporation into polyelectrolyte multilayers (Caruso F. et al, 2000). Another effective enzyme container are alginate particles combined with polyelectrolyte coatings (Srivastava R. et al, 2005). Controllability of release is essential, by decreasing the number of layers in the polyelectrolyte coating (Marchenko I. et al, 2012) or by using controllable cross-linking (Liang K. et al, 2012), the release can be slowed down. By using enzymes, the capsules shell can be destroyed, with the consequence of the permanently release of their molecules. This is for example interesting in the oral administering of protein and peptide drugs. Normally this is restricted to intravenous administration, because of the easy hydrolysis in the acidic stomach. By using disulphide cross-linked nanocapsules the physical

stability against acidic pH conditions are enhanced, compared to un-cross-linked ones. An often-used trigger to disassemble the capsule with an external stimulus or in an intracellular environment is glutathione reduction, releasing encapsulated substances. Glutathione (GSH) is a tripeptide in blood, in extracellular matrices and on the cell surface, the proteins are rich in stabilizing disulphides because of a relatively high redox potential due to the low concentration of GSH. Inside the cells the concentration GSH is higher, thus maintaining a highly reducing environment inside cells (Shu S. et al, 2010).

Lastly there are also physical methods, by controlling the temperature the stability and permeability of polyelectrolytes can be controlled. By using laser-light, UV and microwave radiation, the temperature can be increased locally, which will modify the permeability (Kolesnikova T. A. et al, 2010; Zhou J. et al, 2014). Another promising method is based on the use of ultrasound due to its effective non-invasive, local action and as it is already approved and commonly used for detection and imaging in the medical sector. The integrity and permeability of the microcapsules depend on the duration and power of ultrasonic treatment and on the shell thickness and composition. The fabrication of microcapsules with high ultrasound sensitivity is achieved by embedding ZnO nanoparticles in the polyelectrolyte multilayer shell (Kolesnikova T. A. et al, 2010). An ultrasound wave undergoes viscous and thermal absorption and scattering in the surrounding medium. Through the collapse of generated microbubbles and the resulting shear forces, there will be an occurrence of cavitation, which will cause the destruction of polyelectrolyte capsules (Skirtach A. G. et al, 2006). Permeability control can also be achieved by embedding ferromagnetic nanoparticles into the capsule walls. An external oscillating magnetic field can modulate the capsules and thus control the release of substances in the capsules. The problem by using a magnetic field is the long exposure time and the relatively strong magnetic field to permeate the capsule, which will result in an increase in temperature (Lu Z. et al, 2005). Another physical method is mechanical deformation, where pressure is applied on the microcapsules, which will induce the release (Wuytens P. et al, 2014), but can also be achieved by stretching (Vogt C. et al, 2012).

Metastable carriers, such as vaterite, undergo a crystal phase transition from vaterite to calcite, during which the loaded substance is released almost completely. This mechanism allows a control of the payload delivery time via the properties of the particles and the environment. The recrystallization process starts when vaterite particles are immersed in a water-based solution. This will slowly turn into the calcite phase, because of the dissolution and ionization of the external layer of vaterite. Scheduled administration and time-consuming transport in drug delivery is possible before reaching the release site, where it has advantages over common carrier systems, which exhibit a burst release directly after suspension. Results of biocompatibility tests showed no indications of cytotoxicity and no influences on viability or metabolic activity. Cellular uptake experiments demonstrated fast penetration into cells (Kolesnikova T. A. et al, 2010).

4.5 Enzymes

Proteins present a great source of potential therapeutics, because the structure-function relationship plays a critical role in the biological activity and the potency of the protein to the target receptor (Leader B. et al, 2008). It presents also an opportunity in terms of harnessing protein therapeutics to soften diseases. These protein therapeutics have several advantages over small-molecules drugs. Firstly, proteins comprise highly specific and complex functions, which cannot be mimicked with chemical compounds. Next, because of the specificity there is less potential for interference with normal biological processes and it will cause less adverse effects. Also, because the body naturally produces many of these proteins, these agents are often tolerated and are less likely to cause immune responses. A fourth advantage is that protein therapeutics could provide an effective replacement treatment, if the disease is caused by a mutation or deleted gene. Lastly there are also financial advantages: the FDA approval time of protein therapeutics may be faster than of small-molecule drugs and as the proteins are unique in form and function, companies are also able to obtain far-reaching patent protection for protein therapeutics (Leader B. et al, 2008).

In drug delivery, molecules with medical properties will be loaded in the particles. An example of an important therapeutic enzyme is L-asparaginase, which is used in certain therapies like leukaemia (Karamitros C. S. et al, 2013). Enzymes are proteins and consist of amino acids linked together by a polymer chain. These amino acids can interact with their hydrogen bonds, hydrophobic interactions and sulphite bonds. These interactions create a structure of α -helixes and β -sheets of amino acids, that will form enzymes for catalytic purposes. Enzymes are catalysts for specific reactions by binding the substrate to a binding place on the enzyme and let it react to create the product. This is why there is a growing interest in the development of novel therapeutically procedures and biotechnological processes, in which various proteins play a crucial role (Harder J. et al, 2007).

The use of therapeutic enzymes instead of chemical drugs, has its advantages for the use of drug delivery. Enzymes are more specific and efficient, in contrary to chemical oxidants, so there is less collateral damage. The use of nano- and microcarriers with proteins is a main strategy for site-specific and prolonged drug delivery, but the major challenge in protein drug delivery is the formation of the protein particles with well-defined characteristics, such as size, morphology, composition and density, which are important to achieve bioavailability with a particular administration route (Volodkin D. V. et al, 2010).

4.5.1 Alkaline phosphatase

Alkaline phosphatase (ALP) is a hydrolase enzyme, that catalyses dephosphorylation of various esters. In the human body, there is a presence of ALP, but there is especially a high concentration in the liver, bone, kidney, central nervous system, fibroblasts, endothelial and other cell types. The skeletal and liver ALP isozymes predominate, but in children the majority is of a skeletal origin (Millan J. L. & Whyte M. P., 2016; Reiss I. et al, 1996).

ALP can detoxify lipopolysaccharides (LPS), which is important because LPS contribute to the maintenance of chronic multifactorial inflammatory bowel diseases (IBDs). Examples of IBDs are Crohn's disease (CD) and ulcerative colitis (UC), where a deregulated mucosal immune response to gut derived bacterial antigens is thought to be involved (Podolsky D. K., 2002; Tuin A. et al, 2009). ALP succeeds in the dephosphorylation of one of the toxic phosphate groups of LPS (Domar U. et al, 1992).

ALP can also be used for treatment to improve the renal function in sepsis-induced acute kidney injury (AKI). The most common cause of AKI is septic shock and is associated with considerable morbidity and mortality. Currently there is no single drug approved for the treatment of sepsis-induced AKI. It is thought that the renal protective effects are related to dephosphorylation and thereby detoxification of detrimental molecules involved in the pathogenesis of sepsis-associated AKI. The endotoxin liposaccharide might be a potential candidate target molecule from the cell wall of Gram-negative bacteria. These are associated with the development of sepsis and becomes nontoxic after being dephosphorylated by ALP. Adenosine-5'-triphosphate (ATP) could also be a potential target of ALP, because it is a proinflammatory mediator released during cellular stress. This can be converted into the tissue-protective and anti-inflammatory molecule adenosine (Peters E. et al, 2014; Pickkers P. et al, 2012).

ALP is also involved in the mineralization of the bone by cleavage of phosphate from organic phosphate (Orimo H., 2010). It provokes the mineralization of hydrogels to increase their mechanical strength or render them more suitable for bone replacement applications (Filmon R. et al, 2002). The advantages of hydrogels are the injectability and exact fitting to defect sites and the ease of incorporation of cells and bioactive substances, such as growth factors or enzymes (Leeuwenburgh S. C. et al, 2010). However hydrogels are not able to mineralize and form strong interactions with hard tissues, such as bone (Leeuwenburgh S. C. et al, 2007).

Another use of ALP is in enzyme replacement therapy (ERT), for patients afflicted by hereditary metabolic diseases, in which genetic defects result in the structural defect or absence of endogenous enzymes, that are critical for metabolic pathways. These defects result in the accumulation of substrate and/or its intermediates, leading to pathological states. Hypophosphatasia is a hereditary metabolic disorder, which is caused by the deficiency of tissue-nonspecific alkaline phosphatase (TNSALP). This deficiency results in defective bone mineralization (Fraser D., 1957). The function of TNSALP is the anchoring to the plasma membrane of specialized vesicles in the osteoblasts through a posttranslationally added glucosylphosphatidylinositol moiety (GPI) located on the C-terminal end of the enzyme, forming a specialized sheltered environment in which inorganic phosphates are hydrolysed for the formation of hydroxyapatite bone crystals (Anderson H. C., 1995; Jemerson R. & Low M. G., 1987). Currently a variant of TNSALP entered clinical trials, this variant is a human TNSALP with a C-terminal extension of a human immunoglobulin G (IgG) Fc region for rapid purification and a deca-aspartate sequence for targeting bone tissues (Millan J. L. et al, 2008).

4.5.2 Human guanylate kinase

Human Guanylate kinase (hGMPK) is a phosphotransferase that transfers a phosphoryl group from adenosine-5'-triphosphate (ATP) to guanosine-5'-monophosphate (GMP), which results in adenosine-5'-diphosphate (ADP) and guanosine-5'-monophosphate (GDP) (Jain R. et al, 2015). hGMPK regulates the supply of guanine nucleotides to various signal transduction pathways (Hall S. W. & Kuhn H., 1986; Konrad M., 1992). The medicinal importance in cancer chemotherapy of GMPK is in the activation pathway of guanosine-analogue prodrug. Examples of potent antitumor drugs are 6-thioguanine and 6-mercaptopurine used for the treatment of acute lymphoblastic leukaemia and as immunosuppressive agents (Elion G. B., 1989; Jain R. et al, 2015; Miech R. P. et al, 1969; Zschocke P. D. et al, 1993). Guanylate kinase activity also required for the potentiation of antiviral drug activity in virus-infected cells (Brady W. A. et al, 1996; Sekulic N. et al, 2002).

4.6 Drug delivery

A crucial challenge faced in improving therapies is the efficient delivery and release of the drugs to a target (Timko B. P. et al, 2011). A lot of these drugs don't reach their destination and capsules seem promising for improving drug efficacy through enhanced delivery, targeting and protection. Efficient drug delivery also leads to a reduction in toxicity and the maintenance of its concentration at the target site for a sufficient period of time (De M. et al, 2008; Duncan B. et al, 2010; Peer D. et al, 2007).

There are two systems of drug delivery, namely non-covalent and covalent. Non-covalent drug delivery can include any form of transport, that does not involve a direct chemical bond to the drug. The environment of the drug ensures the stabilization of the drug until release and this has several advantages. Firstly, the drug does not have to be modified, which retains therapeutic efficacy. Next, the optimization of the transport of one drug can be applied to other drugs and these drugs can mostly be released from the capsules by changes in the local environment (Cheng Y. et al, 2010). If the drugs are encapsulated in the capsules, the pH temperature or those induced by other external stimuli are required to modify the capsules for drug diffusion.

In contrary, in covalent drug delivery the drug is covalently bound to the transport vector and it requires the direct breaking of the chemical bond. Thus, the drug is only as flexible as the linker to which it is attached, providing further control over the vector until it reaches the target. Through this linker, site specific cleavage based on enzymatic, thermal or pH induced release can be achieved, which is often not available in a non-covalent system (Doane T. L. & Burda C., 2011).

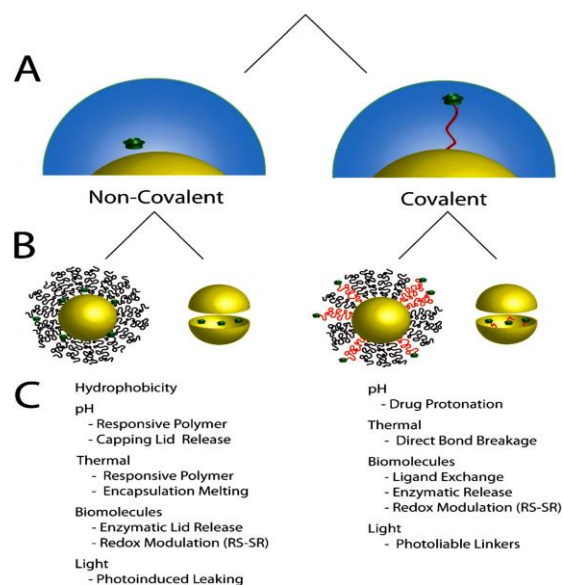


Figure 3: Covalent or non-covalent systems in drug delivery. (A) After identifying whether surface immobilized or encapsulated delivery is preferred (B), a variety of triggers can be utilized for controlled release (C) (Doane T. L. & Burda C., 2011)

Several parameters, such as hydrophobicity, pH, temperature, biomolecular reactions and light, can be used to control drug delivery. These hydrophobic and hydrophilic forces are mostly applied to non-covalently bound drugs. External changes in hydrophobicity will dictate whether the drug will be delivered efficiently. A disadvantage of this method is the risk of non-selective release of drugs before reaching the target (Doane T. L. & Burda C., 2011).

pH induced drug release is governed by the difference in physiological pH (pH 7,4) from the endosomal and lysosomal pH (pH 5-6) (Bae Y. et al, 2005). This is especially interesting in cancer specific drug delivery, because these tumour tissues are known to have a lower pH than regular tissues (Helmlinger G. et al, 1997).

Drug delivery induced by the temperature comprises changes to water-polymer interactions through heating, which allows the encapsulated drug to diffuse out of the capsule and into the target (Alarcon C. d. I. H. et al, 2005; Strong L. E. & West J. L., 2011). The release of the drug is achieved by either swelling or shrinkage of the polymer coating (Liechty W. B. et al, 2010).

In biomolecular induced drug delivery, the capsules are mainly transport agents and they are not chemically active participants in drug release. This methodology can generally be divided in ligand exchange mediated release, enzymatic release and chemical reduction based release. In surface exchange mediated drug delivery certain biological molecules are produced in excess at a target site in comparison to healthy cells (Duncan B. et al, 2010). By using enzymatic triggered drug delivery, specific therapy is possible without prior location of diseased cells (Andresen T. L. et al, 2010). Finally, cellular redox chemistry can also be an effective trigger in drug release. By using for example dithiol bonds, the environment of the cells remain reductive (Sen C. K., 1998), which will induce the breakage of the linker between the drug and the transport vector (Doane T. L. & Burda C., 2011).

4.7 Cellular uptake and intracellular release

A lot of enzymes and other proteins have the potential to being used as therapeutic agents in clinical practice. However due to the high degradability in the digestive tract and the low skin permeability, the proteins should be currently administered by multiple injections. This route is often compromised by low patient compliance and low therapeutic performance. Therefore drug delivery systems are researched for targeted delivery, sustained release and protection against degradation (Volodkin D. V. et al, 2012). Mostly the capsules will enter the cell through endocytosis, but the mechanical properties of the delivery systems are critical, because they may sustain shear forces during delivery. This can cause the unwanted release of the drug before the entering of the cell. Moreover, in endocytosis the encapsulated drugs mostly end up in the endosomes, which will be degraded by the lysosome (Bareford L. M. & Swaan P. W., 2007; Bruno B. J. et al, 2013; Delcea M. et al, 2010; Volodkin D. V. et al, 2012).

4.7.1 Mechanical stability of polymeric capsules

The mechanical properties of the microcapsules are controlled by several parameters, such as the temperature, the number of layers and the encapsulated contents (Köhler K. et al, 2005). Insufficiently stiff capsules tend to release material within or outside of the cell. Increasing the temperature results in an increasing stiffness, due to the interplay of electrostatic and hydrophobic forces which results in capsules which almost all sustain the shear stress of cellular uptake (Delcea M. et al, 2010). The shrinkage is accompanied with the densification of the polymeric shell, this leads to a decrease in capsule size and subsequently leads to an increase in mechanical stiffness (Mueller R. et al, 2005).

4.7.2 Influence of the size and shape on the cellular uptake

Various physicochemical properties, such as size (Chithrani B. D. et al, 2006; Lerch S. et al, 2013), shape (Bhaskar S. et al, 2010; Chithrani B. D. et al, 2006; Daum N. et al, 2012; Holt B. et al, 2007; Lerch S. et al, 2013; Meng H. et al, 2011; Shimoni O. et al, 2013), charge (Hühn D. et al, 2013; Javier A. M. et al, 2006), surface chemistry (Delehanty J. B. et al, 2013; Jiang X. et al, 2010; Parakhonskiy B. V. et al, 2013; Tang R. et al, 2014; Wattendorf U. et al, 2008), the aggregation state and colloidal stability (Caballero-Diaz E. et al, 2013), stiffness (Delcea M. et al, 2010) directly influences the cellular uptake, intracellular trafficking, exocytosis (Kim C. S. et al, 2014) and cytoskeleton re-organization (Wang B. et al, 2012). The effect of one of these parameters is challenging to determine, because for example the aggregation state of the particles can disclaim the influence of size and charge (Yan Y. et al, 2013). Therefore, to achieve a meaningful analysis of the size and shape, it is important that the particles are not aggregated (Hutter E. et al, 2010; Liu S. et al, 2009).

In a study it was found, that particles of various shapes are taken up by phagocytosis in alveolar macrophages (Decuzzi P. & Ferrari M., 2008), but the internalization velocity was determined by the angle between the particle and the initial contact point with the macrophage (Champion J. A. & Mitragotri S., 2006).

Also, the geometry has an influence on the velocity of endocytosis. When there is an increase in the aspect ratio, which is the ratio of the diameters perpendicular to each other, the internalization rate will also increase, except for very long fibres and wires (Parakhonskiy B. et al, 2015).

4.7.3 Intracellular release of content from capsule

Available methods for intracellular delivery include permeabilization of the membrane (Johnson J. A. et al, 1996), electroporation (Vigneron N. et al, 2004), microinjection (Neijssen J. et al, 2005) and photolysis of caged precursors (Adams S. R. & Tsien R. Y., 1993). Inside the cells, the opening of the capsules can be achieved by using infrared laser pulse and with the presence of gold nanoparticles in the walls of the capsules. These gold nanoparticles adsorb the laser energy, which causes local heating and release of the content of the capsule (Radt B. et al, 2004; Skirtach A. G. et al, 2005). Polyelectrolyte multilayer capsules, made by the alternate deposition of charged species, respond to various parameters, such as temperature, pH, sugar concentration,... and they can carry encapsulated materials. They can release these materials in response to external stimuli such as a magnetic field, light or ultrasound (Bedard M. F. et al, 2008; Gorin D. A. et al, 2006; Kolesnikova T. A. et al, 2010; Kolesnikova T. A. et al, 2008; Koyama D. et al, 2004; Lu Z. et al, 2005; Petrov A. I. et al, 2005). For a better response to these external stimuli, there can be golden nanoparticles embedded in the wall (Pavlov A. M. et al, 2011). Other methods for release are pH- and redox-responsive microcapsules, that make use of the different intra- and extracellular environments (Gao L. et al, 2012).

Besides the release of the capsule content, the content also has to quit the endosome in which the capsule undergoes cellular uptake (Bruno B. J. et al, 2013). A method to achieve this, is by pore-forming in the endosomal membrane. In general this is an interplay between membrane tension, that enlarges the pore, and line tension to close the pore (Huang H. W. et al, 2004). Some components, such as cationic amphiphilic peptides, will bind to the lipid bilayer, which leads to internal stress or internal membrane tension sufficiently to create pores (Jenssen H. et al, 2006). Another method is the proton sponge effect, which is mediated by agents with high buffering capacity and the flexibility to swell when protonated. Due to protonation, an extensive inflow of ions and water is induced, which leads to the rupture of the endosomal membrane and release of the entrapped components (Miller D. K. et al, 1983). Another mechanism the fusion with the endosomal membrane, through destabilization of the endosomal membrane by fusogenic peptides. This has an important role in cellular trafficking and endocytosis (Horth M. et al, 1991; Marsh M. & Helenius A., 1989). A final method for endosomal escape is photochemical disruption of the endosomal membrane. A few photosensitizers are primarily localized in the membrane of endosomes and lysosomes (Nishiyama N. et al, 2006; Prasmickaite L. et al, 2001). Through exposure of light, these photosensitizers will induce the formation of reactive singlet oxygen, which destroys the endosomal and lysosomal membrane, but don't affect the content that will be delivered to the cytosol (Berg K. et al, 1999; Lou P. et al, 2006).

5 Goals

5.1 CaCO₃ particles and encapsulated CaCO₃ particles

5.1.1 Loading capacity

The optimal time of incubation and the initial ALP concentration will be determined, to achieve the best loading capacity possible. This will give an indication how long the incubation should be and which ALP concentration should be used. When a more expensive enzyme is used, it is also interesting to consider the loading efficiency.

5.1.2 Stability

Recrystallization from vaterite to calcite is an interesting way to release ALP from the particles and this will start when the vaterite particles are immersed in a water-based solution. So it is interesting to understand when this process starts and how long it process will continue.

5.1.3 Activity of the enzyme loaded to the particles

After the determination of the loading capacity, it is interesting to understand how much of the loaded enzyme is active and thus accessible for the substrate.

5.2 Comparison of the liposomes with CaCO₃ particles

Liposomes are already frequently used in controlled drug delivery and they are the most common and well-investigated nanocarriers for targeted drug delivery. Thus, it is interesting to develop liposomes and load them with ALP to compare the loading capacity and the activity of the enzyme loaded to these particles with the CaCO₃ particles.

6 Material and Methods

6.1 Calcium carbonate particles

6.1.1 Formation of calcium carbonate particles

6.1.1.1 "Small" particles with size $1.150 (\pm 0.074) \mu\text{m}$

All used chemicals were purchased from Sigma Aldrich and used without any further purification. The following processing conditions were chosen: CaCl_2 and Na_2CO_3 concentrations of 0.33 M, magnetic stirring with a rotation speed of 500 rpm (2mag magnetic motion) at room temperature and reaction time of 3 hours. To prepare these particles, ethylene glycol (EG) was added to the reaction solution. Na_2CO_3 and CaCl_2 were each dissolved in 2 mL water and 10 mL EG. When the process was finished, CaCO_3 particles were precipitated by centrifugation (3000 rpm, 3 minutes). Hereafter, ethanol was added and again centrifuged. This washing procedure as executed three times. Finally, they were dried overnight at 70°C and stored in the freezer. This adjusted protocol is based on (Parakhonskiy B. V. et al, 2014b).

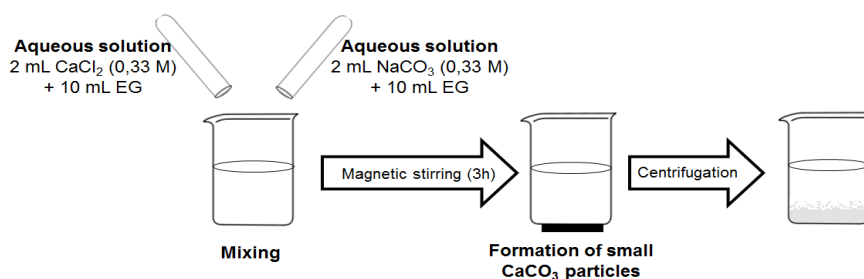


Figure 4. Chemical precipitation procedure for small particles. The reaction between calcium ions and carbonate ions with addition of ethylene glycol (EG) (in aqueous solution)

6.1.1.2 "Large" particles with size $2.307 (\pm 0.385) \mu\text{m}$

All used chemicals were purchased from Sigma Aldrich and used without any further purification. The following processing conditions were chosen: CaCl_2 and Na_2CO_3 concentrations (0.33 M), rotation speed of 500 rpm with magnetic stirring (2 mag magnetic motion) at room temperature and reaction time of 2 minutes. When the process was finished, CaCO_3 particles were precipitated by centrifugation (Sigma laborzentrifugen) at (3000 rpm, 3 minutes). Next, ethanol was added and centrifuged. This procedure was executed three times. Finally, they were dried overnight at 70°C and stored in the freezer. This adjusted protocol is based on (Parakhonskiy B. V. et al, 2014b).

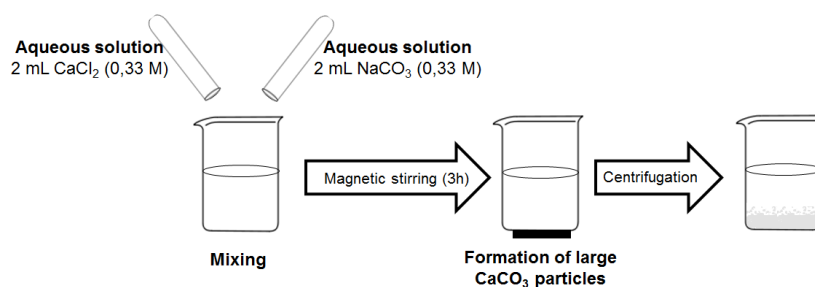


Figure 5. Chemical precipitation procedure for large particles. The reaction between calcium ions and carbonate ions (in aqueous solution)

6.1.2 ALP loading

All used chemicals were purchased from Sigma Aldrich and used without any further purification. Alkaline phosphatase (ALP) (from bovine intestinal mucosa, ≥ 10 DEA U/mg) dissolved in water is loaded in and on the CaCO_3 particles, by adding 2 mL of ALP to 20 mg ($\text{Weight}_{\text{particles}}$) of CaCO_3 particles. Two sizes of particles were tested, that have different characteristics when it comes to loading enzymes and their resulting activity. After incubation and mixing in a vortex (IKA® Vortex genius 3), the particles were isolated from the ALP solution and washed three times by centrifugation (3000 rpm, 3 minutes).

To understand the optimal mixing time and initial ALP concentration, these parameters were varied. For the optimal mixing time, samples with similar concentration, namely 5 mg/mL, were mixed for different time intervals between the range of 30 minutes up to 24 hours. Hereafter, the mixing time was kept constant, namely 2 hours, and the ALP concentration was varied between an ALP concentration of 0.5 and 10 mg/mL.

There are two methods to measure the absorbed concentration, namely the dissolution and the supernatans method. For the supernatans method, the samples are centrifugated (3000 rpm, 3 minutes) and the supernatans is removed. The absorption spectra was measured of this supernatans using the UV-VIS spectrophotometer at 297 nm. There was an ALP-curve set up at 297 nm between the range of 0,26 and 10 mg/mL ALP.

For the dissolution method, was the loading capacity and loading efficiency of the initial concentration of ALP (c_{initial}) determined by measuring the optical absorption of the particles by adding 1 mL of EDTA (MW = 372.23 g/mol, Acros organics) to the CaCO_3 particles. To calculate the absorbed concentration (c_{absorbed}) of the ALP present in the particles, an ALP curve should be set up with a dilution of ALP in EDTA with an UV-VIS spectrophotometer (UVIKON XL Secomam). The range of this curve is between 0.36 and 5 mg/mL, measured at 297 nm in the UV-VIS spectrophotometer. This ALP curve is used to determine the concentration of ALP released from the CaCO_3 particles.

The loading capacity (LC) is calculated by dividing concentration per mL by the total weight of the particles. The loading efficiency (LE) is calculated by dividing the measured concentration by the initial concentration of ALP, that was added to the CaCO_3 particles.

$$\text{LC} = \frac{(c_{\text{initial}} - c_{\text{absorbed}})}{\text{Weight}_{\text{particles}}} * 100\% \quad \text{LE} = \frac{c_{\text{initial}} - c_{\text{absorbed}}}{c_{\text{initial}}} * 100\%$$

6.1.3 Optical Microscopy

To analyse what the stability of the CaCO_3 particles is and if ALP has an influence on the stability and thus the structure of CaCO_3 particles, the particles are examined with an optical microscope. The analysis of the particles was performed with an optical microscope (Leitz Wetzlab) with a 100x oil lens. The images were taken with a colour CCD camera (Monacor) and with the computer program Pinnacle Studio 15.

6.1.4 Scanning Electron Microscopy

Particle morphology characterization was performed by using images obtained by the scanning electron microscopy (SEM). SEM measurements were performed with MIRA II LMU (Tescan) at the operating voltage of (30.00 kV) in second electron and back scattering electron mode. Magnification was ranged from 100 to 40 000 times. Samples were prepared by drying a drop of the aqueous suspension of microparticles on the silicon wafer.

6.1.5 FTIR spectroscopy

The molecular structure of the CaCO_3 particles with and without ALP were examined using Fourier Transform Infrared (FTIR) Spectroscopy (Vertex 70, Bruker). These particles were dried before the measurement. One spectrum per sample was collected in the 250 and 4205 cm^{-1} spectral range with a resolution of 4 cm^{-1} and an average of 25 scans.

6.1.6 Stability of the particles

In this procedure, the ALP loaded CaCO_3 particles were examined to determine the stability of the vaterite, how long it takes to recrystallize to calcite and what the activity of the particles is after recrystallization. For this procedure, optical microscopy and SEM images were used to investigate the recrystallization and release process. The CaCO_3 particles (20 mg) were immersed in various media (2 mL), namely in water, NaCl (Carl Roth GmbH) and phosphate buffered saline (PBS), that is composed out of NaCl (Carl Roth GmbH), KCl (Merck), $\text{Na}_2\text{HPO}_4 \cdot 2\text{H}_2\text{O}$ (Merck) and KH_2PO_4 (Duchefa Biochemie).

This was constantly vortexed (IKA® Vortex genius 3) in Eppendorf tubes. When the recrystallization of the CaCO_3 particles was completed, the particles were centrifuged (Sigma laborzentrifugen) at 3000 rpm for 3 minutes. Hereafter the ALP activity assay was performed to understand the activity of the recrystallized particles.

In this experiment, there was a variation in initial concentration of ALP, the size of the particles, the solvent where the particles were diluted and the dilution of the samples. The two-tested initial ALP concentration were 0, 0.5 and 10 mg/mL absorbed in small and large particles. These particles were dissolved in PBS, water and physiological solution.

6.1.7 Enzymatic activity measurements

To determine the amount of active ALP captured by the particles an activity assay was performed based on (Douglas T. E. L. et al, 2012). Before the activity assay, the particles were washed with ethanol and dried overnight, to remove the residual free enzyme. A weight of 1 mg of particles containing ALP was diluted in 500 μL of water. The concentration of active ALP was determined using a standard ALP activity assay, with modifications. To measure this in the microplate reader, 100 μL of the sample containing released ALP were transferred to a well of a 96 well cell culture plate. 50 μL of a substrate solution consisting of 5×10^{-3} M *p*-nitrophenylphosphate disodium salt (pNPP) (Sigma Aldrich, P5994) in 0.5 M alkaline buffer was added. This buffer was prepared by diluting 1.5 M alkaline buffer (Sigma-Aldrich, A9226) with water in the volumetric ratio 1:2. After incubation, the reaction was stopped by the addition of 100 μL of 0.3 M NaOH (Sigma Aldrich). Absorbance was measured at 405 nm with a Benchmark Plus microplate spectrophotometer (Bio-Rad). This protocol can also be performed by measuring in a UV-VIS spectrophotometer (UVIKON XL Secomam), but because of the need for a higher volume the particles were be diluted in 500 μL and next 250 μL of pNPP was added and finally 500 μL stop solution was added to stop the reaction.

In this experiment, the initial concentration of ALP, the size of the particles and the incubation time of the substrate pNPP will be varied. The four tested initial ALP concentrations were 0.5, 1, 4 and 10 mg/mL absorbed in small and large particles. In this experiment, the incubation time was varied, by adding the stop solution at different time points, namely 2, 3, 5, 8, 10 and 12 minutes. A calibration curve of ALP in water was set up with concentrations ranging from 0.05 to 3 mg/mL that served as reference. To calculate the percentage of active ALP (%active ALP) the measured concentration of active ALP (c_{active}) was divided by the absorbed concentration of ALP (c_{absorbed}).

$$\% \text{ active ALP} = \frac{c_{\text{active}}}{c_{\text{absorbed}}} * 100\%$$

6.1.8 XPS measurements

XPS measurements were performed to quantify the nitrogen on the surface in a PHI 5000 Versaprobe 2, using a monochromatic Al K α ($h\nu = 1486.6$ eV) X-ray source operating at 50 W. For each condition, 4 random points were measured on a single sample. Vacuum within the XPS analysis chamber was always kept below 10^{-6} Pa and the emitted photoelectrons were collected at an angle of 45° with respect to the normal of the sample. Both surveys and high-resolution spectra (C1s, O1s) were recorded at pass energies of 187.85 eV (0.8 eV step) and 23.5 eV (0.1 eV step) respectively. All spectra were analysed and fitted using Multipak software.

6.1.9 Toxicity test

First, 20 μL of particles (10 mg/mL) in 50% ethanol solution were deposited on the 96-microwell plate and will give a monolayer. These wells had been sterilized shortly before the experiment by adding 100 μL of ethanol to each well and then letting the ethanol evaporate. Next, the HeLa cells were brought into a 96-microwell plate with a cell density of 20×10^4 cell per well and cultivated for 24 hours with a temperature of 37°C with 5% of CO_2 . After incubation, 0.5 mL of fresh medium and 50 μL of fluorescent dye AlamarBlue (Sigma Aldrich) was added to each well. After 3 hours of incubation, the intensity of the fluorescence was measured with the spectrophotometer (Gemini XPS Microplate Reader, Molecular Devices). For each type of particles, three independent samples were measured. The fluorescent signal was normalized on the data from the control cell line, namely the cells without any additives.

6.2 Alginate particles

6.2.1 Particles synthesis

To produce silver alginate hydrogel microspheres, 10 mg of large and small CaCO_3 particles were placed in a 2 mL Eppendorf tube. Hereafter, 1 mL of sodium alginate (5 mg/mL) was injected into the tube and left under intensive agitation for 10 minutes in a shaker. This produces sodium alginate particles containing CaCO_3 (AlgCaCO_3). These particles were precipitated via centrifugation (1500 rpm, 3 minutes) and were washed in pure water. The washing procedure was repeated 3 times. Next 1 mL of AgNO_3 (0.5 M) was added to AlgCaCO_3 , which initiates cross-linking of the sodium alginate. The mixture was agitated for 10 minutes in a shaker and then precipitated via centrifugation (1500 rpm, 3 minutes) and washed with pure water. Finally, there was an addition of 5 times 200 μL of ascorbic acid (0.1 M), which initiates the growth of silver nanoparticles and the dissolving of the CaCO_3 structure. The formed microspheres were collected using centrifugation (1500 rpm, 3 minutes) and thoroughly washed.

As a control for enzyme activity in hydrogels, calcium linked alginate particles are used. To produce these, 10 mg of CaCO_3 of 10 mg of large and small CaCO_3 particles were placed in a 2 mL Eppendorf tube. Hereafter, 1 mL of sodium alginate (5 mg/mL) was injected into the tube and left under intensive agitation for 10 minutes in a shaker. This produces sodium alginate particles containing CaCO_3 (AlgCaCO_3). These particles were precipitated via centrifugation (1500 rpm, 3 minutes) and were washed in pure water. The washing procedure was repeated 3 times. Next 1 mL of CaCl_2 (0.5 M) is added to AlgCaCO_3 , which initiates cross-linking of the sodium alginate. The mixture was agitated for 10 minutes in a shaker and then precipitated via centrifugation (1500 rpm, 3 minutes) and washed with pure water. Finally, there was an addition of 5 times 200 μL of ascorbic acid (0.1 M), which initiates the growth of silver nanoparticles and the dissolving of the CaCO_3 structure. The formed microspheres were collected using centrifugation (1500 rpm, 3 minutes) and thoroughly washed.

6.2.2 Stability of the particles

In this procedure, the alginate based hydrogels are examined to determine the stability in comparison with the CaCO₃ particles. For this procedure, optical microscopy and SEM images were used to investigate the recrystallization and release process. The alginate based hydrogels (20 mg) were immersed in water (2 mL). This was constantly vortexed (IKA® Vortex genius 3) in Eppendorf tubes.

6.2.3 Enzymatic activity measurements

To determine the amount of active ALP captured by the particles an activity assay was performed. A weight of 20 mg of alginate based hydrogels containing ALP were diluted in 500 µL of water. The concentration of active ALP was determined using a standard ALP activity assay, with modifications. To measure this in the microplate reader, 100 µL of the sample containing released ALP was transferred to a well of a 96 well cell culture plate. 50 µL of a substrate solution consisting of 5 x 10⁻³ M *p*-nitrophenylphosphate disodium salt (pNPP) (Sigma Aldrich, P5994) in 0.5 M alkaline buffer was added. This buffer was prepared by diluting 1.5 M alkaline buffer (Sigma-Aldrich, A9226) with water in the volumetric ratio 1:2. After incubation, the reaction was stopped by the addition of 100 µL of 0.3 M NaOH (Sigma Aldrich). Absorbance was measured at 405 nm with a Benchmark Plus microplate spectrophotometer (Bio-Rad). This protocol can also be performed by measuring in a UV-VIS spectrophotometer (UVIKON XL Secomam), but because of the need for a higher volume the particles were to be diluted in 500 µL and thereafter 250 µL of pNPP was added and finally 500 µL stop solution was added to stop the reaction.

In this experiment the concentration of alginate, AgNO₃ and CaCl₂ is varied. A calibration curve of ALP in water was set up with concentrations ranging from 0.05 to 3 mg/mL that served as reference. To calculate the percentage of active ALP (%active ALP) the measured concentration of active ALP (c_{active}) is divided by the absorbed concentration (c_{absorbed}).

$$\% \text{ active ALP} = \frac{c_{\text{active}}}{c_{\text{absorbed}}} * 100\%$$

6.3 Liposomes

6.3.1 Particles synthesis

In these experiments 1,2-dioleoyl-*sn*-glycero-3-phosphocoline (DOPC) (Avanti) liposomes are used. DOPC is a zwitterionic natural phospholipid, that is frequently used to form flexible liposomes, because its transition temperature is -17°C, so it is in the fluid phase at room temperature. This is a first experiment with liposomes, so only one lipid was chosen to have a simple formulation to check the interaction between enzymes and liposomes. To prepare 2 mL of liposomes (1 mg/mL), 80 µL of DOPC (25 mg/mL) as transferred in a round bottom flask. Hereafter, 2 mL of chloroform (Avanti) was added and this chloroform is evaporated during 30 minutes in a revaporator (IKA RV 10 Rotary Evaporator with Chemistry Vacuum Pumping Unit PC 2001 VARIO) to form a lipid film on the bottom of the flask. Hereafter 2 mL of buffer (5 mM

Tris-HCl (pH 7,5) with 2 mM MgCl₂) was added and vortex 2 minutes to completely recover the film. Finally, ultrasonicate (Branson Ultrasonics Sonifier S-450 Digital Ultrasonic Cell Disruptor/Homogenizer) 3 times 1 minutes, with 10 seconds of sonification and 15 seconds pause at a power of 10%.

To encapsulate ALP, 1 mL of the liposomes (20 mg/mL) were incubated with ALP (1 mg/mL) for 2 hours. Next, the samples were ultracentrifugated at 35 000 g for 1 hour to separate the liposomes from the supernatans. To understand the amount of ALP that is loaded the supernatans was measured at 297 nm with the UV-VIS spectrophotometer. This protocol is based on the protocol of (Camolezi F. L. et al, 2002).

6.3.2 Enzymatic activity measurements

To determine the amount of active ALP captured by the liposomes an activity assay was performed. The liposome (1 mg/mL) solution containing ALP was ten times diluted to a concentration of 0,1 mg/mL with a volume of 500 µL of water. The concentration of active ALP was determined using a standard ALP activity assay, with modifications. To measure this in the microplate reader, 100 µL of the sample containing released ALP was transferred to a well of a 96 well cell culture plate. 50 µL of a substrate solution consisting of 5 x 10⁻³ M *p*-nitrophenylphosphate disodium salt (pNPP) (Sigma Aldrich, P5994) in 0.5 M alkaline buffer was added. This buffer was prepared by diluting 1.5 M alkaline buffer (Sigma-Aldrich, A9226) with water in the volumetric ratio 1:2. After incubation, the reaction was stopped by the addition of 100 µL of 0.3 M NaOH (Sigma Aldrich). Absorbance was measured at 405 nm with a Benchmark Plus microplate spectrophotometer (Bio-Rad). This protocol can also be performed by measuring in a UV-VIS spectrophotometer (UVIKON XL Secomam), but because of the need for a higher volume the particles were to be diluted in 500 µL and thereafter 250 µL of pNPP was added and finally 500 µL stop solution was added to stop the reaction.

A calibration curve of ALP in water was set up with concentrations ranging from 0.05 to 3 mg/mL that served as reference. To calculate the percentage of active ALP (%active ALP) the measured concentration of active ALP (c_{active}) was divided by the absorbed concentration of ALP

$$\text{ALP\% active ALP} = \frac{c_{\text{active}}}{c_{\text{absorbed}}} * 100\%$$

7 Results and discussion

7.1 Calcium carbonate particles

CaCO₃ particles are very useful microparticles, because of its low synthesis costs, a simple synthesis method, its porosity that leads to easy loading, its biocompatibility, its low toxicity and mild decomposition conditions (Donatan S. et al, 2016; Parakhonskiy B. et al, 2015). Also CaCO₃ particles are frequently used as templates for the assembly of microparticles built by the LbL technique or as template for other applications, such as alginate based hydrogels (Donatan S. et al, 2016). There are three forms of anhydrous polymorphs of CaCO₃ with different characteristic properties, namely aragonite, vaterite and calcite. Vaterite has a hexagonal unit cell and is the most promising polymorph, because of its high porosity and surface area, which can result in a high loading capacity and the potential release of the therapeutic compound (Kirboga S. & Oner M., 2013; Parakhonskiy B. et al, 2012; Svenskaya Y. et al, 2016; Volodkin D. V. et al, 2010).

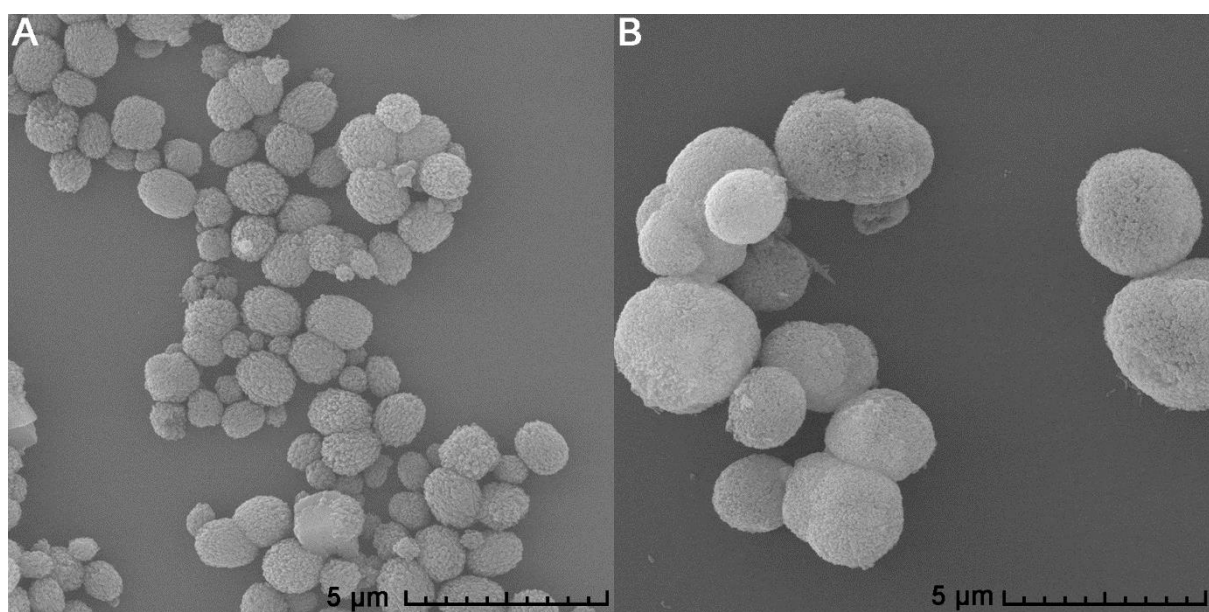


Figure 6: SEM images of small (A) with a size of 1.150 (\pm 0,074) μ m and large (B) with a size of 2.307 (\pm 0.385) μ m vaterite particles.

In the following experiments, two different sizes of vaterite are examined, namely small particles with a size of 1.15 (\pm 0,07) μ m and large particles with a size of 2.3 (\pm 0.4) μ m. These can be observed in the SEM images in Figure 6. Both are synthesized by mixing two salts, namely NaCO₃ and CaCl₂ in equimolar concentrations. Large particles are mixed for 2 minutes and small particles for 3 hours, which results in a reduction in size. For the synthesis of small vaterite particles, EG is added to increase the viscosity, leading to a lesser movement of ions, thus reducing the size and the solubility of CaCO₃ particles.

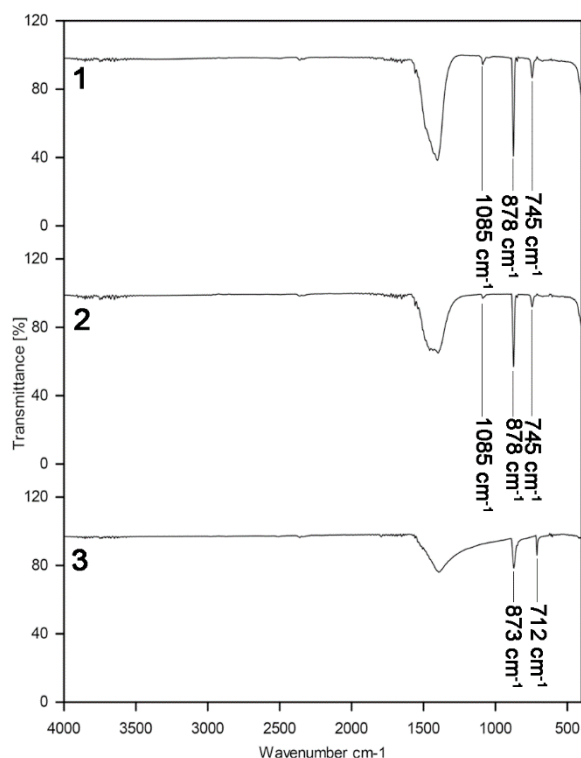


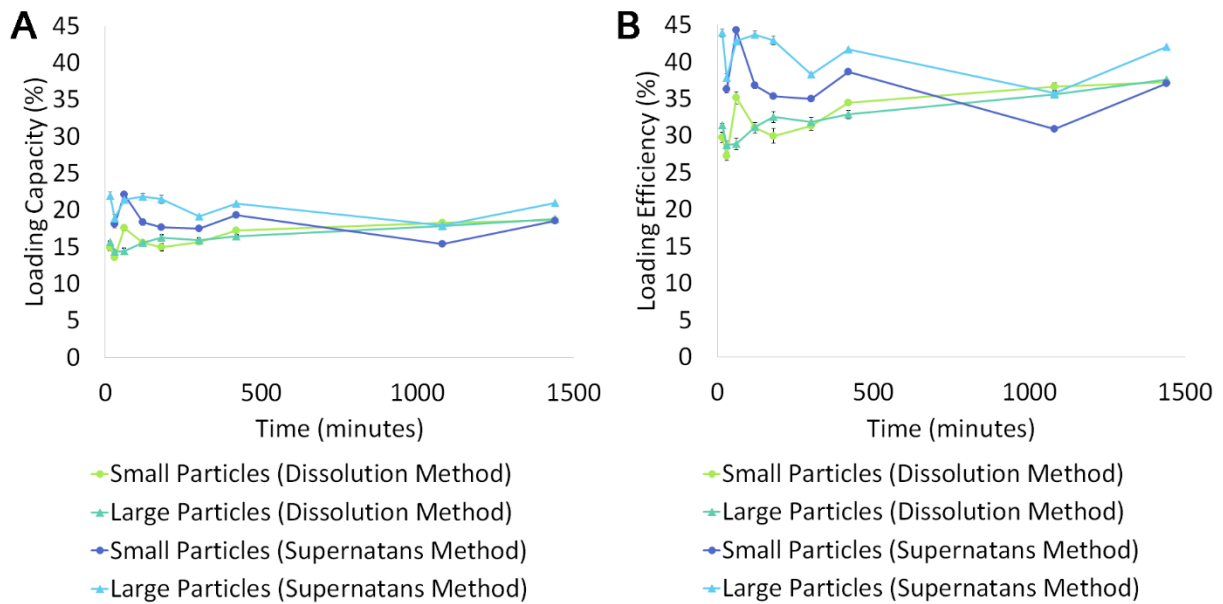
Figure 7: FTIR spectra of small vaterite particles (1), large vaterite particles (2) and calcite particles (3) without ALP. A band typical for calcite is marked at 712 cm^{-1} and 873 cm^{-1} and band characteristic for vaterite is marked at 745 cm^{-1} , 878 cm^{-1} and 1085 cm^{-1} .

In Figure 7, the FTIR spectra of the small and large vaterite particles are displayed in contrast to calcite particles. The observed absorption bands for calcium carbonate phases are due to the planar CO_3^{2-} ion. There are four vibrational modes in the free CO_3^{2-} ion, namely the symmetric stretching at 1080 cm^{-1} (ν_1), the out-of-plane bend at 870 cm^{-1} (ν_2), the asymmetric stretch 1400 cm^{-1} (ν_3) and the split in-plane bending vibrations at 700 cm^{-1} (ν_4). The spectra with bands centered at 712 cm^{-1} (ν_4) and 873 cm^{-1} (ν_2) reveal the presence of calcite. While bands centered at 745 cm^{-1} (ν_4), 878 cm^{-1} (ν_2) and 1085 cm^{-1} (ν_1), which indicates vaterite. In all samples there is a band at 1400 (ν_3), which indicates an asymmetric stretch of the carbonate ion (Saraya M. E. I. & Rokbaa H. H. A. L., 2016).

7.1.1 Optimization of time and concentration for ALP loading

For studying the influence of the time and concentration on the loading of the CaCO_3 particles, different concentrations and time intervals of absorption were examined to define the optimal parameters. To demonstrate the influence of the size of particles, all the experiments are performed on two sizes of particles, shown in Figure 6. After the absorption, the samples are centrifuged and subsequently the ALP loading is measured with the UV-VIS spectrometer. To define ALP loading, the samples are centrifuged after the absorption and the supernatans is removed. There are two methods to define the ALP loading, namely the measurement of the supernatans or the dissolution of the particles in EDTA, thus releasing all the ALP absorbed by the particles. The latter method gives a more accurate result of the ALP concentration absorbed

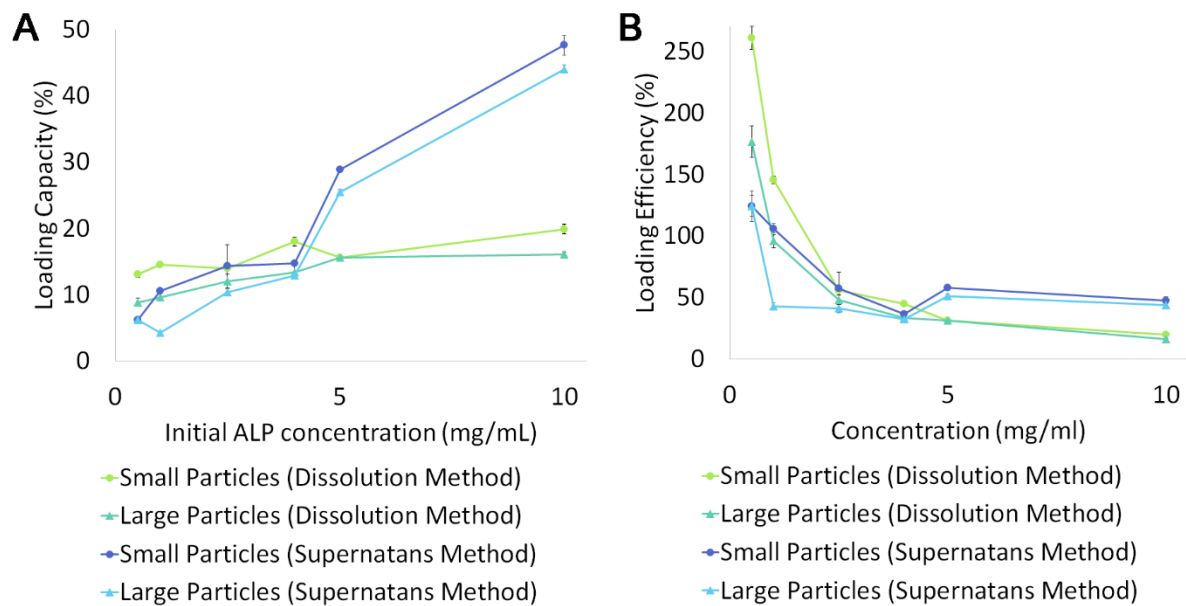
in the particles, however this is a destructive method, thus can rarely be performed. With the use of a calibration curve can the concentration be calculated.



Graph 1: Loading capacity (A) and loading efficiency (B) for small (●) and large (▲) vaterite particles dependent on the time of ALP absorption, by measuring the ALP concentration after dissolving the particles in EDTA (Dissolution method) and measuring the ALP concentration in the supernatans (Supernatans method).

Shown on Graph 1 are the loading capacity and loading efficiency of the ALP absorption, obtained by the two methods. The loading capacity concludes the absorbed concentration regarding the total weight of the particles. The loading efficiency is the absorbed concentration regarding the initial ALP concentration. After 1 to 2 hours, the loading capacity and efficiency will not increase anymore and will remain constant at approximately 16% and 32% respectively, when the dissolution method is used. When the supernatans method is used, the loading capacity of the small particles is 18% and 22% for the large particles after 2 hours of incubation. The loading efficiency of the small and large particles is 37% and 43% respectively after 2 hours of incubation.. For all the following experiments, an adsorption time of 2 hours is used.

To understand the influence of the initial ALP concentration on the absorption, 6 different initial concentrations between 0.5 and 10 mg/mL were tested.



Graph 2: Loading capacity (A) and loading efficiency (B) for small (●) and large (▲) particles dependent on the of the initial ALP concentrations, by measuring the ALP concentration after dissolving the particles in EDTA (Dissolution method) and measuring the ALP concentration in the supernatans (Supernatans method).

As seen in Graph 2, an initial ALP concentration of 5 and 10 mg/mL will give the highest loading capacity, namely 20% for the small particles and for the large particles 19% with a concentration of 5 mg/mL and 16% for a concentration of 10 mg/mL, when the dissolution method is used. The supernatans method gives a much higher loading capacity when an initial concentration of 10 mg/mL is used, namely 48% for the small particles and 44% for the large particles. The loading efficiency of the small particles 48% and of the large particles 44%. Because of the high loading capacity, 10 mg/mL is used in most of the next experiments, sometimes in comparison with 0.5 mg/mL to understand to influence of ALP on the particles. However, ALP is a relatively inexpensive enzyme, so if a more expensive enzyme is used, it is more interesting to take in account the loading efficiency to not lose too much of the enzyme.

The results of the supernatans method is higher in regard to the dissolution method. The dissolution method will give a more accurate result, but is however a destructive method. This is why the supernatans method is interesting, because other containers, such as liposomes, cannot be dissolved and the supernatans method provides a way to compare the loading capacity of these containers.

7.1.2 Stability of the particles

Recrystallization from vaterite to calcite is an interesting way to release ALP from the particles. The recrystallization process starts when vaterite particles are immersed in a water-based solution. Vaterite will slowly turn into the calcite phase, because of the dissolution and ionization of the external layer of vaterite. Vaterite can easily recrystallize to calcite due to the growing surface-to-volume ratio and enhanced solubility with decreasing particles size. It is energetically favourable, because vaterite particles have a higher Gibbs free energy than calcite particles (Kirboga S. & Oner M., 2013; Parakhonskiy B. et al, 2012; Parakhonskiy B. V. et al, 2014a;

Sawada K., 1997; Svenskaya Y. et al, 2016; Volodkin D. V. et al, 2010). During this process, the loaded ALP is released almost completely. Therefore, during the synthesis of three hours of small vaterite particles EG is added. EG will offer an enhanced density and reduced solubility of CaCO_3 . This will diminish the molecular diffusion, reducing the crystal growth rate and the probability of nucleation, which finally stabilized the vaterite crystals (Parakhonskiy B. et al, 2012).

To understand the duration of this process, large and small particles are diluted in three different solutions, namely PBS, physiological solution and water.

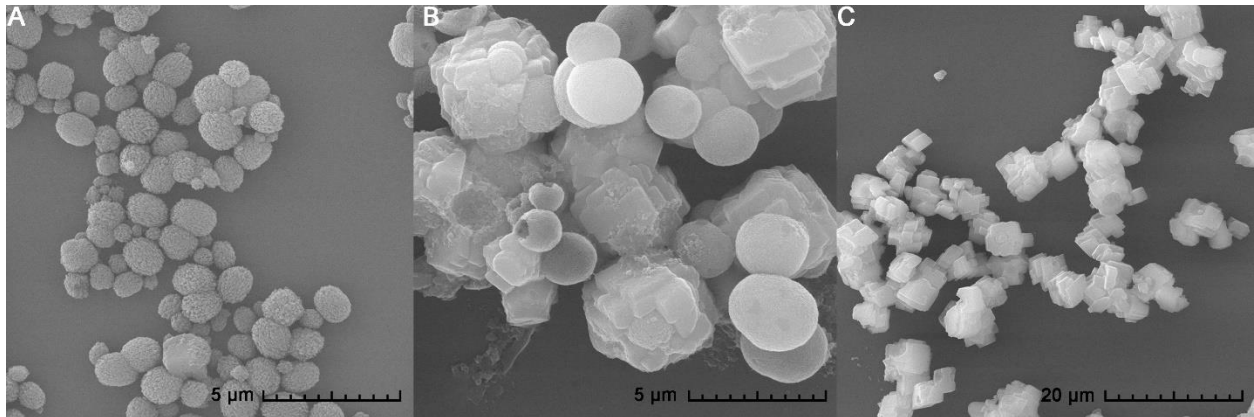


Figure 8: Scanning Electron Microscopy images of the recrystallization process from vaterite particles (A), to vaterite and calcite particles (B), to calcite (C) particles

In Figure 8 the different stages of recrystallization are displayed from vaterite to vaterite and calcite and eventually to calcite. Vaterite and calcite can be clearly distinguished by their shape. Vaterite has a spherical shape and calcite has a cubic-like shape.

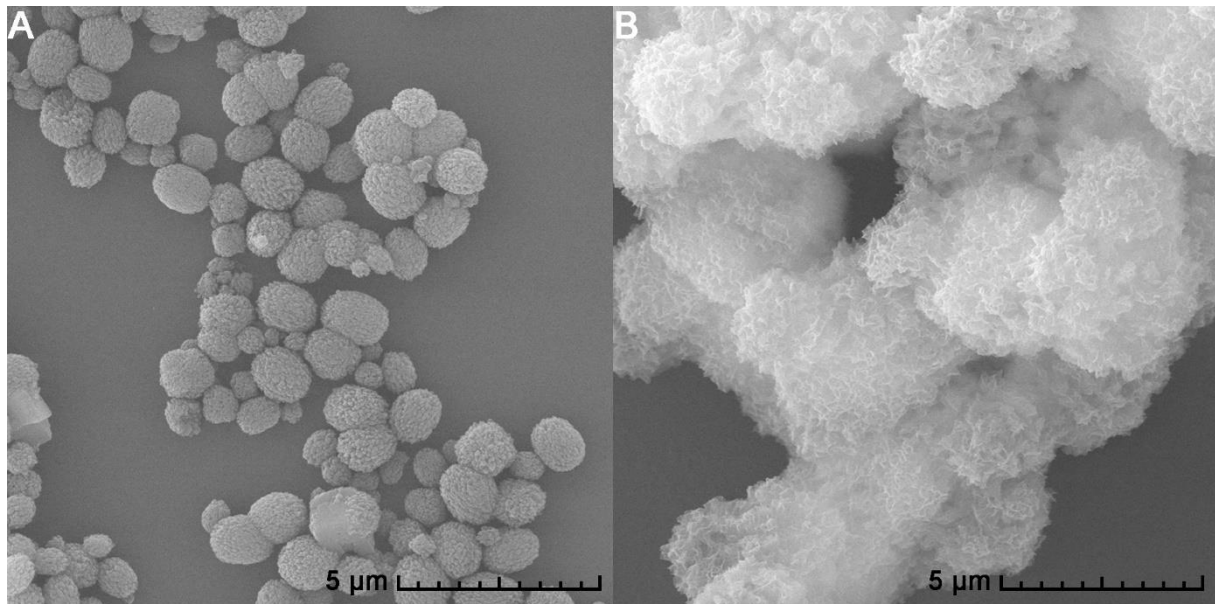


Figure 9: Scanning Electron Microscopy images of the transformation of vaterite particles (A) to hydroxyapatite (B) particles

However, this recrystallization process from vaterite to calcite is only attained in physiological solution and water. In PBS, there are strong indication that vaterite is altered to hydroxyapatite ($\text{Ca}_5(\text{PO}_4)_3\text{OH}$) after an ion-exchange reaction with the phosphate ions of the medium.

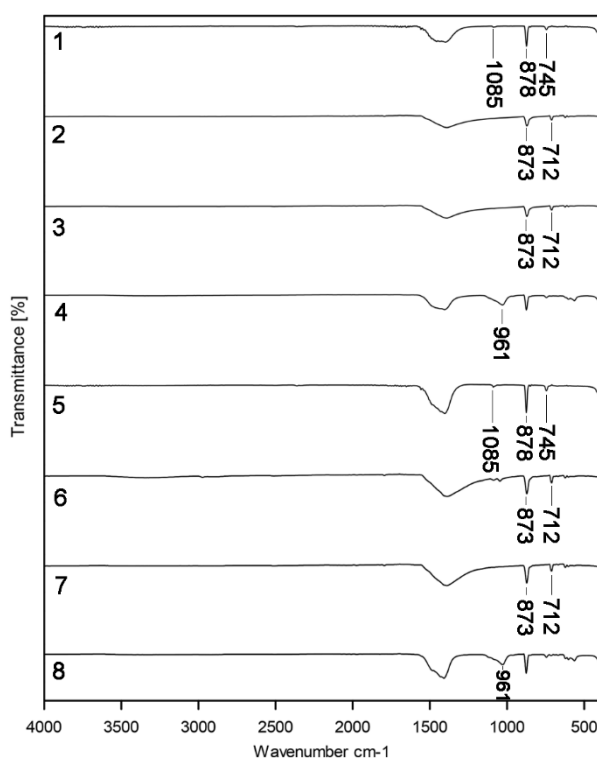


Figure 10: FTIR spectra of calcium carbonate particles without ALP before (1 and 5) and after (2, 3, 4, 6, 7, 8) one week of incubation in the different solvents. (1) Initial large vaterite particles; (2) Large particles incubated in H_2O ; (3) Large particles incubated in NaCl ; (4) Large particles incubated in PBS; (5) Initial small vaterite particles; (6) Small particles incubated in H_2O ; (7) Small particles incubated in NaCl ; (8) Small particles incubated in PBS. A band typical for hydroxyapatite is marked at 961 cm^{-1} , a band typical for calcite is marked at 873 cm^{-1} and 712 cm^{-1} and a band typical for vaterite is marked at 1085 cm^{-1} , 878 cm^{-1} and 745 cm^{-1} .

In Figure 10, the FTIR spectra are displayed confirming that if vaterite particles are incubated in PBS buffer, the phosphate ions will interact with the vaterite particles. The specific bands of vaterite, calcite and hydroxyapatite are marked on Figure 10. A band specific for hydroxyapatite can be seen at 961 cm^{-1} . This band is specific for PO_4^{3-} , which is a strong indication of hydroxyapatite. There are four vibrational modes in the free CO_3^{2-} ion, namely the symmetric stretching at 1080 cm^{-1} (ν_1), the out-of-plane bend at 870 cm^{-1} (ν_2), the asymmetric stretch 1400 cm^{-1} (ν_3) and the split in-plane bending vibrations at 700 cm^{-1} (ν_4). The spectra with bands centered at 712 cm^{-1} (ν_4) and 873 cm^{-1} (ν_2) reveal the presence of calcite. While bands centered at 745 cm^{-1} (ν_4), 878 cm^{-1} (ν_2) and 1085 cm^{-1} (ν_1), which indicates vaterite. In all samples, there is a band at 1400 (ν_3), which indicates an asymmetric stretch of the carbonate ion.

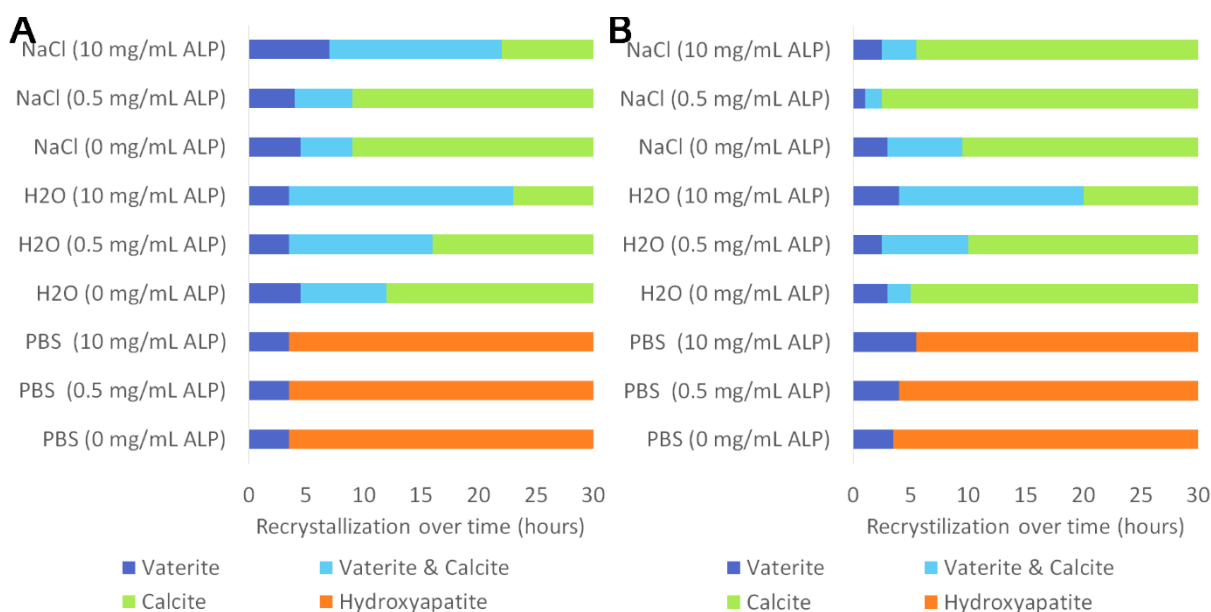
On the FTIR spectra there can be seen that if the vaterite particles are incubated in H_2O and NaCl , they are transformed to calcite. If vaterite particles are incubated in PBS buffer, it will become hydroxyapatite.

Table 1: Results of EDX of large particles dissolved in PBS

Spectrum	O	Na	Si	P	Cl	K	Ca	Total
Spectrum 2	41.37	11.01	19.74	3.20	5.87	0.84	17.97	100.00

The transition of vaterite to hydroxyapatite in PBS is also confirmed with energy-dispersive X-ray spectroscopy (EDX). The results in Table 1 indicates the presence of phosphor ions in the particles. EDX is used for elemental analysis or chemical characterization of a sample. It is based on the fundamental principle that each element has a unique atomic structure, which allows to obtain a unique set of peaks on its electromagnetic emission spectrum, which is stimulated by a high-energy beam.

This recrystallization experiment is performed for two different ALP concentrations, namely 0.5 and 10 mg/mL ALP, loaded on small and large particles and particles without ALP. This was done to examine the influence of the ALP on the stability of the particles. ALP is loaded during two hours of absorption of ALP diluted in water. These particles were diluted in three different solvents, namely physiological solution, water and PBS. There should also be considered that the loading of ALP takes 2 hours of absorption.



Graph 3: The dynamics of the composition of the samples for different ALP concentrations, namely 0, 0.5 and 10 mg/mL, with different sizes, namely small (A) and large (B) particles, incubated in different solutions, namely PBS, NaCl and H₂O. The recrystallization process started after 2 hours of ALP loading.

In Graph 3, there can be concluded that all particles are recrystallized after 24 hours. The recrystallization of large particles diluted in a NaCl solution is the shortest, namely after 2.5 hour. The recrystallization of the small particles diluted in H₂O is the longest, namely after 23 hours. There can also be observed that the small particles have a slightly longer stability in contrast to the large particles. Another observation that can be made, is that the concentration of ALP has an influence on the stability of the particles. A concentration of 10 mg/mL mostly gives a longer presence of vaterite in contrast to the particles loaded with 0.5 mg/mL ALP or no ALP.

Small particles in H₂O are recrystallized between 12 and 23 hours, depending on their ALP concentration. The recrystallization of large particles in H₂O is slightly quicker namely between 5 hours and 20 hours. The small particles are longer stable in H₂O than in NaCl, they are recrystallized in NaCl between 9 and 22 hours. Also, the large particles are longer stable, the recrystallization of these particles is completed between 2.5 and 9.5 hours. The shorter recrystallization process of the particles is because the CaCO₃ particles are negatively charged, which will be neutralized by NaCl. The negative charge slows the aggregation down, but due to neutralisation the particles will aggregate and the crystal growth and molecular diffusion will be enhanced. This will lead to the recrystallization of vaterite to calcite. The samples dissolved in PBS are all transformed after 5 hours of incubation to hydroxyapatite.

7.1.3 Amount of active ALP in the particles

To understand how much ALP is active in the particles with different initial ALP concentrations, a standard ALP activity assay was performed. After the dilution of the particles in water, the substrate *p*NPP reacts with ALP and forms *p*-nitrophenol with a yellow colour, shown in Figure 11. Hereafter the reaction is stopped by adding NaOH.

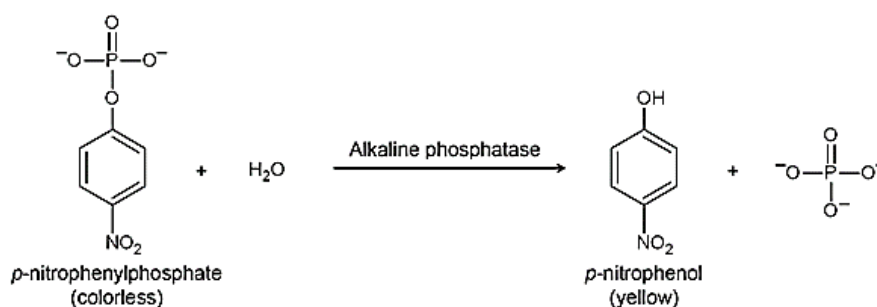
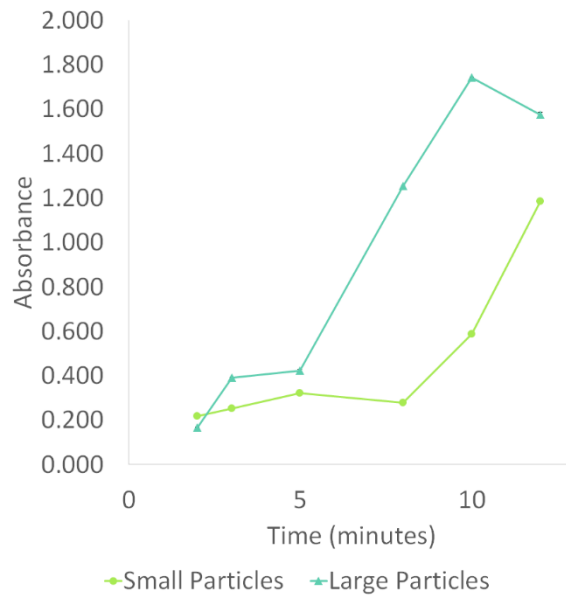


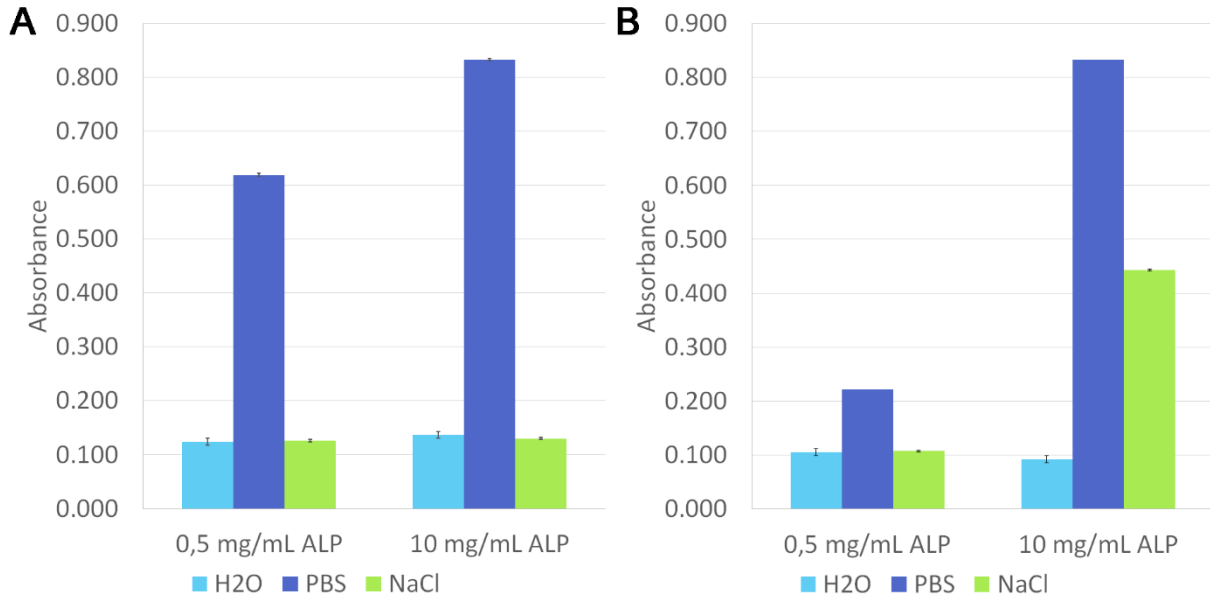
Figure 11: Enzymatic reaction mechanism of *p*-nitrophenylphosphate to *p*-nitrophenol with ALP.

To understand which incubation time of the enzyme gives the best results and is always situated in the linear part of the calibration curve, different time intervals of adding the stop solution were tested on small and large vaterite particles.



Graph 4: Absorbance spectra with a low standard deviation ($\pm 0,005$) of 1 mg of small (●) and large (▲) vaterite particles loaded with an initial concentration of 10 mg/mL ALP after the addition of substrate pNPP in function of different time intervals of adding stop solution.

In Graph 4, there can be seen that the absorbance of the activity of 1 mg of CaCO_3 increases with the length of the incubation time, so for the next experiments the incubation time of 5 minutes is chosen, because the absorbance for this concentration always is in the linear part of the calibration curve.



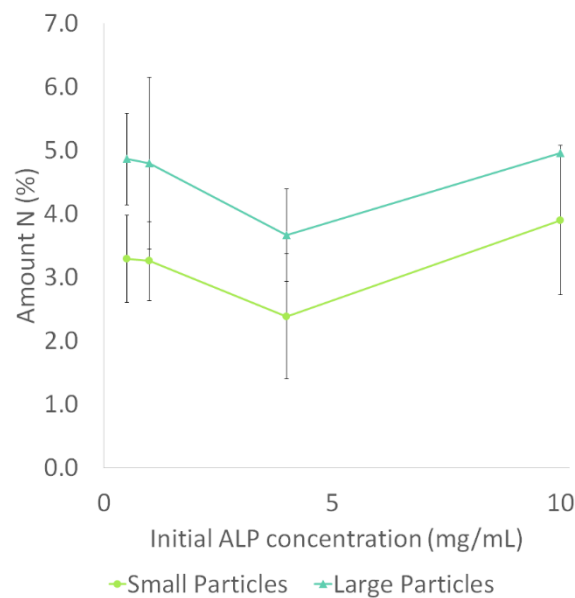
Graph 5: Intensity of the absorbance of the enzyme activity measurement measured at 405 nm of recrystallized small (A) and large (B) particles loaded with an initial concentration of 0,5 mg/mL ALP and 10 mg/mL. The particles are incubated in three solvents, namely H₂O, PBS and NaCl.

After the recrystallization of the particles, there can still be active ALP present in the particles. To understand how much of the ALP remained in the particles, an enzyme activity assay was performed on the particles after recrystallization. From Graph 5, there can be concluded that

there was almost no activity in the recrystallized particles diluted in H₂O. In the large particles diluted in NaCl there is still activity detected, namely with an absorbance of 0.443, but in the small particles there is also no activity. Finally, the particles diluted in PBS still show high activity. Small particles loaded with an initial concentration of 0.5 mg/mL have an absorbance of 0.619 and the large particles have a lower absorbance, namely 0.222. Small and large particles diluted in PBS with an initial concentration of 10 mg/mL show the highest absorbance, namely 0.833. To conclude, the calcite structure provides the release of ALP and in the hydroxyapatite, structure a fraction of the ALP remains in the particle.

7.1.4 XPS measurements

XPS is a spectroscopic technique that measures the elemental composition on the surface of the particles. These measurements were performed for small and large particles, where different ALP concentrations are absorbed in and on the particles.

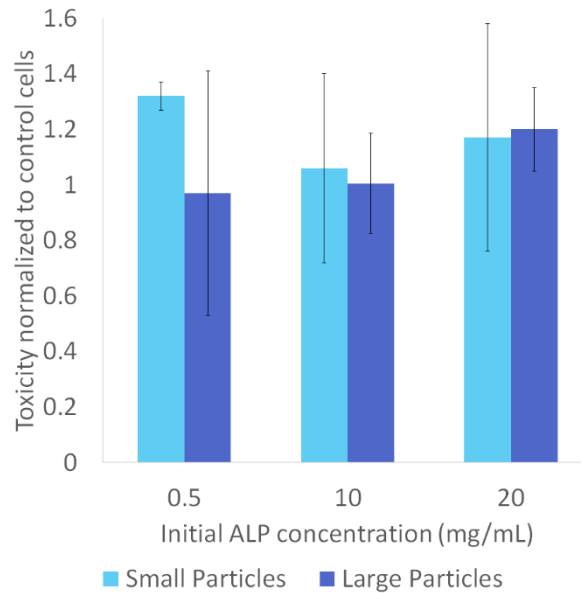


Graph 6: Amount of nitrogen in the small (●) and large (▲) particles, dependent on the different initial ALP concentrations, namely 0.5, 1, 4 and 10 mg/mL.

Shown on Graph 6 is the percentage of nitrogen present on the surface of the particles. Nitrogen indicates the presence of ALP. For the different concentrations, the percentage of nitrogen is approximately the same for the particles. The percentage of nitrogen on the surface of the small particles is approximately 3.2%, which is slightly lower than on the surface of the large particles, namely approximately 4.6%. This can be explained by the smaller surface area of the small particles, however the amount of absorbed ALP concentration is higher, so this could be an indication of the presence of ALP in the particles.

7.1.5 Toxicity

To understand the toxicity of the CaCO_3 particles loaded with ALP, three different ALP concentrations are used. Next, HeLa cells are used to see if the particles are toxic, with the use of a fluorescent dye AlamarBlue. The results are already normalized to the controls, which are HeLa cells with the addition of the particles.



Graph 7: Results of the toxicity normalized to the control cells of small and large particles, loaded with different initial ALP concentrations, namely 0.5, 10 and 20 mg/mL.

The results in Graph 7 are normalized to the control cells and don't show toxicity, because they are above the value of 1. For the small particles, an initial ALP concentration of 0.5 mg/mL gives the best result, namely 1.32 and decreases to 1.06 for an initial ALP concentration of 10 mg/mL and increases slightly to 1.17 for an initial ALP concentration of 20 mg/mL. For the large particles, when loaded with an initial ALP concentration of 0.5 mg/mL this gives the minimum, namely 0.97. For an initial ALP concentration of 10 mg/mL it increases to 1 and for 20 mg/mL to 1.2.

7.2 Alginate particles

CaCO₃ particles can't easily be used by itself, due to its instability in water based solutions and weak protection of loaded materials (Svenskaya Y. et al, 2013) therefore protection is needed. A less time consuming and expensive method than using polyelectrolytes, is by using alginate based hydrogels. In these experiments, alginate, silver alginate with and without CaCO₃ core and calcium alginate particles with and without CaCO₃ core are compared to the CaCO₃ particles. The absorption of alginate, the gelation and dissolving of the CaCO₃ does not have an influence on the morphology of the particles as can be seen in Table 2.

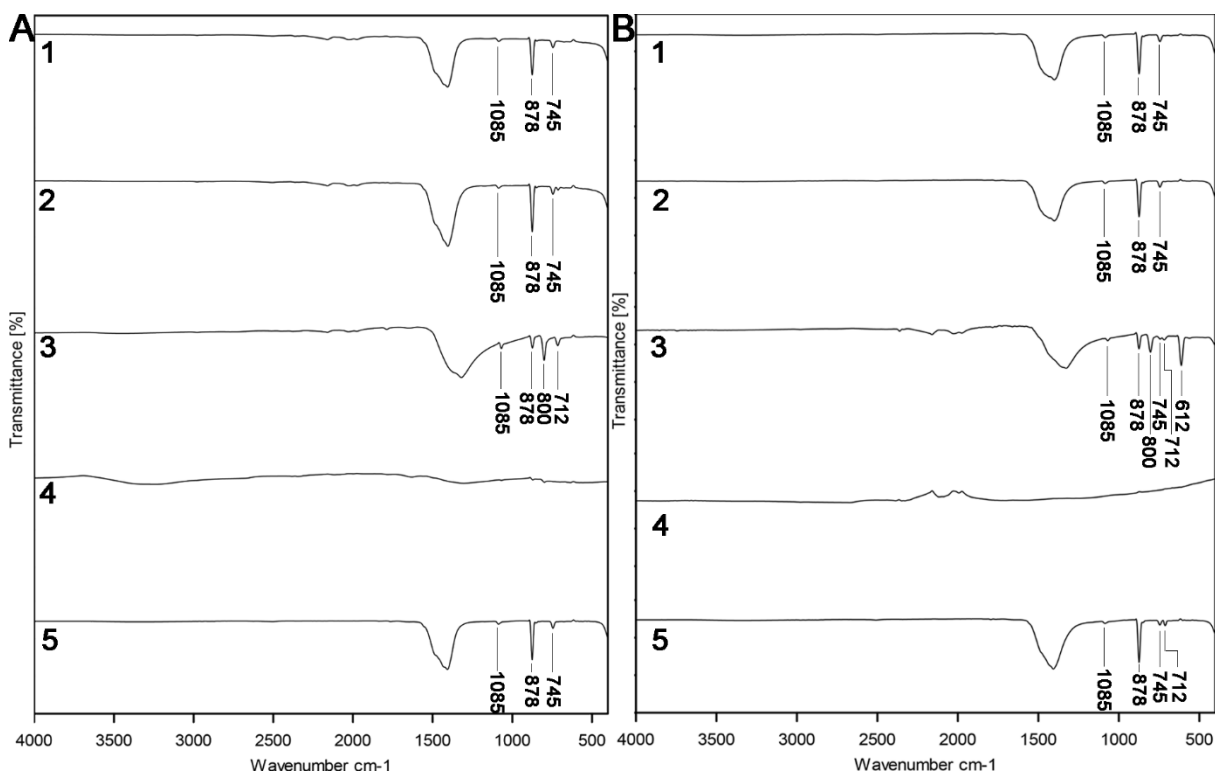


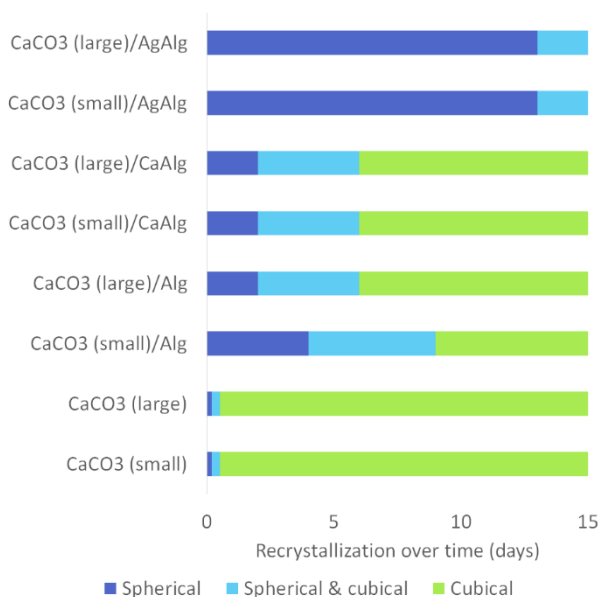
Figure 12: FTIR spectra of small (A) and large (B) alginate based hydrogels in comparison with CaCO₃ particles (1); (2) alginate particles; (3) silver alginate particles with a CaCO₃ core; (4) silver alginate particles after addition of ascorbic acid; (5) calcium alginate particles with a CaCO₃ core. Bands characteristic for small silver alginate particles are 712 cm⁻¹, 800 cm⁻¹, 878 cm⁻¹ and 1085 cm⁻¹. Bands characteristic for large silver alginate particles are 612 cm⁻¹, 712 cm⁻¹, 745 cm⁻¹, 800 cm⁻¹, 878 cm⁻¹ and 1085 cm⁻¹. Specific bands for calcium alginate particles with a CaCO₃ core are 745 cm⁻¹, 878 cm⁻¹ and 1085 cm⁻¹.

The FTIR spectra of the different particles are displayed in Figure 12 with the specific bands for each particle marked. There are four vibrational modes in the free CO₃²⁻ ion, namely the symmetric stretching at 1080 cm⁻¹ (v₁), the out-of-plane bend at 870 cm⁻¹ (v₂), the asymmetric stretch 1400 cm⁻¹ (v₃) and the split in-plane bending vibrations at 700 cm⁻¹ (v₄). However, there is no difference between the CaCO₃ particles and the alginate particles. This can be due to the very small layer of alginate and in its dried state it could be perceived more as separate molecules, which cannot be detected by FTIR and the CaCO₃ will dominate. Also, the calcium alginate particles have similar FTIR spectra. The characteristic bands for these particles are 745 cm⁻¹ (v₄), 878 cm⁻¹ (v₂) and 1085 cm⁻¹ (v₁). For the large calcium alginate particles with a CaCO₃ core there are bands at 712 cm⁻¹ and 745 cm⁻¹, which indicates the presence of vaterite and

calcite. Bands specific for small silver alginate with a CaCO_3 core are 712 cm^{-1} (ν_4), 800 cm^{-1} , 878 cm^{-1} (ν_2) and 1085 cm^{-1} (ν_1). Bands specific for large silver alginate particles with a CaCO_3 core are 612 cm^{-1} , 712 cm^{-1} (ν_4), 800 cm^{-1} , 878 cm^{-1} (ν_2) and 1085 cm^{-1} (ν_1). The spectra of the silver alginate after the addition of ascorbic acid don't show any specific peaks in contrast to the other spectra.

7.2.1 Stability of the particles

After one day, all CaCO_3 particles are recrystallized to calcite, so these particles are very unstable. Alginate based hydrogels have a longer stability and to prove this, these particles are incubated in water and the recrystallization process is observed through optical microscopy and SEM images.

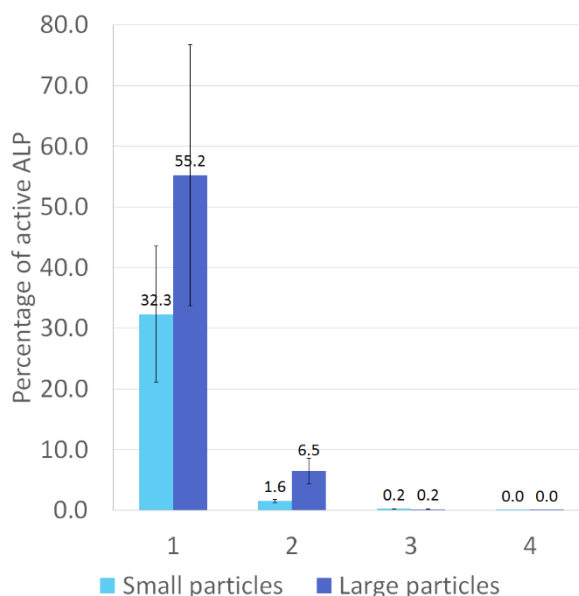


Graph 8: The dynamics of the composition of the samples of small and large CaCO_3 particles in comparison with different alginate based hydrogels, such as alginate particles (CaCO_3/Alg), silver alginate particles with CaCO_3 core ($\text{CaCO}_3/\text{AgAlg}$) and calcium alginate particles with CaCO_3 core ($\text{CaCO}_3/\text{CaAlg}$).

In Graph 8, there can be concluded that the alginate based hydrogels have a higher stability in comparison with CaCO_3 particles, that has a stability of less than one day. The alginate based hydrogels have a stability of minimum 6 days and the silver alginate particles with CaCO_3 core show some cubic-like particles after 13 days. The calcium alginate particles with CaCO_3 core are all recrystallized after 6 days, also large alginate particles are recrystallized after 6 days. Small alginate particles are all recrystallized after 9 days.

7.2.2 Amount of active ALP in the particles

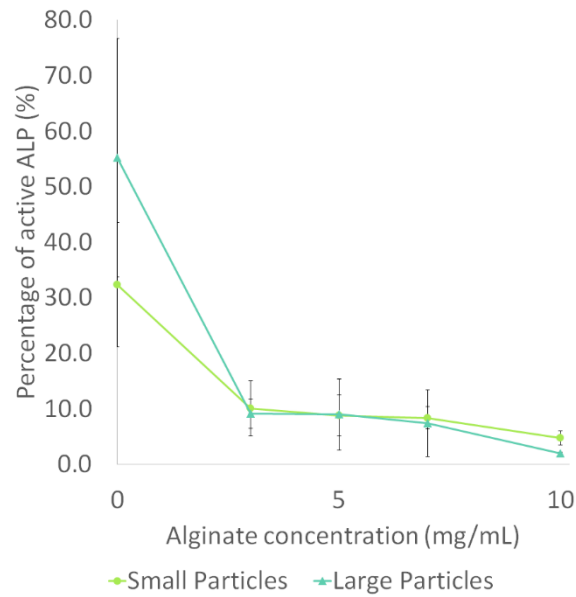
To form silver alginate particles the CaCO_3 particles are filled with alginate (10 mg/mL) and hereafter AgNO_3 (0.5 M) is added to achieve the alginate gelation and finally ascorbic acid (0.1 M) is added, which initiates the silver reduction process of the particles and the dissolution of calcium carbonate. To understand what the influence of this procedure is on the percentage of active ALP, the concentration of the active ALP is measured in all intermediate steps.



Graph 9: The percentage of active ALP in the intermediate steps of the formation of silver alginate particles, namely starting with ALP loaded CaCO_3 particles (1), next the addition of alginate (10 mg/mL) (2), subsequently AgNO_3 (0.5 M) (3) is added and finally ascorbic acid (0.1 M) (4) is added.

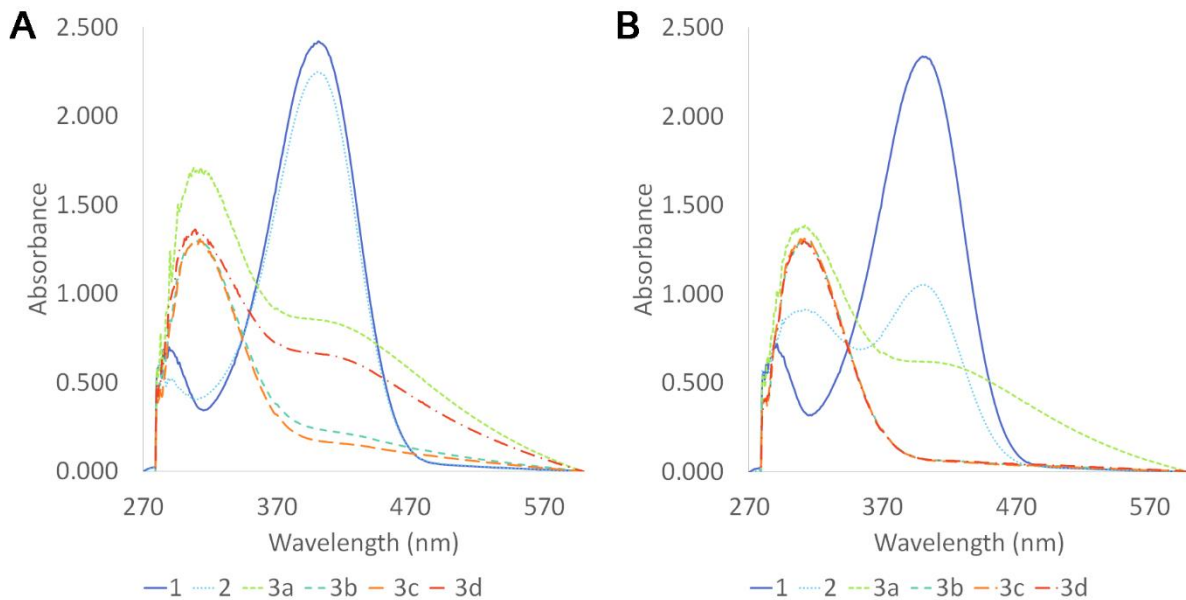
Shown in Graph 9, there is a decrease in active ALP in all steps. In the small vaterite particles 32.3% of the ALP is active and this decreases after the addition of alginate (10 mg/mL) to 1.6%. After the addition of AgNO_3 (0.5 M) only 0.2% is active and finally after the addition of ascorbic acid (0.1 M) there was no activity detected. The large particles are slightly more active than the small particles. In the large vaterite particles 55.2% of the ALP is active and this decreases after the addition of alginate (10 mg/mL) to 6.5%. After the addition of AgNO_3 (0.5 M) only 0.2% is active and finally after the addition of ascorbic acid (0.1 M) there was no activity detected. To optimize this, several concentrations of alginate and AgNO_3 are used.

To reduce the loss of active ALP, an experiment was performed with four different concentrations, namely 3, 5, 7 and 10 mg/mL.



Graph 10: The percentage of active ALP in small (●) and large (▲) particles dependent on the different alginate concentrations, namely 0, 3, 5, 7, and 10 mg/mL.

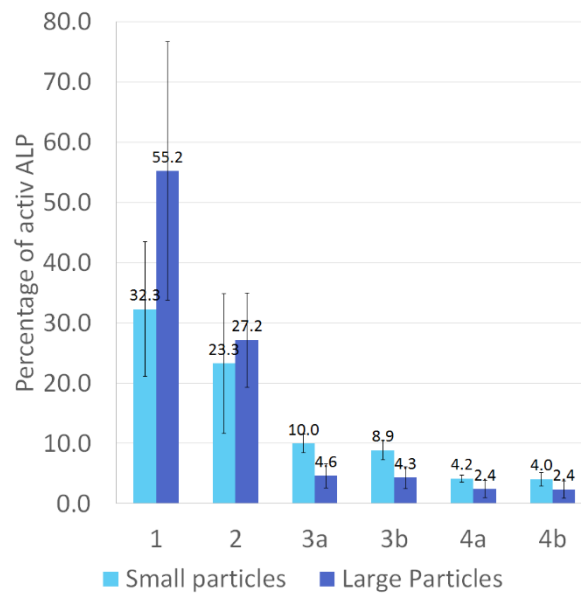
In Graph 10, a reduction in activity can be seen, when the alginate concentration is higher. The activity of the particles without the addition of alginate is 55.2% for the large particles and 32.3% for the small particles. With the addition of alginate, the activity decreases, if the alginate concentration is 3 mg/mL the activity of the small particles is 10.0% and of the large particles 9.2%. The activity slightly decreases with a higher alginate concentration. The activity of the particles after the addition of 10 mg/mL alginate is 4.7% for the small particles and 2.0% for the large particles.



Graph 11: Absorption spectra of ALP loaded small (A) and large (B) particles with different coating: CaCO₃ particles (1), CaCO₃ particles with alginate (5 mg/mL) layer (2) and CaCO₃ particles with alginate layer crosslinked with different AgNO₃ concentrations, namely 0.1 M (3a), 0.25 M (3b), 0.5 M (3c) and 0.75 M (3d).

To optimize the AgNO_3 concentration, different concentrations of AgNO_3 were tested. However, there is no detection of active ALP at 405 in Graph 11. There is a peak at 320 nm, this indicates the pNPP that has not reacted to p-nitrophenol. This is displayed in contrast to the activity of 20 mg of CaCO_3 particles, where most of the substrate has reacted.

To demonstrate that ALP is still active in hydrogels, the alginate particles are linked by adding CaCl_2 . To understand if the concentration of CaCl_2 to the amount of active ALP, two different concentrations of CaCl_2 are used.

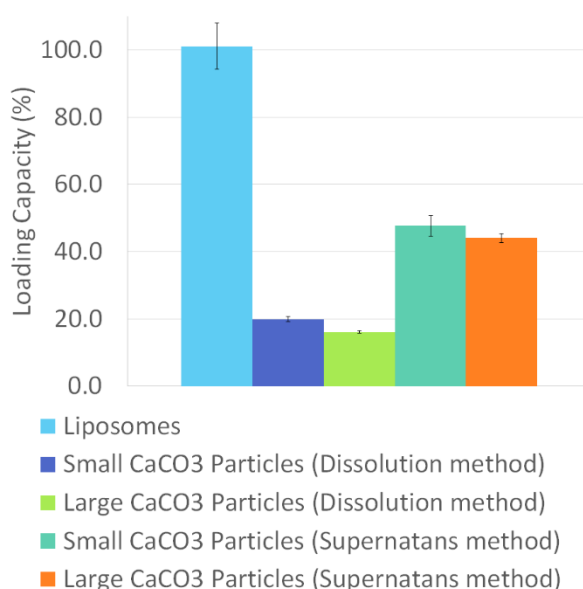


Graph 12: The percentage of active ALP in small and large ALP loaded CaCO_3 (1) particles, alginate particles (2), alginate particles linked with different concentration of CaCl_2 , namely 0.1 M (3a) and 0.5 M (3b) and finally after the addition of ascorbic acid (0.1M) to the alginate particles linked with 0.1 M CaCl_2 (4a) and 0.5 M CaCl_2 (4b).

In Graph 12, a decrease in the percentage of active ALP can be seen. In the small vaterite particles 32.3% of the ALP is active and this decreases after the addition of alginate (10 mg/mL) to 23.3%. After the addition of CaCl_2 10.0% is active if the concentration is 0.1 M and 8.9% if the concentration is 0.5 M, so there is a slight decrease in activity if the concentration of CaCl_2 increases. After the addition of ascorbic acid (0.1 M) the activity of the calcium alginate particles with CaCO_3 core formed with CaCl_2 with a concentration 0.1 M is 4.2% and with a concentration of 0.5 M it is 4.0%. In the large vaterite particles 55.2% of the ALP is active and this decreases after the addition of alginate (10 mg/mL) to 27.2%. After the addition of CaCl_2 4.6% is active if the concentration is 0.1 M and 4.3% if the concentration is 0.5 M, so there is a slight decrease in activity if the concentration of CaCl_2 increases. After the addition of ascorbic acid (0.1 M) the activity of the calcium alginate particles is 2.4%.

7.3 Liposomes

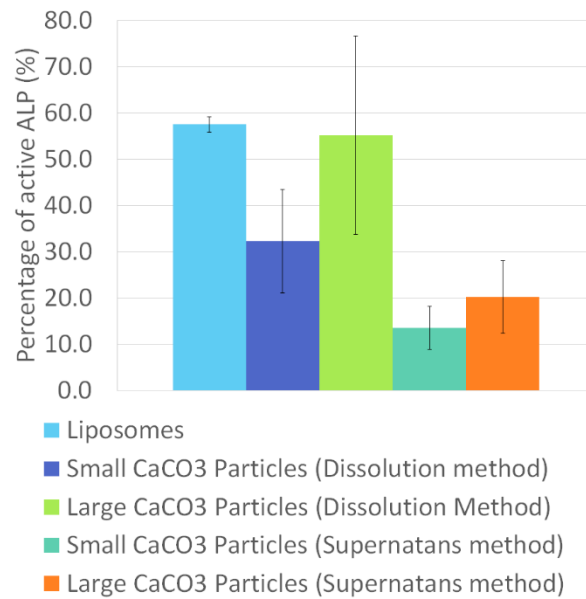
Liposomes are already frequently used in controlled drug delivery and for encapsulating enzymes in biosensing applications. They are the most common and well-investigated nanocarriers for targeted drug delivery. Therefore, ALP is loaded onto liposomes, to compare the CaCO_3 particles with these loaded liposomes. In these experiments DOPC is used and ALP is loaded on the surface of the liposomes through incubation of the liposomes with the enzyme solution for 2 hours. DOPC is a zwitterionic natural phospholipid, that is frequently used to form flexible liposomes, because its transition temperature is -17°C , so it is in the fluid phase at room temperature. After the incubation, the liposomes are ultracentrifuged and hereafter the supernatans is removed. To understand the loading capacity of the liposomes the absorbance of the supernatans is measured with the UV-VIS spectrophotometer at 297 nm.



Graph 13: Loading capacity of the liposomes, small vaterite particles and large vaterite particles, measured with the dissolution method and the supernatans method, loaded with an initial ALP concentration of 10 mg/mL.

In Graph 13, there can be seen that the liposomes have a loading capacity of 100%, which is much higher than the small vaterite particles with 19.9% or the large vaterite particles with 16.1%, measured with the dissolution method. However the concentration of ALP captured by the liposomes is measured using the supernatans method. For a better comparison, it is thus interesting to compare this with the results of the supernatans method for the CaCO_3 particles. The loading capacity of the small vaterite particles is 47.7% and of the large vaterite particles 44.0%, measured using the supernatans method.

Next, the activity of the liposomes is measured with the enzymatic activity assay in comparison with the vaterite particles.



Graph 14: The percentage of active ALP of the liposomes, small vaterite particles and large vaterite particles, measured with the dissolution method and the supernatans method, loaded with an initial ALP concentration of 10 mg/mL.

The ALP in the liposomes is the most active with 57.5% of active ALP, shown in Graph 14. In the small vaterite particles 32.3% is active and in the large vaterite particles 55.2% of the absorbed ALP is active, measured with the dissolution method. However, because the concentration in the particles, measured with the supernatans method, is the amount of active ALP lower, namely 13.5% for the small particles and 20.2% for the large particles..

From these results, it can be concluded that the liposomes have a higher loading capacity, but the percentage of the ALP is only 57.5%. This means that 42.5% of the ALP is not accessible for the substrate. A possible explanation could be that some of the enzyme penetrated the liposomes and the substrate could not penetrate the liposomes. The large vaterite particles have approximately the same percentage of active ALP, which is higher than the percentage of active ALP in the small vaterite particles. However, the enzyme is loaded on the surface of the liposomes, thus the enzyme can easily interact with the proteins in biological fluids. After the incubation of the enzyme with the CaCO₃ particles, the enzyme will not only be present on the surface of the particles, but also inside the particles, thus protecting the enzyme more from its environment.

This is a first experiment with liposomes, so only one lipid is chosen to have a simple formulation to check the interaction between enzymes and liposomes. To examine these liposomes further PEGylation can be considered as the next step in the formulation. This is necessary to avoid immune recognition after intravenous injection.

8 Conclusion

The aim of this thesis was the development of various carriers loaded with ALP and to compare these carriers based on their loading capacity, their stability and their enzyme activity. Seven types of carriers were obtained, namely CaCO_3 particles, alginate based hydrogels, calcium alginate based hydrogels and silver alginate based hydrogels with and without a CaCO_3 core and finally liposomes.

First, the maximal **loading capacity** is determined by optimizing the time of incubation and the initial concentration of the ALP solution for the small and large vaterite particles are optimized. The loading capacity for an initial concentration of 10 mg/mL ALP is 19.9% for the small particles and 16.1% for the large particles after 2 hours of incubation. However, ALP is a relatively inexpensive enzyme, so if a more expensive enzyme is used, it will be more interesting to consider the loading efficiency. The loading capacity of the liposomes is much higher, namely 100%.

Through recrystallization of the vaterite particles, ALP can be released. So it is interesting to understand what the **stability** is of the vaterite particles and thus understand how long the process takes before all particles are calcite. All vaterite particles are recrystallized after 24 hours, but depending on the size of the particles, the amount of ALP that is loaded onto the particles and the solvent in which the particles were incubated. The stability of the small vaterite particles is higher, in contrast to the large particles. Also, a higher amount of loaded ALP indicates a longer stability of the particles. Finally, in H_2O the vaterite particles are stable and for a longer time, then in NaCl and the particles incubated in PBS will transform into hydroxyapatite particles. The stability of the alginate based hydrogels is 6 approximately days for the large particles and approximately 9 days for the small particles, before all particles are transformed. Also, the stability of the calcium alginate based hydrogels is 6 days. The silver alginate based hydrogels with a CaCO_3 core remain almost all stable after approximately 13 days.

After the determination of the loading capacity, it is interesting to understand **how much of the loaded enzyme is active** and thus accessible for the substrate. Even though the small vaterite particles have a higher loading capacity than the large vaterite particles, the percentage of active ALP of the large particles is higher. In the XPS data it is indicated that there is more ALP on the surface of the large particles. The higher loading capacity and the lower amount of ALP for the small vaterite particles could indicate that there is ALP present in the particles. When these loaded vaterite particles are coated with alginate, the percentage of active ALP decreases. The small vaterite particles decreases from 32.3% active ALP to 23.3% active ALP after the addition of alginate and the large particles decrease from 55.2% to 27.2%. When these alginate based hydrogels are linked with silver, no activity can be detected. However, when these links are made with CaCl_2 , the activity decreases, but is still 10% for the small particles and 4.6% for the large particles. After the removal of the CaCO_3 , the activity decreases to 4.2% for the small particles and 2.4% for the large particles. To compare the percentage of activity of the CaCO_3 based particles with an already well investigated carrier, an activity assay is performed on the liposomes and the percentage of active ALP is 57.5%. This means that 42.5%

of the ALP is not accessible for the substrate. A possible explanation could be that some of the enzyme penetrated the liposomes and the substrate could not penetrate the liposomes.

Liposomes are already frequently used in controlled drug delivery and they are the most common and well-investigated nanocarriers for targeted drug delivery. This makes it very interesting to compare with the CaCO_3 particles. To conclude is the loading capacity and the percentage of the active ALP higher in the liposomes, but there was a simple formulation used, so that the interaction between the enzymes and the liposomes could be checked. When these are further investigated, there should be considered to PEGylate these particles. However, PEGylation can decrease the activity and the formulation can become very complex.

9 Future perspectives

To compare the performance of the particles used in this thesis, it would be interesting to load ALP in and on other containers, that are already frequently used. Interesting containers would be silica and PLGA particles. Silica particles have the advantage that it can be easily removed with hydrofluoric acid, when it is used for encapsulation. PLGA is of considerable interest to use as a base material for biomedical applications because of its biocompatibility, it is approved for clinical use in humans by the U.S. Food and Drug Administration (FDA), the biodegradation rate is tailored depending on the molecular weight and the copolymer ratio, it has potential to modify surface properties to provide better interaction with biological materials and it is suitable for export to countries where implantation of animal-derived products is unpopular. Another container, that would be interesting are RBCs. However, RBCs produces ALP, so to understand the loading of the enzyme, another model enzyme should be used.

In this thesis, there is already some research to the stability of the particles in different solvents, namely PBS, NaCl and H₂O. These particles are designed to be delivered in the blood of patients. Therefore experiments, where the particles are incubated in blood, would be interesting to understand the effect of the blood on the particles, but also if there is a formation of the protein corona and if this influences the uptake by the cells. It would also be interesting to understand how many cycles of adding substrate to the particles it takes, before there is a significantly decrease in activity.

There should also be a cell study, where the uptake, the entering through the membrane, the toxicity and the release in the cell is studied. Also, antibacterial tests should be carried out to understand if the particles are susceptible to bacterial contamination. A final experiment that should be considered is the use of mice to test the effect of the particles on the mice.

9.1 Expected manuscripts

1. Vaterite composed particles loaded with the therapeutic enzyme alkaline phosphatase
2. Microparticles and nanoparticles loaded with the therapeutic enzyme alkaline phosphatase

10 References

- Adams S. R., Tsien R. Y. (1993) Controlling cell chemistry with caged compounds. *Annual Review of Physiology* **55**: 755-784
- Alarcon C. d. I. H., Pennadam S., Alexander C. (2005) Stimuli responsive polymers for biomedical applications. *Chemical Society Reviews* **34**: 276-285
- Amsden B., Turner N. (1999) Diffusion characteristics of calcium alginate gels. *Biotechnology and Bioengineering* **65**: 605-610
- Anderson H. C. (1995) Molecular biology of matrix vesicles. *Clinical orthopaedics and related research*: 266-280
- Andreeva D. V., Gorin D. A., Shchukin D. G., Sukhorukov G.B. (2006) Magnetic Microcapsules with Low Permeable Polypyrrole Skin Layer. *Macromolecular Rapid Communications* **27**: 931-936
- Andresen T. L., Thompson D. H., Kaasgaard T. (2010) Enzyme-triggered nanomedicine: drug release strategies in cancer therapy. *Molecular Membrane Biology* **27**: 353-363
- Antipov A. A., Shchukin D., Fedutik Y., Petrov A. I., Sukhorukov G.B., Möhwald H. (2003) Carbonate microparticles for hollow polyelectrolyte capsules fabrication. *Colloids and Surfaces A: Physicochemical Engineering Aspects* **224**: 175-183
- Bae Y., Nishiyama N., Fukushima S., Koyama H., Yasuhiro M., Kataoka K. (2005) Preparation and biological characterization of polymeric micelle drug carriers with intracellular pH-triggered drug release property: tumor permeability, controlled subcellular drug distribution, and enhanced in vivo antitumor efficacy. *Bioconjugate Chemistry* **16**: 122-130
- Balabushevitch N. G., Sukhorukov G.B., Moroz N. A., Volodkin D. V., Larionova N. I., Donath E., Möhwald H. (2001) Encapsulation of Proteins by Layer-by-Layer Adsorption of Polyelectrolytes onto Protein Aggregates: Factors Regulating the Protein Release. *Biotechnology and Bioengineering* **76**: 207-213
- Balabushevitch N. G., Tiourina O. P., Volodkin D. V., Larionova N. I., Sukhorukov G.B. (2003) Loading the Multilayer Dextran Sulfate/Protamine Microsized Capsules with Peroxidase. *Biomacromolecules* **4**: 1191-1197
- Bareford L. M., Swaan P. W. (2007) Endocytic Mechanisms for Targeted Drug Delivery. *Advanced Drug Delivery Reviews* **59**: 748-758
- Bäumler H., Artman G., Voigt A., Mitlöhner R., Neu B., Kiesewetter H. (2000) Plastic behaviour of polyelectrolyte microcapsules derived from colloid templates. *Journal of Microencapsulation* **17**: 651-655
- Bedard M. F., Braun D., Sukhorukov G.B., Skirtach A. G. (2008) Towards self-assembly of nanoparticles on polymeric capsules: release threshold and permeability. *ACS Nano* **2**: 1807-1816

- Berg K., Selbo P. K., Prasmickaite L., Tjelle T. E., Sandvig K., Moan J., Gaudernack G., Fodstad O., Kjolsrud S., Anholt H., Rodal G. H., Rodal S. K., Hogset A. (1999) Photochemical internalization: a novel technology for delivery of macromolecules into cytosol. *Cancer Research* **59**: 1180-1183
- Bhaskar S., Pollock K. M., Yoshida M., Lahann J. (2010) Towards designer microparticles: simultaneous control of anisotropy, shape, and size. *Small (Weinheim an der Bergstrasse, Germany)* **6**: 404-411
- Biagiotti S., Paoletti M. F., Fraternali A., Rossi L., Magnani M. (2011) Drug Delivery by Red Blood Cells. *Life* **63**: 621-631
- Blandino A., Macias M., Cantero D. (2000) Glucose oxidase release from calcium alginate gel capsules. *Enzyme and Microbial Technology* **27**: 319-324
- Brady W. A., Kokoris M. S., Fitzgibbon M., Black M. E. (1996) Cloning, Characterization and Modeling of Mouse and Human Guanylate Kinases. *The Journal of Biological Chemistry* **271**
- Bruno B. J., Miller G. D., Lim C. S. (2013) Basics and Recent Advances in Peptide and Protein Drug Delivery. *Therapeutic Delivery* **4**: 1443-1467
- Caballero-Diaz E., Pfeiffer C., Kastl L., Rivera-Gil P., Simonet B., Valcarcel M., Jiménez-Lamana J., Laborda F., Parak W. J. (2013) The Toxicity of Silver Nanoparticles Depends on Their Uptake by Cells and Thus on Their Surface Chemistry. *Particle & Particle Systems Characterization* **30**: 1079-1085
- Camolezi F. L., Daghasanli K. R. P., Magalhaes P. P., Pizauro J. M., Ciancaglini P. (2002) Construction of an alkaline phosphatase-liposome system: A tool for biomineralization study. *The International Journal of Biochemistry & Cell Biology* **34**: 1091-1101
- Caruso F., Möhwald H. (1999) Protein Multilayer Formation on Colloids through a Stepwise Self-Assembly Technique. *Journal of American Chemical Society* **121**: 6039-6046
- Caruso F., Niikura K, Furlong D. N., Okahata Y. (1997) Assembly of Alternating Polyelectrolyte and Protein Multilayer Films for Immunosensing. *Langmuir* **13**: 3427-3433
- Caruso F., Trau D., Möhwald H., Renneberg R. (2000) Enzyme Encapsulation in Layer-by-Layer Engineered Polymer Multilayer Capsules. *Langmuir* **16**: 1485-1488
- Champion J. A., Mitragotri S. (2006) Role of target geometry in phagocytosis. *Proceedings of the National Academy of Sciences of the United States* **103**: 4930-4934
- Chasis J. A., Mohandas N. (1986) Erythrocyte Membrane Deformability and Stability: Two Distinct Membrane Properties That Are Independently Regulated by Skeletal Protein Associations. *The Journal of Cell Biology* **103**
- Cheng Y., Samia A. C., Li J., Kenney M. E., Resnick A., Burda C. (2010) Delivery and efficacy of a cancer drug as a function of the bond to the gold nanoparticle surface. *Langmuir* **26**: 2248-2255

- Chithrani B. D., Ghazani A. A., Chan W. C. W. (2006) Determining the Size and Shape Dependence of Gold Nanoparticle Uptake into Mammalian Cells. *Nano Letters* **6**: 662-668
- Daum N., Tscheka C., Neumeyer A., Schneider M. (2012) Novel approaches for drug delivery systems in nanomedicine: effects of particle design and shape. *Wiley Interdisciplinary reviews Nanomedicine and nanobiotechnology* **4**: 52-65
- De M., Ghosh P. S., Rotello V. M. (2008) Applications of Nanoparticles in Biology. *Advanced Materials* **20**: 4225-4241
- Decuzzi P., Ferrari M. (2008) The Receptor-Mediated Endocytosis of Nonspherical Particles. *Biophysical Journal* **94**: 3790-3797
- Dejugnat C., Sukhorukov G.B. (2004) pH-Responsive Properties of Hollow Polyelectrolyte Microcapsules Templated on Various Cores. *Langmuir* **20**: 7265-7269
- Delcea M., Möhwald H., Skirtach A. G. (2011) Stimuli-responsive LbL capsules and nanoshells for drug delivery. *Advanced Drug Delivery Reviews*
- Delcea M., Schmidt S., Palankar R., Fernandes P. A. L., Fery A., Möhwald H., Skirtach A. G. (2010) Mechanobiology: Correlation Between Mechanical Stability of Microcapsules Studied by AFM and Impact of Cell-Induced Stresses. *Cell Mechanics* **6**: 2858-2862
- Delehanty J. B., Blanco-Canosa J. B., Bradburne C. E., Susumu K., Stewart M. H., Prasuhn D. E., Dawson P. E., Medintz I. L. (2013) Site-specific cellular delivery of quantum dots with chemoselectively-assembled modular peptides. *Chemical Communications* **49**: 7878-7880
- Discher D. E., Eisenber A. (2002) Polymer Vesicles. *Materials Science: Soft Surfaces* **297**
- Doane T. L., Burda C. (2011) The unique role of nanoparticles in nanomedicine: imaging, drug delivery and therapy. *Chemical Society Reviews* **41**: 2885-2911
- Domar U., Nilsson B., Baranov V., Gerdes U., Stigbrand T. (1992) Expression of intestinal alkaline phosphatase in human organs. *Histochemistry* **98**: 359-364
- Donatan S., Yashchenok A., Khan N., Parakhonskiy B., Cocquyt M., Pinchasik B., Khalenkow D., Möhwald H., Konrad M., Skirtach A. G. (2016) Loading Capacity versus Enzyme Activity in Anisotropic and Spherical Calcium Carbonate Microparticles. *Applied Materials & Interfaces* **8**: 14284-14292
- Donath E., Budde A., Knippel E., Bäuml H. (1996) "Hairy Surface Layer" Concept of Electrophoresis Combined with Local Fixed Surface Charge Density Isotherms: Application to Human Erythrocyte Electrophoretic Fingerprinting. *Langmuir* **12**: 4832-4839
- Donath E., Voigt A. (1986) Electrophoretic mobility of human erythrocytes. On the applicability of the charged layer model. *Biophysical Journal* **49**: 493
- Donath E., Walther D., Shilov V. N., Knippel E., Budde A., Lowack K., Helm C. A., Möhwald H. (1997) Nonlinear Hairy Layer Theory of Electrophoretic Fingerprinting Applied to Consecutive Layer by Layer Polyelectrolyte Adsorption onto Charged Polystyrene Latex Particles. *Langmuir* **13**: 5294-5305

- Dong W., Ferri J. K., Adalsteinsson T., Schönhoff M., Sukhorukov G.B., Möhwald H. (2005) Influence of Shell Structure on Stability, Integrity, and Mesh Size of Polyelectrolyte Capsules: Mechanism and Strategy for Improved Preparation. *Chemistry of Materials* **17**: 2603-2611
- Doshi N., Zahr A. S., Bhaskar S., Lahann J., Mitragotri S. (2009) Red blood cell-mimicking synthetic biomaterial particles. *Proceedings of the National Academy of Sciences of the United States* **106**: 21495-21499
- Douglas T. E. L., Messersmith P. B., Chasan S., Mikos A. G., de Mulder E. L. W., Dickson G., Schaubroeck D., Balcaen L., Vanhaecke F., Dubruel P., Jansen J. A., Leeuwenburgh S. C. G. (2012) Enzymatic Mineralization of Hydrogels for Bone Tissue Engineering by Incorporation of Alkaline Phosphatase. *Macromolecular Bioscience* **12**: 1077-1089
- Duan L., He Q., Yan X., Cui Y., Wang K., Li J. (2007) Hemoglobin protein hollow shells fabricated through covalent layer-by-layer technique. *Biochemical and biophysical research communications* **354**: 357-362
- Duncan B., Kim C., Rotello V. M. (2010) Gold nanoparticle platforms as drug and biomacromolecule delivery systems. *Journal of Controlled Release* **148**: 122-127
- Elion G. B. (1989) The Purine Path to Chemotherapy. *Angewandte Chemie International Edition* **28**: 870-878
- Filmon R., Baslé M. F., Atmani H., Chappard D. (2002) Adherence of osteoblast-like cells on calcospherites developed on a biomaterial combining poly(2-hydroxyethyl) methacrylate and alkaline phosphatase. *Bone* **30**
- Fraser D. (1957) Hypophosphatasia. *The American Journal of Medicine* **22**: 730-746
- Gao L., Fei J., Zhao J., Cui W., Cui Y., Li J. (2012) pH- and Redox-Responsive Polysaccharide-Based Microcapsules with Autofluorescence for Biomedical Applications. *Chemistry - A European Journal* **18**: 3185-3192
- Gåserød O., Smidsrod O., G. S-b (1998) Microcapsules of alginate-chitosan – I: A quantitative study of the interaction between alginate and chitosan. *Biomaterials* **19**: 1815-1825
- Gentile P., Chiono V., Carmacnola I., Hatton P. V. (2014) An Overview of Poly(lactic-co-glycolic) Acid (PLGA)-Based Biomaterials for Bone Tissue Engineering. *International Journal of Molecular Sciences* **15**: 3640-3659
- Ghan R., Shutava T., Patel A., John V. T., Lvov Y. M. (2004) Enzyme-Catalyzed Polymerization of Phenols within Polyelectrolyte Microcapsules. *Macromolecules* **37**: 4519-4524
- Glinel K., Moussa A., Jonas A. M., Laschewsky A. (2002) Influence of Polyelectrolyte Charge Density on the Formation of Multilayers of Strong Polyelectrolytes at Low Ionic Strength. *Langmuir* **18**: 1408-1412
- Gorin D. A., Schchukin D. G., Mikhailov A. I., Köhler K., Sergeev S. A., Portnov S. A., Taranov I. V., Kislov V. V., Sukhorukov G.B. (2006) Effect of microwave radiation on polymer microcapsules containing inorganic nanoparticles. *Technical Physics Letters* **32**: 70-72

- Graff A., Winterhalter M., Meier W. (2001) Nanoreactors from Polymer-Stabilized Liposomes. *Langmuir* **17**: 919-923
- Haghooie R., Toner M., Doyle P. S. (2010) Squishy Non-Spherical Hydrogel Microparticles. *Macromolecular Rapid Communications* **31**: 128-134
- Hall S. W., Kuhn H. (1986) Purification and properties of guanylate kinase from bovine retinas and rod outer segments. *European Journal of Biochemistry* **161**: 551-556
- Han M. R., Kwon M. C., Lee H. Y., Kim J. C., Yoo S. K., Sin I. S., Kim S. M. (2007) pH-dependent release property of alginate beads containing calcium carbonate particles. *Journal of Microencapsulation* **24**: 787-796
- Harder J., Gläser R., Schröder J. M. (2007) The role and potential therapeutical applications of antimicrobial proteins in infectious and inflammatory diseases. *Endocrine, metabolic & immuno disorders drug targets* **7**: 78-82
- Hardikar V. V., Matijevic E. (2001) Influence of ionic and nonionic dextrans on the formation of calcium hydroxide and calcium carbonate particles. *Colloids and Surfaces A: Physicochemical Engineering Aspects* **186**: 23-31
- Haug A., Larsen B., Smidsrod O. (1966) A Study of the constitution of alginic acid by partial acid hydrolysis. *Acta Chemica Scandinavia* **20**: 183-190
- Helmlinger G., Yuan F., Dellian M., Jain R. K. (1997) Interstitial pH and pO₂ gradients in solid tumors in vivo: high-resolution measurements reveal a lack of correlation. *Nature Medicine* **3**: 177-182
- Holt B., Lam R., Meldrum F. C., Stoyanov S. D., Paunov V. N. (2007) Anisotropic nano-papier mache microcapsules. *Soft Matter* **3**: 188-190
- Horth M., Lambrecht B., Khim M. C., Bex F., Thiriart C., Ruysschaert J. M., Burny A., Brasseur R. (1991) Theoretical and functional analysis of the SIV fusion peptide. *Embo Journal* **10**: 2747-2755
- Hotz J., Meier W. (1998) Vesicle-Templated Polymer Hollow Spheres. *Langmuir* **14**: 1031-1036
- Huang H. W., Chen F. Y., Lee M. T. (2004) Molecular mechanism of Peptide-induced pores in membranes. *Physical Review Letters* **92**
- Hühn D., Kantnert K., Geidel C., Brandholt S., De Cock I., Soenen S. J. H., Rivera P., Montenegro J., Braeckman K., Müllen K., Nienhaus G. U., Klapper M., Parak W. J. (2013) Polymer-Coated Nanoparticles Interacting with Proteins and Cells: Focusing on the Sign of the Net Charge. *ACS Nano* **7**: 3253-3263
- Husain Q., Iqbal J., Saleemuddin M. (1985) Entrapment of concanavalin A-glycoenzyme complexes in calcium alginate gels. *Biotechnology and Bioengineering* **27**: 1102-1107
- Hutter E., Boridy S., Labrecque S., Lalancette-Hébert M., Kriz J., Winnik F. M., Maysinger D. (2010) Microglial Response to Gold Nanoparticles. *ACS Nano* **4**: 2595-2606

- Islam K. N., Bakar Z. A. B., Noordin M. N., Hussein M. Z. B., Rahman N. S. B. A., Ali E. (2011) Characterisation of Calcium Carbonate and its polymorphs form cock shells (*Anadara granosa*). *Powder Technology* **213**
- Itoh Y., Matsusaki M., Kida T., Akashi M. (2004) Preparation of Biodegradable Hollow Nanocapsules by Silica Template Method. *Chemistry Letters* **33**: 1552-1553
- Jain R., Khan N., Menzel A., Rajkovic I., Konrad M., Techert S. (2015) Insights into open/closed conformations of the catalytically active human guanylate kinase as investigated by small-angle X-ray scattering. *European Biophysics Journal* **45**
- James J. P., Yan Y., Caruso F. (2012) The Role of Particle Geometry and Mechanics in the Biological Domain. *Advanced Healthcare Materials* **1**: 35-47
- Javier A. M., Kreft O., Alberola A. P., Kirchner C., Zebli B., Suha A. S., Horn E., Kempter S., Skirtach A. G., Rogach A. L., Rädler J., Sukhorukov G.B., Benoit M., Parak W. J. (2006) Combined Atomic Force Microscopy and Optical Microscopy Measurements as a Method To Investigate Particle Uptake by Cells. *Small (Weinheim an der Bergstrasse, Germany)* **2**: 394-400
- Jemmerson R., Low M. G. (1987) Phosphatidylinositol anchor of HeLa cell alkaline phosphatase. *Biochemistry* **26**: 5703-5709
- Jenssen H., Hamill P., Hancock R. E. (2006) Peptide antimicrobial agents. *Clinical Microbiology Reviews* **19**: 491-511
- Jiang X., Dausend J., Hafner M., Musyanovych A., Röcker C., Landfester K., Mailänder V., Nienhaus G. U. (2010) Specific Effects of Surface Amines on Polystyrene Nanoparticles in their Interactions with Mesenchymal Stem Cells. *Biomacromolecules* **11**: 748-753
- Johnson J. A., Gray M. O., Karliner J. S., Chen C. H., Mochly-Rosen D. (1996) An improved permeabilization protocol for the introduction of peptides into cardiac myocytes. Application to protein kinase C research. *Circulation Research* **79**: 1086-1099
- Karamitros C. S., Yashchenok A. M., Möhwald H., Skirtach A. G., Konrad M. (2013) Preserving Catalytic Activity and Enhancing Biochemical Stability of the Therapeutic Enzyme Asparaginase by Biocompatible Multilayered Polyelectrolyte Microcapsules. *Biomacromolecules* **14**
- Kierstan M., Bucke C. (1977) The immobilization of microbial cells, subcellular organelles, and enzymes in calcium alginate gels. *Biotechnology and Bioengineering* **19**: 387-397
- Kikuchi A., Kawabuchi M., Sugihara M., Sakurai Y., Okano T. (1997) Pulsed dextran release from calcium-alginate gel beads. *Journal of Controlled Release* **47**: 21-29
- Kim C. S., Le N. D. B., Xing Y., Yan B., Tonga G. Y., Kim C., Vachet R. W., Rotello V. M. (2014) The Role of Surface Functionality in Nanoparticle Exocytosis. *Advanced Healthcare Materials* **3**: 1200-1202
- Kirboga S., Oner M. (2013) Effect of the Experimental Parameters on Calcium Carbonate Precipitation. *The Italian Association of Chemical Engineering* **32**

- Köhler K., Shchukin D. G., Möhwald H., Sukhorukov G. B. (2005) Thermal Behavior of Polyelectrolyte Multilayer Microcapsules. 1. The Effect of Odd and Even Layer Number. *Journal of Physical Chemistry* **109**: 18250-18259
- Kohn R., Larsen B. (1972) Preparation of water-soluble polyuronic acids and their calcium salts, and the determination of calcium ion activity in relation to the degree of polymerization. *Acta Chemica Scandinavia* **26**: 2455-2468
- Kolesnikova T. A., Gorin D. A., Fernandes P., Kessel S., Khomutov G. B., Fery A., Shchukin D. G., Möhwald H. (2010) Nanocomposite Microcontainers with High Ultrasound Sensitivity. *Materials Views* **20**: 1189-1195
- Kolesnikova T. A., Khlebtsov B. N., Shchukin D. G., Gorin D. A. (2008) Atomic force microscopy characterization of ultrasound-sensitive nanocomposite microcapsules. *Nanotechnologies in Russia* **3**: 560-569
- Konrad M. (1992) Cloning and expression of the essential gene for guanylate kinase from yeast. *Journal of Biological Chemistry* **267**: 25652-25655
- Koyama D., Kiyama W., Watanabe Y. (2004) Micro-capsule destruction using ultrasound for drug delivery system. *IEEE Ultrasonics Symposium* **Vol 1-3**
- Lasic D. D. (1994) Liposomes: From Physics to Applications. *Biophysical Journal* **67**: 1358-1362
- Leader B., Baca Q. J., Golan D. E. (2008) Protein therapeutics: a summary and pharmacological classification. *Nature Reviews* **7**: 21-39
- Lee K. Y., Mooney D. J. (2012) Alginate: properties and biomedical applications. *Progress in polymer science* **37**: 106-126
- Leeuwenburgh S. C., Ana I. D., Jansen J. A. (2010) Sodium citrate as an effective dispersant for the synthesis of inorganic-organic composites with a nanodispersed mineral phase. *Acta Biomaterialia* **6**: 836-844
- Leeuwenburgh S. C., Jansen J. A., Mikos A. G. (2007) Functionalization of oligo(poly(ethylene glycol)fumarate) hydrogels with finely dispersed calcium phosphate nanocrystals for bone-substituting purposes. *Journal of Biomaterials Science* **18**: 1547-1564
- Lengert E., Yashchenok A., Atkin V., Lapanje A., Gorin D. A., Sukhorukov G.B., Parakhonskiy B. V. (2016) Hollow silver alginate microspheres for drug delivery and surface enhanced Raman scattering detection. *RSC Advances* **6**
- Lerch S., Dass M., Landfester K., Mailänder V. (2013) Polymeric nanoparticles of different sizes overcome the cell membrane barrier. *European Journal of Pharmaceutics and Biopharmaceutics* **84**
- Liang K., Such G. K., Johnston A. P. R., Zhu Z., Ejima H., Richardson J. J., Cui J., Caruso F. (2014) Endocytic pH-Triggered Degradation of Nanoengineered Multilayer Capsules. *Advanced Materials* **26**: 1901-1905

- Liang K., Such G. K., Zhu Z., Dodds S. J., Johnston A. P. R., Cui J., Ejima H., Caruso F. (2012) Engineering Cellular Degradation of Multilayered Capsules through Controlled Cross-Linking. *ACS Nano* **6**
- Liechty W. B., Kryscio D. R., Slaughter B. V., Peppas N. A. (2010) Polymers for drug delivery systems. *Annual Review of Chemical and Biomolecular Engineering* **1**: 149-173
- Liu L., Liu S., Ng S. Y., Froix M., Ohno T., Heller J. (1997) Controlled release of interleukin-2 for tumour immunotherapy using alginate/chitosan porous microspheres. *Journal of Controlled Release* **43**: 65-74
- Liu S., Wei L., Hao L., Fang N., Chang M. W., Xu R., Yang Y., Chen Y. (2009) Sharper and Faster "Nano Darts" Kill More Bacteria: A Study of Antibacterial Activity of Individually Dispersed Pristine Single-Walled Carbon Nanotube. *ACS Nano* **3**: 3891-3902
- Lou P., Lai P., Shieh M., MacRobert A. J., Berg K., Bown S. G. (2006) Reversal of doxorubicin resistance in breast cancer cells by photochemical internalization. *International Journal of Cancer* **119**: 2692-2698
- Lu Z., Prouty M. D., Guo Z., Golub V. O., Kumar C. S. S. R., Lvov Y. M. (2005) Magnetic Switch of Permeability for Polyelectrolyte Microcapsules Embedded with Co@Au Nanoparticles. *Langmuir* **21**: 2042-2050
- Lvov Y. M., Patekari P., Zhang X., Tochilin V. (2010) Converting Poorly Soluble Materials into Stable Aqueous Nanocolloids. *Langmuir* **27**: 1212-1217
- Magnani M., Rossi L., Fraternali A., Bianchi M., Antonelli A., Crinelli R., Chiarantini L. (2002) Erythrocyte-mediated delivery of drugs, peptides and modified oligonucleotides. *Gene Therapy* **9**: 749-751
- Manning G. S. (1977) Limiting Laws and Counterion Condensation in Polyelectrolyte Solutions. *Biophysical Chemistry* **7**: 95
- Marchenko I., Yashchenok A., Borodina T., Bukreeva T. V., Konrad M., Möhwald H., Skirtach A. G. (2012) Controlled enzyme-catalyzed degradation of polymeric capsules templated on CaCO₃: Influence of the number of LbL layers, conditions of degradation, and disassembly of multicompartments. *Journal of Controlled Release* **162**: 599-605
- Marsh M., Helenius A. (1989) Virus entry into animal cells. *Advances in Virus Research* **36**: 107-151
- Melvik J. E., Dornish M. (2004) Alginate as a carrier for cell immobilisation. *Fundamentals of Cell Immobilisation Biotechnology* **8**: 33-51
- Melzoch K., Rychtera M., Hábová (1994) Effect of immobilization upon the properties and behaviour of *Saccharomyces cerevisiae* cells. *Journal of Biotechnology* **32**: 59-65
- Meng H., Yang S., Li Z., Xia T., Chen J., Ji Z., Zhang H., Wang X., Lin S., Huang C., Zhou Z. H., Zink J. I., Nel A. E. (2011) Aspect Ratio Determines the Quantity of Mesoporous Silica

Nanoparticle Uptake by a Small GTPase-Dependent Macropinocytosis Mechanism. *ACS Nano* **5**: 4434-4447

Merkel T. J., Jones S. W., Herlihy K. P., Kersey F. R., Shields A. R., Napier M., Luft J. C., Wu H., Zamboni W. C., Wang A. Z., Bear J. E., DeSimone J. M. (2011) Using mechanobiological mimicry of red blood cells to extend circulation times of hydrogel microparticles. *Proceedings of the National Academy of Sciences of the United States* **108**: 586-591

Miech R. P., York R., Parks R. E. (1969) Adenosine triphosphate-guanosine 5'-phosphate phosphotransferase. II. Inhibition by 6-thioguanosine 5'-phosphate of the enzyme isolated from hog brain and sarcoma 180 ascites cells. *Molecular Pharmacology* **5**: 30-37

Millan J. L., Narisawa S., Lemire I., Lolsel T. P., Bolleau G., Leonard P., Gramatikova S., Terkeltaub R., Camacho N. P., McKee M. D., Crine P., Whyte M. P. (2008) Enzyme replacement therapy for murine hypophosphatasia. *Journal of Bone and Mineral Research* **23**: 777-787

Millan J. L., Whyte M. P. (2016) Alkaline Phosphatase and Hypophosphatasia. *Calcified Tissue International* **98**: 398-416

Miller D. K., Griffiths E., Lenard J., Firestone R. A. (1983) Cell killing by lysosomotropic detergents. *Journal of Cell Biology* **97**: 1841-1851

Moya S., Dähne L. VA, Leporatti S. DE, Möhwald H. (2001) Polyelectrolyte multilayer capsules templated on biological cells: core oxidation influences layer chemistry. *Colloids and Surfaces A: Physicochemical Engineering Aspects* **183-185**: 27-40

Mozafari M. R., Johnson C., Hatziantoniou S., Demetzos C. (2008) Nanoliposomes and Their Applications in Food Nanotechnology. *Journal of Liposome Research* **18**: 309-327

Mueller R., Köhler K., Weinkamer R., Sukhorukov G.B., Fery A. (2005) Melting of PDADMAC/PSS Capsules Investigated with AFM Force Spectroscopy. *Macromolecules* **38**: 9766-9771

Neijssen J., Herberts C., Drijfhout J. W., Reits E., Janssen L., Neefjes J. (2005) Cross-presentation by intercellular peptide transfer through gap junctions. *Nature* **434**: 83-88

Neu B., Voigt R., Mitlöhner R., Leporatti S., Gao C. Y., Donath E., Kiesewetter H., Möhwald H., Meiselman H. J., Bäuml H. (2008) Biological Cells as Templates for Hollow Microcapsules. *Journal of Microencapsulation* **18**: 385-395

Nishiyama N., Amida W. D., Date K., Miyata K., Kataoka K. (2006) Photochemical enhancement of transgene expression by polymeric micelles incorporating plasmid DNA and dendrimer-based photosensitizer. *Journal of Drug Targeting* **14**: 413-424

Ogino T., Suzuki T., Sawada K. (1987) The formation and transformation mechanism of calcium carbonate in water. *Geochimica et Cosmochimica Acta* **51**: 2757-2767

Orimo H. (2010) The mechanism of mineralization and the role of alkaline phosphatase in health and disease. *Journal of Nippon Medical School* **77**: 4-12

- Ouwerx C., Velings N., Mestdagh M. M., Axelos M. A. V. (1998) Physico-chemical properties and rheology of alginate gel beads formed with various divalent cations. *Polymer Gels and Networks* **6**: 393-408
- Parakhonskiy B., Haase A., Antolini R. (2012) Sub-Micrometer Vaterite Containers: Synthesis, Substance Loading and Release. *Angewandte Chemie International Edition* **51**
- Parakhonskiy B., Zyuzin M., Yashchenok A., Carregal-Romero S., Rejman J., Möhwald H., Parak W. J., Skirtach A. G. (2015) The influence of the size and aspect ratio of anisotropic, porous CaCO₃ particles on their uptake by cells. *Journal of Nanobiotechnology*: 13
- Parakhonskiy B. V., Foss C., Carletti E., Fedel M., Haase A., Motta A., Migliaresi C., Antolini R. (2013) Tailored intracellular delivery via a crystal phase transition in 400 nm vaterite particles†. *Biomaterial Science*
- Parakhonskiy B. V., Yashchenok A. M., Donatan S., Volodkin D. V., Tessarolo F., Antolini R., Möhwald H., Skirtach A. G. (2014a) Macromolecule Loading into Spherical, Elliptical, Star-Like and Cubic Calcium Carbonate Carriers. *ChemPhysChem* **15**: 2817-2822
- Parakhonskiy B. V., Yashchenok A. M., Konrad M., Skirtach A. G. (2014b) Colloidal micro- and nano-particles as templates for polyelectrolyte multilayer capsules. *Advances in Colloid and Interface Science* **207**: 253-264
- Park B., Yoon D., Kim D. (2010) Recent progress in bio-sensing techniques with encapsulated enzymes. *Biosensors & Bioelectronics* **26**: 1-10
- Pavlov A. M., Saez V., Cobley A., Graves J., G.B. S, Mason T. J. (2011) Controlled protein release from microcapsules with composite shells using high frequency ultrasound—potential for in vivo medical use. *Soft Matter* **7**: 4341-4347
- Peer D., Karp J. M., Hong S., Langer R. (2007) Nanocarriers as an emerging platform for cancer therapy. *Nature Nanotechnology* **2**: 751-760
- Peters E., Masereeuw R., Pickkers P. (2014) The Potential of Alkaline Phosphatase as a Treatment for Sepsis-Associated Acute Kidney Injury. *Clinical Practice* **127**
- Petrov A. I., Volodkin D. V., Sukhorukov G. B. (2005) Protein-Calcium Carbonate Coprecipitation: A Tool for Protein Encapsulation. *Biotechnology Progress* **21**: 918-925
- Pickkers P., Heemskerk S., Schouten J., Laterre P., Vincent J., Beishuizen A., Jorens P. G., Spapen H., Bulitta M., Peters W. H. M., van der Hoeven J. G. (2012) Alkaline phosphatase for treatment of sepsis-induced acute kidney injury: a prospective randomized double-blind placebo-controlled trial. *Critical Care* **16**
- Podolsky D. K. (2002) Inflammatory Bowel Disease. *The New England Journal of Medicine: Research & Review Articles* **437**
- Prasmickaite L., Hogset A., Berg K. (2001) Evaluation of different photosensitizers for use in photochemical gene transfection. *Photochemistry and Photobiology* **73**: 388-395

- Radt B., Smith T. A., Caruso F. (2004) Optically Addressable Nanostructured Capsules. *Advanced Materials* **16**: 2184-2189
- Raj N. K. K., Sharma C. P. (2003) Oral insulin—a perspective. *Journal of Biomaterials Applications* **17**: 183-196
- Ramundo-Orlando A., Morbiducci U., Mossa G., D'Inzeo G. (2000) Effect of Low Frequency, Low Amplitude Magnetic Fields on the Permeability of Cationic Liposomes Entrapping Carbonic Anhydrase. *Bioelectromagnetics* **21**: 491-498
- Reiss I., Inderrieden D., Kruse K. (1996) Measurement of skeletal specific alkaline phosphatase in disorders of calcium metabolism in childhood. *Monatsschrift Kinderheilkunde* **144**: 885-890
- Rother C., Nidetzky B. (2014) Enzyme Immobilization by Microencapsulation: Methods, Materials and Technological Applications. In Flickinger MC (ed.), *Encyclopedia of Industrial Biotechnology: Bioprocess, Bioseparation and Cell Technology*. John Wiley & Sons, Inc.
- Ruysschaert T., Germain M., Gomes J. F. P., Fournier D., SUkhorukov G.B., Meier W., Winterhalter M. (2004) Liposome-Based Nanocapsules. *Transactions on Nanobioscience* **3**: 49-55
- Sakr O. S., Borchard G. (2013) Encapsulation of Enzymes in Layer-by-Layer (LbL) Structures: Latest Advances and Applications. *Biomacromolecules* **14**: 2117-2135
- Saraya M. E. I., Rokbaa H. H. A. L. (2016) Preparation of Vaterite Calcium Carbonate in the Form of Spherical Nano-size Particles with the Aid of Polycarboxylate Superplasticizer as a Capping Agent. *American Journal of Nanomaterials* **4**: 44-51
- Sawada K. (1997) The Mechanisms of Crystallization and Transformation of Calcium Carbonates *Pure and Applied Chemistry* **69**: 921-928
- Schlücker S. (2011) *Surface Enhanced Raman Spectroscopy: Analytical, Biophysical and Life Science Applications*.
- Schneider G., Decher G. (2004) From Functional Core/Shell Nanoparticles Prepared via Layer-by-Layer Deposition to Empty Nanospheres. *Nano Letters* **4**: 1833-1839
- Schuetz P., Caruso F. (2003) Copper-Assisted Weak Polyelectrolyte Multilayer Formation on Microspheres and Subsequent Film Crosslinking. *Advanced Functional Materials* **13**: 929-937
- Sekulic N., Shuvalova L., Spangenberg O., Konrad M., Lavie A. (2002) Structural characterization of the Closed Conformation of Mouse Guanylate Kinase. *JBC papers*
- Sen C. K. (1998) Redox signaling and the emerging therapeutic potential of thiol antioxidants. *Biochemical Pharmacology* **55**: 1747-1758
- Sergeeva A., Sergeev R., Lengert E., Zakharevich A., Parakhonskiy B. V., Gorin D. A., Sergeev S., Volodkin D. V. (2015) Composite Magnetite and Protein Containing CaCO₃ Crystals. External Manipulation and Vaterite → Calcite Recrystallization-Mediated Release Performance. *ACS Applied Materials & Interfaces* **7**: 21315-21325

- Sharp K. A., Brooks D. E. (1985) Calculation of the electrophoretic mobility of a particle bearing bound polyelectrolyte using the nonlinear poisson-boltzmann equation. *Biophysical Journal* **47**: 563-566
- Shchepelina O., Kharlampieva E., Mao W., Alexeev A., Tsukruk V. V. (2010) Anisotropic Micro- and Nano-Capsules. *Macromolecular Rapid Communications* **31**: 2041-2046
- She S., Li Q., Shan B., Tong W., Gao C. Y. (2013) Fabrication of Red-Blood-Cell-Like Polyelectrolyte Microcapsules and Their Deformation and Recovery Behavior Through a Microcapillary. *Advanced Materials* **25**: 5814-5818
- She S., Xu C., Yin X., Tong W., Gao C. Y. (2012) Shape Deformation and Recovery of Multilayer Microcapsules after Being Squeezed through a Microchannel. *Langmuir* **28**: 5010-5016
- Shenoy D. B., Antipov A. A., Sukhorukov G.B., Möhwald H. (2003) Layer-by-layer engineering of biocompatible, decomposable core-shell structures. *Biomacromolecules* **4**: 265-272
- Shimoni O., Yan Y., Wang Y., Caruso F. (2013) Shape-Dependent Cellular Processing of Polyelectrolyte Capsules. *ACS Nano* **7**: 522-530
- Shu S., Zhang X., Wu Z., Wang Z., Li C. (2010) Gradientcross-linked Biodegradable Polyelectrolyte Nanocapsules for Intracellular Protein Drug Delivery. *Biomaterials* **31**: 6039-6049
- Singh M. N., Hemant K. S. Y., Ram M., Shivakumar H. G. (2010) Microencapsulation: a Promising Technique for Controlled Drug Delivery. *Research in Pharmaceutical Sciences* **5**: 65-77
- Skirtach A. G., De Geest B. G., Mamedov A., Antipov A. A., Kotov N. A., Sukhorukov G.B. (2006) Ultrasound Stimulated Release and Catalysis using Polyelectrolyte Multilayer Capsules. *Journal of Materials Chemistry* **17**: 1050-1054
- Skirtach A. G., Dejognat C., Braun D., Susa A. S., Rogach A. L., Parak W. J., Möhwald H., Sukhorukov G.B. (2005) The Role of Metal Nanoparticles in Remote Release of Encapsulated Materials. *Nano Letters* **5**: 1371-1377
- Skirtach A. G., Yashchenok A. M., Möhwald H. (2011) Encapsulation, release and applications of LbL polyelectrolyte multilayer capsules. *Chemical Communications* **47**: 12736-12746
- Skjåk-Braek G., Smidsrod O., Larsen B. (1986) Tailoring of alginates by enzymatic modification in vitro. *International Journal of Biological Macromolecules* **8**: 330-336
- Smidsrod O., Haug A. (1968) A Light Scattering Study of Alginate. *Acta Chemica Scandinavia* **22**: 797-810
- Srivastava R., Brown J. Q., Zhu H., McShane M. J. (2005) Stable Encapsulation of Active Enzyme by Application of Multilayer Nanofilm Coatings to Alginate Microspheres. *Macromolecular Bioscience* **5**: 717-727

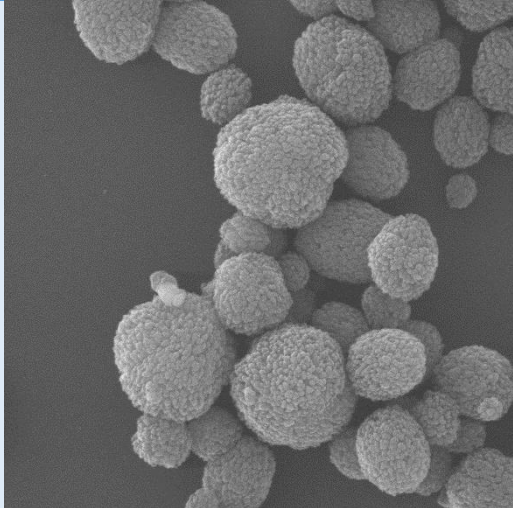
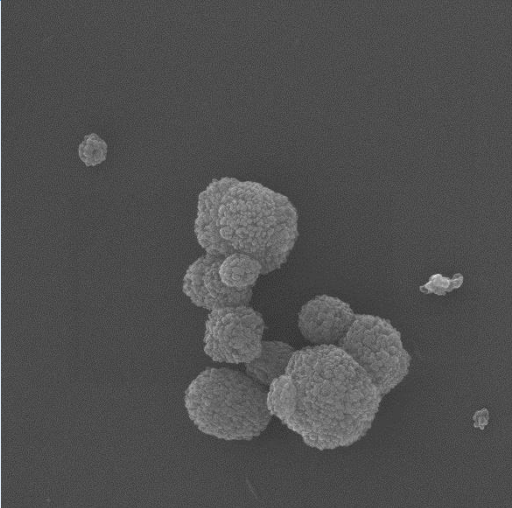
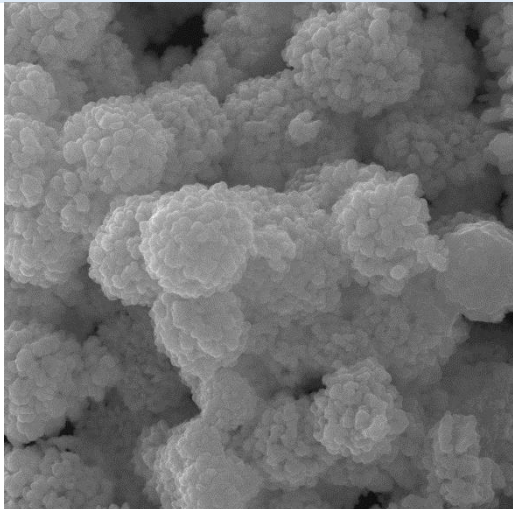
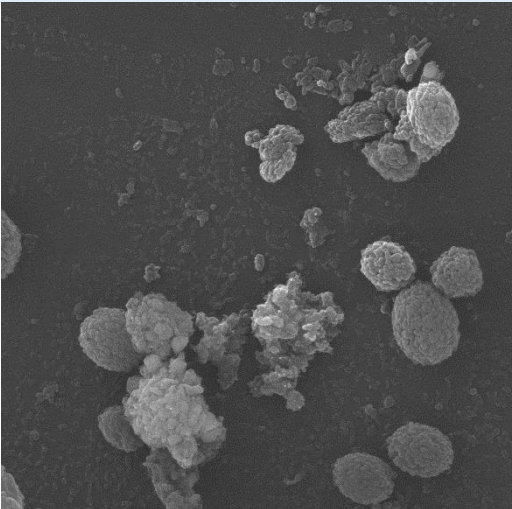
- Stein E. W., Volodkin D. V., McShane M. J., Sukhorukov G.B. (2006) Real-Time Assessment of Spatial and Temporal Coupled Catalysis within Polyelectrolyte Microcapsules Containing Coimmobilized Glucose Oxidase and Peroxidase. *Biomacromolecules* **7**: 710-719
- Stokke B. T., Smidsrod O., Zanetti F., Strand W., Skjakbraek G. (1993) Distribution Of Uronate Residues In Alginate Chains In Relation To Alginate Gelling Properties .2. Enrichment Of Beta-D-Mannuronic Acid Anddepletion Of Alpha-L-Guluronic Acid In Sol Fraction. *Carbohydrate Polymers* **21**: 39-46
- Strand B. L., Gåserød O., Kulseng B., Espevik T., Skjåk-Bræk G. (2008) Alginate-polylysine-alginate microcapsules: effect of size reduction on capsule properties. *Journal of Microencapsulation* **19**: 615-630
- Strong L. E., West J. L. (2011) Thermally responsive polymer-nanoparticle composites for biomedical applications. *Wiley Interdisciplinary reviews Nanomedicine and nanobiotechnology* **3**: 307-317
- Sukhorukov G.B., Brumen M., Donath E., Möhwald H. (1999) Hollow Polyelectrolyte Shells: Exclusion of Polymers and Donnan Equilibrium. *Journal of Physical Chemistry* **103**
- Svenskaya Y., Fattah H., Zakharevich A., Gorin D., Sukhorukov G., Parakhonskiy B. (2016) Ultrasonically Assisted Fabrication of Vaterite Submicron-sized Carriers. *Advanced Powder Technology*
- Svenskaya Y., Parakhonskiy B. V., Haase A., Atkin V., Lukyanets E., Gorin D., Antolini R. (2013) Anticancer drug delivery system based on calcium carbonate particles loaded with a photosensitizer. *Biophysical Chemistry* **182**: 11-15
- Tang R., Moyano D. F., Subramani C., Yan B., Jeoung E., Tonga G. Y., Duncan B., Yeh Y., Jiang Z., Kim C., Rotello V. M. (2014) Rapid Coating of Surfaces with Functionalized Nanoparticles for Regulation of Cell Behavior. *Advanced Materials* **26**: 3310-3314
- Thu B., Bruheim P., Espevik T., Smidsrod O., Soon-Shiong P., Skjak-Braek G. (1996) Alginate polycation microcapsules *Biomaterials* **17**: 1031-1040
- Timko B. P., Whitehead K, Gao W., Kohane D. S., Farokhzad O., Anderson D., Langer R. (2011) Advances in drug delivery. *Annual Review of Materials Research* **41**: 1-20
- Tiourina O. P., Sukhorukov G.B. (2002) Multilayer alginate/protamine microsized capsules: Encapsulation of -chymotrypsin and controlled release study. *International Journal of Pharmaceutics* **242**: 155-161
- Trau D., Renneberg R. (2003) Encapsulation of glucose oxidase microparticles within a nanoscale layer-by-layer film: immobilization and biosensor applications. *Biosensors & Bioelectronics* **18**: 1491-1499
- Trushina D. B., Bukreeva T. V., Kovalchuk M. V., N. AM (2014) CaCO₃ vaterite microparticles for biomedical and personal care applications. *Materials Science and Engineering* **45**: 644-658

- Trushina D. B., Sulyanov S. N., Bukreeva T. V., Kovalchuk M. V. (2015) Size Control and Structure Features of Spherical Calcium Carbonate Particles. *Kristallografiya* **60**: 625-633
- Tuin A., Poelstra K., de Jager-Krikken A., Bok L., Raaben W., Velders M. P., Dijkstra G. (2009) Role of alkaline phosphatase in colitis in man and rats. *Gut* **58**
- Vigneron N., Stroobant V., Chapiro J., Ooms A., Degiovanni G., Morel S., van der Bruggen P., Boon T., Van den Eynde B. J. (2004) An antigenic peptide produced by peptide splicing in the proteasome. *Science* **304**: 587-590
- Vinogradova O. I., Lebedeva O. V., Vasilev K., Gong H., Carcia-Turiel J., Kim B. (2005) Multilayer DNA/Poly(allylamine hydrochloride) Microcapsules: Assembly and Mechanical Properties. *Biomacromolecules* **6**
- Vogt C., Mertz D., Benmlih K., Hemmerlé J., Voegel J., Schaaf P., Lavalle P. (2012) Layer-by-Layer Enzymatic Platform for Stretched-Induced Reactive Release. *ACC Publications* **1**: 797-801
- Voigt A., Lichtenfeld H., Sukhorukov G.B., Zastrow H., Donath E., Bäumlér H., Möhwald H. (1999) Membrane Filtration for Microencapsulation and Microcapsules Fabrication by Layer-by-Layer Polyelectrolyte Adsorption. *Industrial & Engineering Chemistry Research* **38**: 4037-4043
- Volodkin D. V., Larionova N. I., Sukhorukov G. B. (2004) Protein Encapsulation via Porous CaCO₃ Microparticles Templating. *Biomacromolecules* **5**: 1962-1972
- Volodkin D. V., Petrov A. I., Prevot M., Sukhorukov G.B. (2003) Matrix Polyelectrolyte Microcapsules: New System for Macromolecule Encapsulation. *Langmuir*
- Volodkin D. V., Schmidt S., Fernandes P., Larionova N. I., Sukhorukov G.B., Dushl C., Möhwald H., von Klitzing R. (2012) One-Step Formulation of Protein Microparticles with Tailored Properties: Hard Templating at Soft Conditions. *Advanced Functional Materials* **22**: 1914-1922
- Volodkin D. V., von Klitzing R., H. M (2010) Pure Protein Microspheres by Calcium Carbonate Templating. *Angewandte Chemie International Edition* **49**
- Walde P., Ichikawa S. (2001) Enzymes inside lipid vesicles: preparation, reactivity and applications. *Biomolecular Engineering* **18**: 143-177
- Wang B., Zhang Y., Mao Z., Gao C. Y. (2012) Cellular uptake of covalent poly(allylamine hydrochloride) microcapsules and its influences on cell functions. *Macromolecular Bioscience* **12**: 1534-1545
- Wattendorf U., Kreft O., Textor M., Sukhorukov G.B., Merlke H. P. (2008) Stable Stealth Function for Hollow Polyelectrolyte Microcapsules through a Poly(ethylene glycol) Grafted Polyelectrolyte Adlayer. *Biomacromolecules* **9**: 100-108
- Wuytens P., Parakhonskiy B. V., Yashchenok A. M., Winterhalter M., Skirtach A. G. (2014) Pharmacological aspects of release from microcapsules from polymeric multilayers to lipid membranes. *Current Opinion in Pharmacology* **18**: 129-140

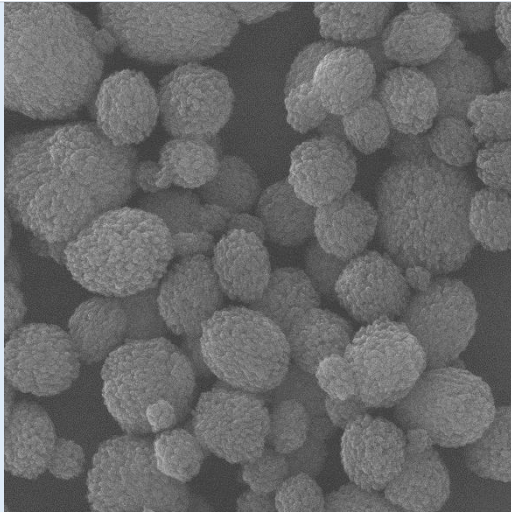
- Yan Y., Gause K. T., Kamphuis M. M. J., Ang C., O'Brien-Simpson N. M., Lenzo J. C., Reynolds E. C., Nice E. C., Caruso F. (2013) Differential Roles of the Protein Corona in the Cellular Uptake of Nanoporous Polymer Particles by Monocyte and Macrophage Cell Lines. *ACS Nano* **7**: 10960-10970
- Yashchenok A., Delcea M., Videnova K., Jares-Erijman A., Jovin T. M., Konrad M., Möhwald H., Skirtach A. G. (2010) Enzyme Reaction in the Pores of CaCO₃ Particles upon Ultrasound Disruption of Attached Substrate-Filled Liposomes. *Angewandte Chemie International Edition* **49**: 8116-8120
- Yilmaz Z. E., Cordonnier T., Debuigne A., Calvignac B., Jerome C., Boury F. (2016) Protein encapsulation and release from PEO-b-polyphosphoester templated calcium carbonate particles. *International Journal of Pharmaceutics* **513**: 130-137
- Yoo P. J., Nam K. T., Qi J., Lee S., Park J., Belcher A. M., Hammond P. T. (2006) Spontaneous assembly of viruses on multilayered polymer surfaces. *Nature Materials* **5**: 234-240
- Yoshimoto M., Wang S., Fukunaga K., Walde P., Kuboi R., Nakao K. (2002) Preparation and Characterization of Reactive and Stable Glucose Oxidase-Containing Liposomes Modulated with Detergent. *Biotechnology and Bioengineering* **81**: 695-704
- Yu A., Wang Y., Barlow E., Caruso F. (2005) Mesoporous Silica Particles as Templates for Preparing Enzyme-Loaded Biocompatible Microcapsules. *Advanced Materials* **17**: 1737-1741
- Zhang R., Köhler K., Kreft O., Skirtach A. G., Möhwald H., Sukhorukov G. B. (2010) Salt-induced fusion of microcapsules of polyelectrolytes. *Soft Matter* **6**
- Zhou J., Pishko M. V., Lutkenhaus J. L. (2014) Thermoresponsive Layer-by-Layer Assemblies for Nanoparticle-Based Drug Delivery. *ACS Publication* **30**: 5903-5910
- Zschocke P. D., Schiltz E., Schulz G. E. (1993) Purification and sequence determination of guanylate kinase from pig brain. *European Journal of Biochemistry* **213**: 263-269

I. Appendix: SEM images of alginate based hydrogels

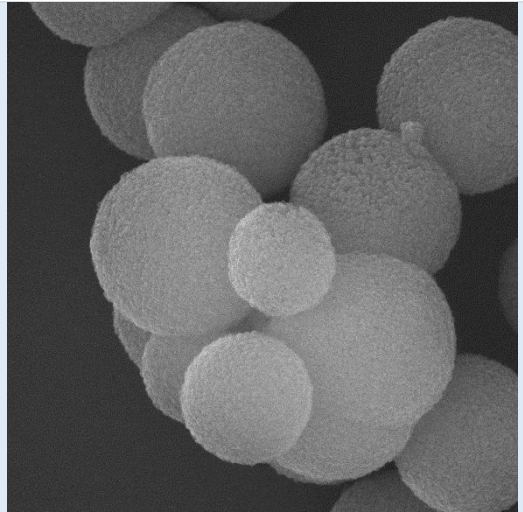
Table 2: SEM images of the various small and large alginate based hydrogels

	Small CaCO ₃ particles	Large CaCO ₃ particles
CaCO₃/Alg	 <p>SEM HV: 30.00 kV View field: 6.613 µm Det: SE SEM MAG: 50.00 kx Date(m/d/y): 05/02/17 Performance in nanospace</p>	 <p>SEM HV: 30.00 kV View field: 6.613 µm Det: SE SEM MAG: 50.00 kx Date(m/d/y): 05/02/17 Performance in nanospace</p>
CaCO₃/AgAlg	 <p>SEM HV: 30.00 kV View field: 6.612 µm Det: SE SEM MAG: 50.01 kx Date(m/d/y): 05/02/17 Performance in nanospace</p>	 <p>SEM HV: 30.00 kV View field: 6.613 µm Det: SE SEM MAG: 50.00 kx Date(m/d/y): 05/02/17 Performance in nanospace</p>

CaCO₃/CaAlg

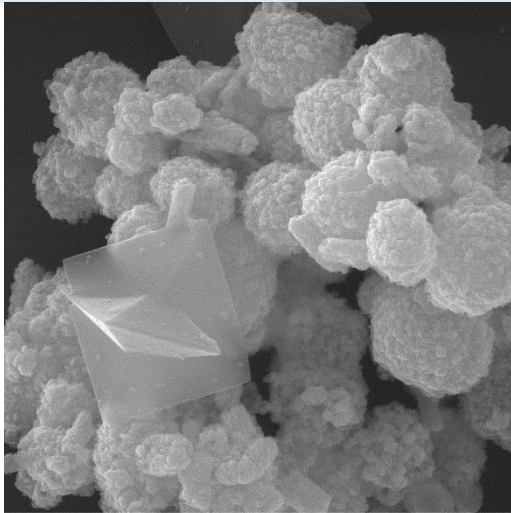


SEM HV: 30.00 kV
View field: 6.613 µm
SEM MAG: 50.00 kx
Det: SE
Date(m/d/y): 05/02/17
MIRA\ TESCAN
2 µm
Performance in nanospace

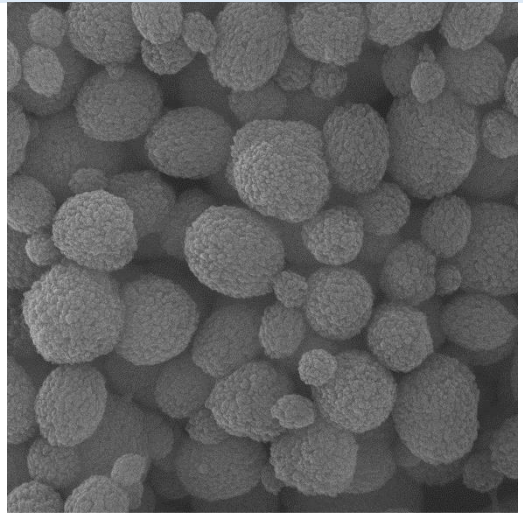


SEM HV: 30.00 kV
View field: 6.613 µm
SEM MAG: 50.00 kx
Det: SE
Date(m/d/y): 05/02/17
MIRA\ TESCAN
2 µm
Performance in nanospace

AgAlg



SEM HV: 30.00 kV
View field: 6.613 µm
SEM MAG: 50.00 kx
Det: SE
Date(m/d/y): 05/02/17
MIRA\ TESCAN
2 µm
Performance in nanospace



SEM HV: 30.00 kV
View field: 6.613 µm
SEM MAG: 50.00 kx
Det: SE
Date(m/d/y): 05/02/17
MIRA\ TESCAN
2 µm
Performance in nanospace